

AMAP 2017



ACA

ADAPTATION ACTIONS FOR A CHANGING ARCTIC

PERSPECTIVES FROM THE BAFFIN BAY/DAVIS STRAIT REGION



AMAP

Arctic Monitoring and Assessment Programme (AMAP)

Educational use: This report (in part or in its entirety) and other AMAP products available from www.amap.no can be used freely as teaching materials and for other educational purposes.

The only condition of such use is acknowledgement of AMAP as the source of the material according to the recommended citation.

In case of questions regarding educational use, please contact the AMAP Secretariat (amap@amap.no).

Note: This report may contain material (e.g. photographs) for which permission for use will need to be obtained from original copyright holders.

Disclaimer: The views expressed in this peer-reviewed report are the responsibility of the authors of the report and do not necessarily reflect the views of the Arctic Council, its members or its observers.

AMAP 2017

Adaptation Actions for a Changing Arctic: Perspectives from the Baffin Bay/Davis Strait Region

AMAP

Arctic Monitoring and Assessment Programme (AMAP)

Oslo, 2017

AMAP 2017 Adaptation Actions for a Changing Arctic: Perspectives from the Baffin Bay/Davis Strait Region

Citing whole report

AMAP, 2018. Adaptation Actions for a Changing Arctic: Perspectives from the Baffin Bay/Davis Strait Region. Arctic Monitoring and Assessment Programme (AMAP), Oslo, Norway. xvi + 354pp

Citing individual chapters

[Lead author list], 2018. [Chapter title]. In: Adaptation Actions for a Changing Arctic: Perspectives from the Baffin Bay/Davis Strait Region. pp. [xx-yy]. Arctic Monitoring and Assessment Programme (AMAP), Oslo, Norway.

ISBN 978-82-7971-105-6

© Arctic Monitoring and Assessment Programme, 2018

Published by

Arctic Monitoring and Assessment Programme (AMAP), Oslo, Norway. (www.amap.no)

Ordering

This report can be ordered from the AMAP Secretariat, The Fram Centre, Box 6606 Langnes, 9296 Tromsø, Norway

This report is also published as electronic documents, available from the AMAP website at www.amap.no

Technical Production

Technical production management

Jan René Larsen, Jon L. Fuglestad and Inger Utne (AMAP Secretariat)

Technical and linguistic editing

Tonya Clayton (tclayton@nasw.org)

Publication design and layout

Burnthebook, United Kingdom (www.burnthebook.co.uk)

Jane White and Simon Duckworth (Burnthebook)

Cover photograph

Downtown Nuuk is a busy area, 16 June 2010

David Boertmann

Printing

Narayana Press, Gylling, DK-8300 Odder, Denmark (www.narayanapress.dk)



AMAP Working Group (during period of preparation of this assessment)

Martin Forsius (Chair, Finland), Morten Olsen (Vice-Chair, Kingdom of Denmark), Sarah Kalhok (Canada), Mikala Klint (Kingdom of Denmark) Nathia Hass Brandtberg (Kingdom of Denmark), Outi Mähönen (Finland), Helgi Jensson (Iceland), Marianne Kroglund (Vice-Chair, Norway), Tove Lundeberg (Sweden), Yuri Tsaturov (Vice-Chair, Russia), J. Michael Kuperberg (United States), Eva Krummel (Inuit Circumpolar Council), Jannie Staffansson (Saami Council), Bob van Dijken (Arctic Athabaskan Council)

AMAP Secretariat

Lars-Otto Reiersen, Jan René Larsen, Janet Pawlak, Jon L. Fuglestad, Simon Wilson, Inger Utne

Arctic Council Member States and Permanent Participants of the Council

Canada, Kingdom of Denmark (Denmark/Greenland/Faroe Islands), Finland, Iceland, Norway, Russia, Sweden, United States, Aleut International Association (AIA), Arctic Athabaskan Council (AAC), Gwitch'in Council International (GCI), Inuit Circumpolar Council (ICC), Russian Association of Indigenous Peoples of the North (RAIPON), Saami Council

Assessment leads:

Anders Mosbech, Mickaël Lemay and Malene Simon

Editorial Committee:

Anders Mosbech, Mickaël Lemay, Malene Simon, Flemming Ravn Merkel, Tom Christensen, Rikke Becker Jacobsen, Parnuna Egede and Knud Falk

Scientific Editors:

Mickaël Lemay and Knud Falk

Authors:

Peter Aastrup, **Maria Ackrén**, Michel Allard, Philippe Archambault, Kristine Arendt, **Carl Barrette**, Simon Bélanger, Trevor Bell, Dominique Berteaux, Kevin Bjella, Lill Rastad Bjorst, **David Boertmann**, **Merete Watt Boolsen**, Heather Brooks, **Ross Brown**, **Tanya Brown**, Andrée-Sylvie Carbonneau, Diane Chaumont, **Tom Christensen**, **Christine Cuyler**, **Jackie Dawson**, Chris Derksen, Émmanuel Devred, Guy Doré, **Sharon Edmunds-Potvin**, **Knud Falk**, Steve Ferguson, Kaitlyn Finner, Niels Foged, **James Ford**, **Alastair Franke**, **Gilles Gauthier**, **Patrick Grenier**, **Emmanuel Guy**, James Hamilton, **Anne Merrild Hansen**, Gwen Healey, **Rasmus B. Hedeholm**, **Chris Hotson**, Stephen Howell, **Hayley Hung**, **Linnea Ingebrigtsen**, **Thomas Ingeman-Nielsen**, Inuit Tapiriit Kanatami, **Rikke Becker Jacobsen**, Thomas James, **Margaret Johnston**, **Berit Kaae**, Tove Lading, Melissa Lafrenière, Scott F. Lamoureux, **Peter Lang Langen**, **Frederic Lasserre**, Diane Lavoie, David Lee, **Mickaël Lemay**, **Esther Lévesque**, Francis Lévesque, Emmanuel L'Hérault, **Wendy Loya**, Sergey Marchenko, Valérie Mathon-Dufour, **Hans Meltofte**, **Flemming Ravn Merkel**, **Anders Mosbech**, Gert Mulvad, **Josephine Nymand**, Darlene O'Leary, Steffen M. Olsen, **Jean-François Pelletier**, Larissa Pizzolato, **Frank Rigét**, Mylène Riva, **Dominique Robert**, Christian B. Rodehacke, **Thierry Rodon**, **Mikael Sejr**, Martin Sharp, **Malene Simon**, Sharon L. Smith, **Chris Southcott**, Sara Statham, Martin Stendel, **Jason Stow**, Pelle Tejsner, **Clive Tesar**, Rasmus T. Tonboe, **Jean-Éric Tremblay**, Fernando Ugarte, Christina Viskum Lytken Larsen, **Fiona Walton**, **Susse Wegeberg**, Hope Weiler, George Wenzel, **Laura Wheeland**

Bold text denotes lead authors

The Executive summary was written by the assessment leads and Knud Falk, and commented by the lead authors

3.1 Climatic drivers

LEAD AUTHORS: PETER LANG LANGEN, PATRICK GRENIER, ROSS BROWN

CONTRIBUTING AUTHORS: CARL BARRETTE, DIANE CHAUMONT, CHRIS DERKSEN, JAMES HAMILTON, STEPHEN HOWELL, THOMAS INGEMAN-NIELSEN, THOMAS JAMES, DIANE LAVOIE, SERGEY MARCHENKO, STEFFEN M. OLSEN, CHRISTIAN B. RODEHACKE, MARTIN SHARP, SHARON L. SMITH, MARTIN STENDEL, RASMUS T. TONBOE

Key messages

- **The Earth's climate is warming due to anthropogenic greenhouse gas emissions, and warming will continue throughout this century.** Climate models are the central tool for constructing physically based scenarios of the future.
- **Climate models do not provide one single projection for the future but rather a range of likely outcomes.** This range arises from differences in imposed greenhouse gas emissions, model structures and processes, and outcomes of natural climate variations. For the Baffin Bay/Davis Strait (BBDS) assessment, medium- and high-emissions scenarios were used for the climate projections.
- **Continued BBDS warming is projected.** Mean near-surface winter air temperatures are projected to increase (relative to 1986–2005) by about 1 to 4°C by 2030 and 1.5 to 10°C by 2080. Summer temperatures are projected to increase by about 0.5 to 2°C by 2030 and 1 to 5°C by 2080. Projected changes tend to be largest in the northwestern part of the region. For the high-emissions scenarios, thawing-season lengths increase by about 1–2 months by the end of the century.
- **An increase in precipitation is generally projected for the BBDS region.** For winter, mean total precipitation is projected to change by about -10% to +25% by 2030 and -10% to +70 % by 2080. For summer, the projected change is about -5% to +15% by 2030 and 0% to +35% by 2080. The projected change is generally toward increasing precipitation, with the largest relative changes being in winter and over the northwestern parts of the region.
- **Mean BBDS near-surface wind speeds are projected to change within ±5% by 2030 and ±10% by 2080 for all seasons.** There is little information on projected changes in prevailing wind direction.
- **Projections of weather extremes show increases in minimum and maximum temperatures and also heavy precipitation.** Annual minimum temperatures are projected to increase by 2–6°C by 2081–2100 under medium emissions and >6°C under high emissions. Annual maximum temperatures increase somewhat less. Both quantities increase more on the Nunavut side of the region than on the Greenland side. Projections show more wet days, shorter dry spells, and more precipitation during very wet days.
- **Projections of snow-cover duration for the late 21st century show a decrease of approximately 40–60 days, mainly due to later snow onset.** Reductions are most pronounced in coastal regions. The results are quite sensitive to imposed emissions—e.g., with stabilization after decline under medium emissions and accelerating decreases under high emissions. Large reductions in May–October snowpack are projected.
- **BBDS permafrost is projected to warm the most in the region's coldest areas and to thaw considerably in the warmest areas.** Ellesmere Island is an example of a cold area that is projected to experience pronounced permafrost warming. Southwestern Greenland is an example of a relatively warm area that is projected to experience pronounced permafrost thawing.
- **The Greenland Ice Sheet is projected to lose mass during the 21st century, with the primary mechanisms being increased freshwater runoff (up to a doubling or tripling) and glacier calving.** Year-to-year variability in freshwater runoff is projected to increase. The Canadian Arctic glaciers and ice caps are similarly projected to lose mass due to increased runoff.
- **Projections for lake ice in 2050 indicate a 10–15 day earlier break-up and a 5–10 day later freeze-up, with a 10–30 cm decrease in maximum ice thickness.** Lake-ice response to warming is influenced by lake morphology (size and depth) and local changes in snow accumulation.
- **Freshening and warming of the Baffin Bay surface layer (about 0.2°C per decade over the next 50 years) is projected under the high-emissions scenario.** Models project an increased inflow of warm Atlantic-origin water into the bay, a decrease of cold Arctic water flow through the Canadian Arctic Archipelago, and an intensification of the Baffin Bay counterclockwise circulation. The duration of ice bridges in Nares Strait, and thus the duration of the North Water Polynya, will likely decrease.
- **Climate models project the largest decreases in sea ice cover to occur in the autumn (15–20% reduction by 2080) due to later freeze-up, with smaller decreases in the spring (10–15% reduction) due to earlier ice break-up.** Winter ice thickness is projected to decrease by about 20–30 cm, with the largest decreases in more northerly regions. The timing of the changes varies considerably across models. For the foreseeable future, multi-year ice is likely to remain a hazard for shipping in the Canadian Arctic Archipelago.
- **Relative sea level in the BBDS region is projected to fall at nearly all locations, due mainly to crustal uplift in response to past and projected ice mass decreases.** For the year 2100 in the high-emissions scenario, projected median relative sea-level changes across the region range from approximately -90 cm to +10 cm.

Introduction

The climate of the BBDS region is undergoing a period of rapid change linked to global warming (Overland et al., 2017) and natural climate variability (Way and Viau, 2014). The increase in atmospheric concentrations of greenhouse gases is significantly affecting the climate of the region, which in turn drives changes in ecosystem services and the populations that rely on these services (see AMAP, 2017b, and Chapter 6 of this report in particular). Climatic drivers are dealt with in this subchapter, which discusses aspects of ongoing and projected climate change relevant for the BBDS region. Section 3.1.1 consists of a general discussion of changes in the global climate system, explaining how such knowledge is obtained and how it must be interpreted. Sections 3.1.2 through 3.1.6 discuss changes taking place specifically in the BBDS region, with each section discussing trends of the recent past, as well as future scenarios for the atmosphere, terrestrial cryosphere, ocean, sea ice, and sea level. The climatic components are discussed separately for convenience, but they are closely interconnected (Hinzman et al., 2013; Overland et al., 2017).

The main role of this subchapter is to provide a synthesis of published information on observed and projected climate change over the BBDS region. However, the authors recognize that traditional and local knowledge (TK) is an important complement to the larger-scale portrait provided in the scientific literature: TK provides the link between large-scale climate change and local impacts. One of the challenges of incorporating TK into scientific assessments is that the observations are anecdotal, are fragmentary in time and space, and are usually not published in citable literature. However, efforts to consolidate TK across Arctic communities reveal a fairly consistent picture of some of the most important climate and environmental changes affecting local communities. From the Gaden and Stern (2015) compilation of traditional climate and environmental observations made by Inuit in the western and central Canadian Arctic, the changes most consistently reported across the 12 communities were the following: warmer summers and/or more extreme warm summer temperatures, more variable and unpredictable weather, a longer ice-free season, thinner ice, earlier snow melt, lower freshwater levels, and the presence of new plant/animal/insect species. These observations are the local footprint of the large-scale climate changes documented in this subchapter.

Reliable information about the future evolution of climate is needed by decision-makers for a wide range of applications (Mote et al., 2011; Huard et al., 2014). The process of providing this information requires a detailed understanding of local needs and the climate sensitivities contained, for instance, in TK, which is difficult to incorporate into decision-making processes (Cuerrier et al., 2015). Making this connection is beyond the scope of this subchapter; the aim here is to present the larger-scale changes in regional climate as documented in the published literature. However, it should be noted that Cuerrier et al. (2015) propose a novel mix of qualitative and quantitative methods to translate TK into evidence for decision-making and for developing environmental policy.

3.1.1 Global and Arctic climate change

The vast majority of climate scientists agree that human activities have put Earth's climate on a warming path (Oreskes, 2004; Cook et al., 2013; IPCC, 2013a), which is amplified in the Arctic by various processes (Pithan and Mauritsen, 2014; Barnes and Polvani, 2015; Overland et al., 2017). This section briefly explains the scientific background on global warming and provides information on the limitations and interpretation of climate scenarios. The processes responsible for Arctic amplification are presented in the supplementary material for this subchapter (Langen et al., 2016).

3.1.1.1 Climate change scenarios

The Earth's climate is warming due to anthropogenic greenhouse gas emissions, and this warming will continue throughout this century. Climate models are the central tool for constructing physically based scenarios of the future.

A steady global climate is the result of an equilibrium between Earth's energy input (solar radiation) and output (infrared radiation). Because greenhouse gases (e.g., carbon dioxide, methane) and aerosol particles (e.g., sulfates, black carbon) affect these radiative fluxes (Arrhenius, 1896; Twomey, 1977; Blanchet and List, 1983), the climate system responds to modifications in the atmospheric concentrations of these constituents. Basically, greenhouse gases (GHGs) absorb a part of the infrared radiation that would normally escape to space, and then reemit it back toward the Earth's surface, resulting in a warming effect. Anthropogenic aerosols have a variety of effects, summing up to a cooling that is insufficient to compensate for the anthropogenic GHG warming. The amplitude of the net response has been assessed with detailed, physically based models, and the results show that human GHG emissions have forced the climate toward a warmer state. Moreover, it is practically certain that this warming process will continue throughout this century and into the next one, at a rate that depends on both past and future emissions (IPCC, 2013a).

Here, we operate with the concept of a *climate scenario*, which is, in essence, one plausible trajectory for one or more climate variables, among many other plausible trajectories. Although there are a number of methods for constructing scenarios (see Mearns et al., 2001, for a discussion of the various methods and their advantages and disadvantages), climate models remain the central tool for scenario construction. These models provide a large ensemble of physically based, plausible responses to the increasing concentrations of greenhouse gases in the atmosphere. Climate model-based scenarios assume external forcings, such as an anthropogenic emissions scenario, as well as a certain level of solar and volcanic activity. The output may take the form of a time series (e.g., one value for the average temperature at Nuuk, Greenland, for each day from here to 2100) or of a climatic change (e.g., the percent change in mean annual total precipitation over Baffin Island between the 1986–2005 reference period and the 2081–2100 future period). As emphasized next, a climate scenario cannot be interpreted as a prediction, and a large ensemble of different scenarios is necessary for developing robust adaptation plans (Charron, 2014).

3.1.1.2 Limitations and interpretation

Climate models do not provide one single projection for the future but rather a range of likely outcomes. This range in climate projections arises from differences in imposed greenhouse gas emissions, different model structures and processes, and different outcomes of natural climate variations. For the Baffin Bay/Davis Strait assessment, climate model projections were used for two scenarios: medium emissions and high emissions.

Considerable progress has been made over the past 30 years in climate modeling. However, this progress does not allow scientists to *predict* the exact future climatic trajectory, because of at least three important sources of uncertainty (Rowell, 2006; Hawkins and Sutton, 2009): (1) uncertainty in future human (and natural) forcings, (2) imperfections in the models' formulations of the physical, chemical, and biological processes that determine the climate, and (3) natural variability in the climate system. The first point refers mainly to the fact that future decisions related to GHG emissions (and land use) cannot be foretold exactly. The second point refers to the fact that different models indicate different responses to assumed external forcings: no single best model can be identified, since each one has its own strengths and weaknesses in representing the climate system. Finally, the third point refers to interannual and interdecadal variations that superimpose on the long-term warming signal. In brief, there exist many plausible combinations of anthropogenic emissions scenarios, model formulations, and natural variability phenomena – which implies many plausible climate scenarios.

The emissions scenarios called “RCP4.5” and “RCP8.5” (van Vuuren et al., 2011) have been adopted as plausible lower and upper bounds for future emissions pathways for this report (“RCPs” refer to representative concentration pathways but are discussed here in terms of emissions, for convenience.). This adoption follows a recommendation to standardize scenarios across the Snow, Water, Ice and Permafrost in the Arctic (SWIPA) report (AMAP, 2017b) and the Adaptation Actions for a Changing Arctic (AACAA) reports. The low-emissions RCP2.6 scenario was not considered (this scenario requires drastic reductions in carbon dioxide emissions); the RCP6.0 scenario is covered by the spread between RCP4.5 and RCP8.5. The model outputs used are representative of the large ensemble of simulations from the Coupled Modeling Intercomparison Project Phase 5 (CMIP5; Taylor et al., 2011), which was used by the Intergovernmental Panel on Climate Change (IPCC) for its fifth assessment report (AR5), published in 2013 (IPCC, 2013a).

Due to computing limitations, global climate model simulations are currently produced at horizontal and vertical resolutions of approximately 100–300 km and 1 km, respectively (the atmosphere's horizontal scale is much greater than its thickness). Processes occurring at a finer scale – such as wind channeling effects in fjords (Maxwell, 1981; Seidel, 1987) and katabatic “piteraq” events (Moore et al., 2015) – cannot be fully represented, which limits the direct utility of such model simulations for many local applications. Various downscaling techniques have been developed to overcome this limitation and produce meaningful local scenarios (Maraun et al., 2010; Hewitson et al., 2014).

It is important to emphasize that climate scenarios inform on what *could happen* on Earth and not what *will happen*. To account for the various plausible responses, climate scenarios may be presented, for example, as confidence intervals or as probabilities of occurrence (Kandlikar et al., 2005). Scenarios presented as multi-model averages have the advantage of synthesizing a vast amount of information. However, these types of scenarios must be interpreted carefully because the averaging procedure smooths out natural variability and between-model variability. A future change represented by a multi-model average often represents a fairly likely outcome among many others, and its sign is generally that of the majority of the models. However, multi-model averages are often misinterpreted as “robust predictions.” Finally, spatial averages over the entire BBDS domain may mask geographical differences.

The following climate projections are generally based on multi-model assessments for the entire BBDS region. In addition to this set of assessments, the Danish Meteorological Institute (DMI) has prepared a series of reports specifically for Greenland, based on downscaling with the DMI climate model system (Christensen et al., 2015). However, because the DMI work relies on a single regional model and a single driving global model and because it covers only a portion of the BBDS region, the DMI results will be used only occasionally throughout the following discussion. The full reports (in Danish) may be downloaded from the DMI website (DMI Scientific Report 15-04, www.dmi.dk/laer-om/generelt/dmi-publikationer/videnskabelige-rapporter/).

3.1.2 Atmosphere

In this section, scenarios are presented for 21st-century changes (relative to the reference period 1986–2005) in near-surface air temperature, precipitation, and wind speed. Expectations related to meteorological extremes are also discussed. The figures represent new calculations that are based on published CMIP5 model results but are specific to the BBDS region (see land and sea boundaries in Figure 2.1). The results are discussed in light of other recent results published in the scientific literature.

3.1.2.1 Temperature

Continued warming is projected for the BBDS region. Mean near-surface winter air temperatures are projected to increase by about 1 to 4°C by 2030 and 1.5 to 10°C by 2080 (relative to 1986–2005). Summer temperatures are projected to increase by about 0.5 to 2°C by 2030 and 1 to 5°C by 2080. Projected changes tend to be largest in the northwestern part of the region and smallest in the southeast. For the high-emissions scenarios, thawing-season lengths increase by about 1–2 months by the end of the century.

Observed trends

Air temperature data from climate stations in the region indicate a slight cooling from 1950 to about the mid-1990s; at that time, a period of rapid warming began, culminating with 2010 as likely the warmest annual mean temperature in the instrumental record. Annual mean near-surface air temperatures in the

region warmed at rates of approximately 1°C per decade over this period (Brown et al., 2018), with the greatest warming occurring over more northerly areas (Hamilton and Wu, 2013). The spatial pattern of this recent warming is characterized by a maximum over the eastern Canadian Arctic, with the seasonal pattern showing the greatest warming in the autumn and early winter period (Rapaić et al., 2015). Near-surface air temperatures indicate regional cooling since 2010, mainly in the winter. This cooling is consistent with a return to more positive values of the North Atlantic Oscillation, which exhibited large negative anomalies in 2010.

Projected changes

In this subsection, temperature-change scenarios based on the CMIP5 ensemble are presented and discussed. A particular focus is placed on natural variability – namely, the year-to-year and decade-to-decade fluctuations that cause the climate to vary around the long-term warming trajectory.

During the current century, average near-surface air temperatures in the BBDS region are expected to increase, with a very high likelihood. However, the magnitude of this warming cannot be exactly predicted due to the reasons stated above, in the discussion of model limitations and interpretation. Figure 3.1 shows the evolution of observed warming (black lines) and projected warming (colored envelopes) for the BBDS region for each season (land area only). Observed interannual variability is much larger in winter than in the other three seasons. The green and red bands summarize the 20-year moving averages of regionally averaged temperature projections from 95 CMIP5 simulations (56 and 39 simulations for the RCP4.5 and RCP8.5 emissions scenarios, respectively). The simulation results show that much larger warming is expected for winter than for the other seasons. At approximately 2035, the RCP4.5 and RCP8.5 envelopes start diverging. Over time, each envelope widens, reflecting model-related uncertainty (primarily) and natural variability (secondarily) (Hawkins and Sutton, 2009).

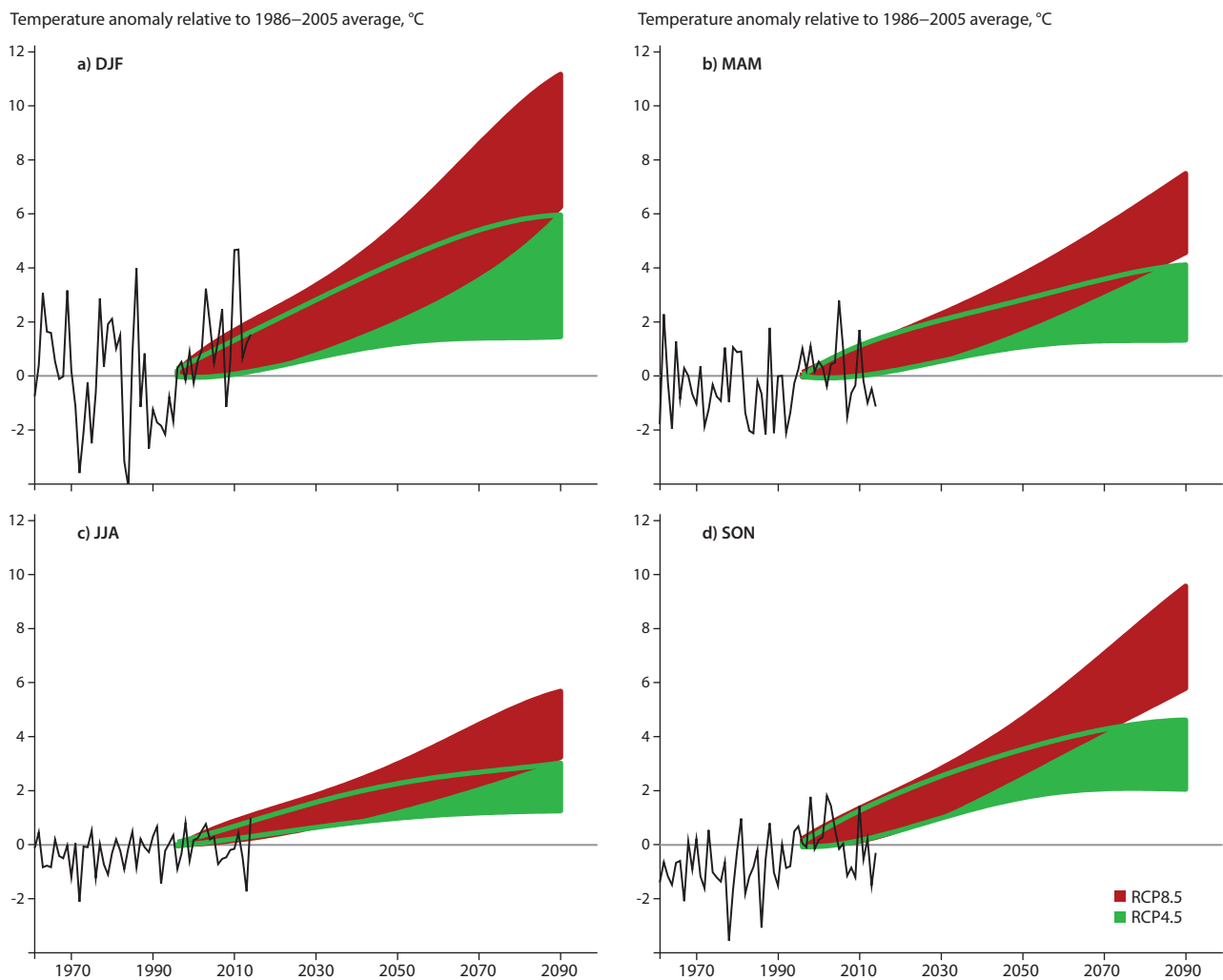


Figure 3.1 Observed and projected anomalies in 2-meter air temperature averaged over the land portion of the BBDS region, relative to the 1986–2005 average. The black lines represent observations (specifically, the CRU TS 3.23 tmp observational product) (Harris et al., 2014). The colored envelopes represent the likely evolution of the 20-year averages up to 2090 under the RCP4.5 (green) and RCP8.5 (red) emissions scenarios, based on CMIP5 simulations for (a) winter (December-January-February, DJF), (b) spring (March-April-May, MAM), (c) summer (June-July-August, JJA), and (d) autumn (September-October-November, SON). The CRU data are presented up to 2014. Average anomalies for each simulation are first calculated for each year and then averaged over 20-year blocks from 1986–2005 (attributed here to the year 1996) through 2080–2099 (attributed to 2090). For each attribution year, the 10th and 90th percentiles among the simulations are next calculated; fourth-order fits on these two percentile times series define the envelope boundaries.

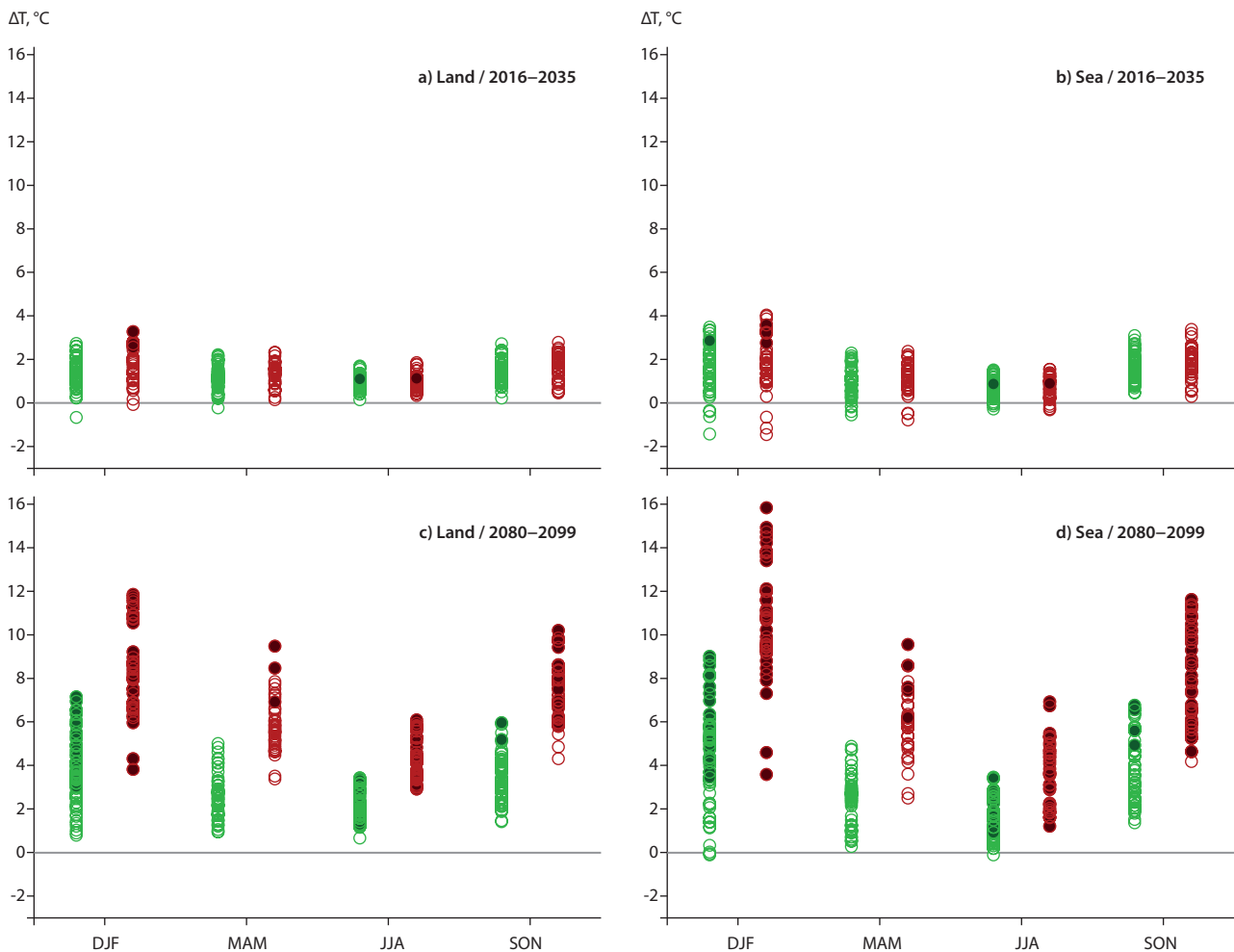


Figure 3.2 Average 2-meter air temperature anomalies (ΔT) relative to 1986–2005 for the BBDS region: (a) land areas for 2025 (2016–2035), (b) sea areas for 2025, (c) land areas for 2090 (2080–2099), and (d) sea areas for 2090. Each circle represents one simulation. A filled circle indicates that the anomaly is larger than the 1986–2005 standard deviation in that same simulation. A total of 95 CMIP5 simulations are used: 56 for RCP4.5 (green) and 39 for RCP8.5 (red).

The expected amount of warming can also be presented as intervals (Figure 3.2). The model results show that a few simulations project negative temperature anomalies for 2016–2035, whereas for 2081–2099 such cases are rare (only for RCP4.5 and only over the sea). The inter-simulation spread in anomalies is larger over sea than over land. Anomaly results for minimum and maximum daily temperature (not shown) are similar to those for average temperature (Figure 3.2).

The spatial pattern of projected temperature change is shown in Figure 3.3, in terms of the 25th, 50th and 75th percentiles for annual mean air temperature. This way of visualizing the spread in the range of changes projected by the climate model ensemble is recognized by the IPCC as “*a simple, albeit imperfect, guide to the range of possible futures (including the effect of natural variability)*” (IPCC, 2013b, p. 1313). (See also the introductory discussion above, regarding limitations and interpretation of climate models.) Overall, the projected warming shows a gradient of greatest warming toward the northwest. This pattern is associated with general Arctic amplification and the gradual disappearance of sea ice in the region. The corresponding seasonal maps for winter and summer reveal similar patterns but with larger amplitudes during winter (see Langen et al., 2016). Although large-scale

patterns emerge in these figures from the model ensemble, it is important to note that the actual climate evolution may turn out to have a significantly different pattern (just as with any single model version) (Deser et al., 2014).

Due to natural variability, which occurs at various timescales, temperatures are not expected to change as smoothly as depicted in the multi-model averages. Natural variability is strong enough that temporary local cooling trends, with durations of up to 25 years or more, can be expected with significant probabilities (Grenier et al., 2015). Figure 3.4 illustrates these concepts by presenting three plausible RCP8.5-based climate scenarios for winter temperature at Clyde River (Baffin Island, Nunavut) over 2011–2035 (following observations over 1962–2010). Each scenario (a, b, and c) is based on a different global climate model (GCM). Successive 15-year trends are represented by the red (warming) and blue (cooling) lines. The FIO-ESM scenario (Figure 3.4a) presents a marked cooling phase centered on ~2020, with average winter temperatures around 2030 being no different than what has been observed in the past. The MIROC-ESM scenario (Figure 3.4b) also presents a temporary cooling centered on 2020, followed by pronounced warming. The GFDL-CM3 scenario, on the other hand, continues the sustained warming observed during 1990–2010 (Figure 3.4c).

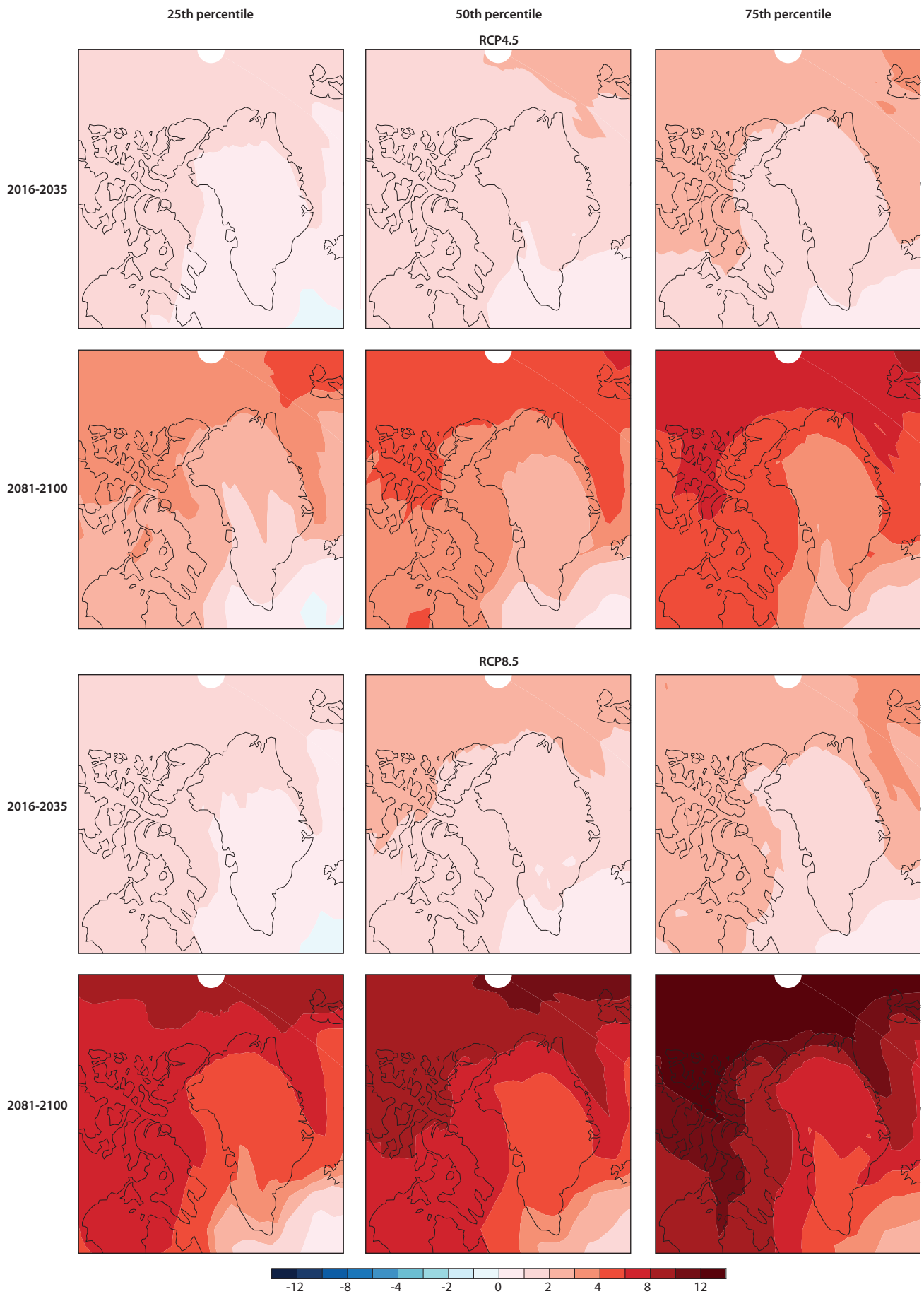


Figure 3.3 Changes in annual mean near-surface air temperature (°C) for RCP4.5 and RCP8.5 for the time periods 2016–2035 and 2081–2100 (relative to 1986–2005): 25th, 50th, and 75th percentiles. The 50th percentile corresponds to the median value, and the 25th and 75th percentiles correspond to the values dividing the distribution of projected changes into the coldest 25% and warmest 25% of models, respectively. (Data source: IPCC, 2013b.)

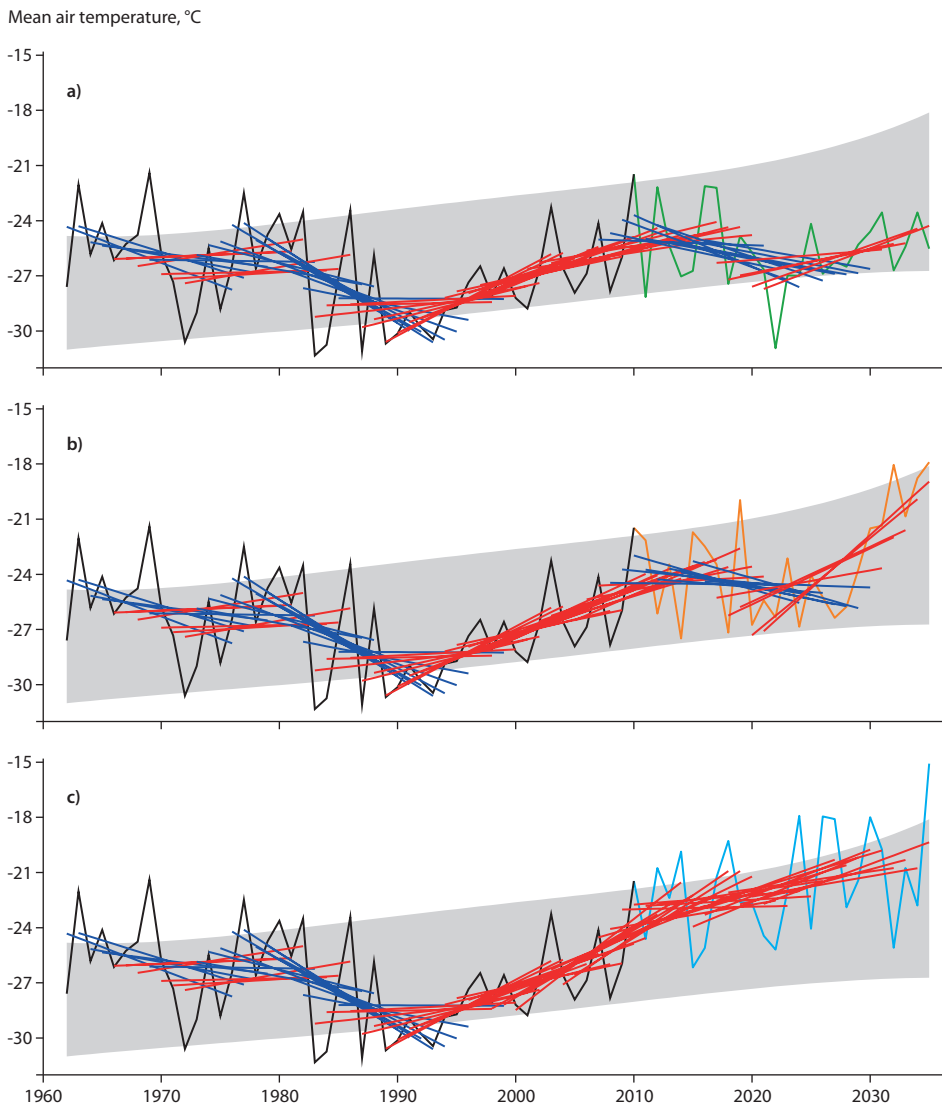


Figure 3.4 Selected winter climate scenarios for Clyde River in Nunavut (70°28'26" N, 68°35'10" W), based on the r11ip1 member of the RCP8.5 experiment performed with the following global climate models: (a) FIO-ESM (green), (b) MIROC-ESM (orange), and (c) GFDL-CM3 (cyan). Gridded (10×10 km) data from Natural Resources Canada (Hopkinson et al., 2011) are used as observations over 1962–2010 (black line). Climate scenarios over 2011–2035 are obtained by statistically adjusting the simulations with a procedure termed quantile mapping (Grenier et al., 2015). Linear trends over 15-year segments are represented in red when positive and blue when negative. The gray envelope represents the time-smoothed 10th and 90th percentiles for yearly values in an ensemble of 15 RCP8.5-based climate scenarios (comprising the three presented here).

With changing annual and seasonal average temperatures, many temperature-derived climate indicators are also projected to change. For example, the Arctic summer length (defined here as the time between melt onset in spring and freeze onset in autumn) is projected by the CMIP5 RCP8.5-based simulations to increase by ~40 days over land and ~80 days over sea ice during the 21st century, with substantial differences among models (Mortin et al., 2014). Sillmann et al. (2013b) report consistent decreases in the number of frost days between the time periods 1981–2000 and 2081–2100, with decreases varying across the domain (land only) by about 0 to 30 days under RCP4.5 and about 5 to 70 days under RCP8.5. For Greenland, Christensen et al. (2015) found thawing season increases of approximately 45 days by 2081–2100 for RCP8.5 (~15 days for RCP4.5), using the HIRHAM5/EC-Earth climate model at 5 km resolution. Other indicators, such as the frequency of freeze–thaw cycles, could change monthly but not necessarily annually, as reported for other northern regions such as Nunavik and Nunatsiavut (Allard and Lemay, 2012). For Greenland, results from the HIRHAM5 model showed marked regional differences but an overall increase in the number of freeze–thaw cycles with projected warming (Christensen et al., 2015). Analysis of the frequency of winter thaw days over Baffin Island showed only small increases projected for 2050 (Barrette, 2013).

3.1.2.2 Precipitation

An increase in precipitation is generally projected for the BBDS region. For winter, mean total precipitation (liquid and solid) is projected to change by about -10% to +25% by 2030 and -10% to +70% by 2080 (relative to 1986–2005). For summer, total precipitation is projected to change by about -5% to +15% by 2030 and 0% to +35% by 2080. The projected change is generally toward an increase in precipitation, with the largest relative changes being in winter and over the northwestern parts of the region.

Observed trends

Estimating trends in precipitation over the BBDS region is a particular challenge, for a number of reasons: precipitation is notoriously difficult to measure in Arctic environments, the surface station network is sparse and biased to coastal locations, there is strong interannual variability in precipitation time series, data sets are rarely homogeneous, and satellite sources do not always provide long enough periods of data for reliable trend analysis. Nevertheless, Mernild et al. (2014) analyzed trends in Greenland precipitation data (derived from coastal meteorological stations and ice cores) for various 30-year periods during

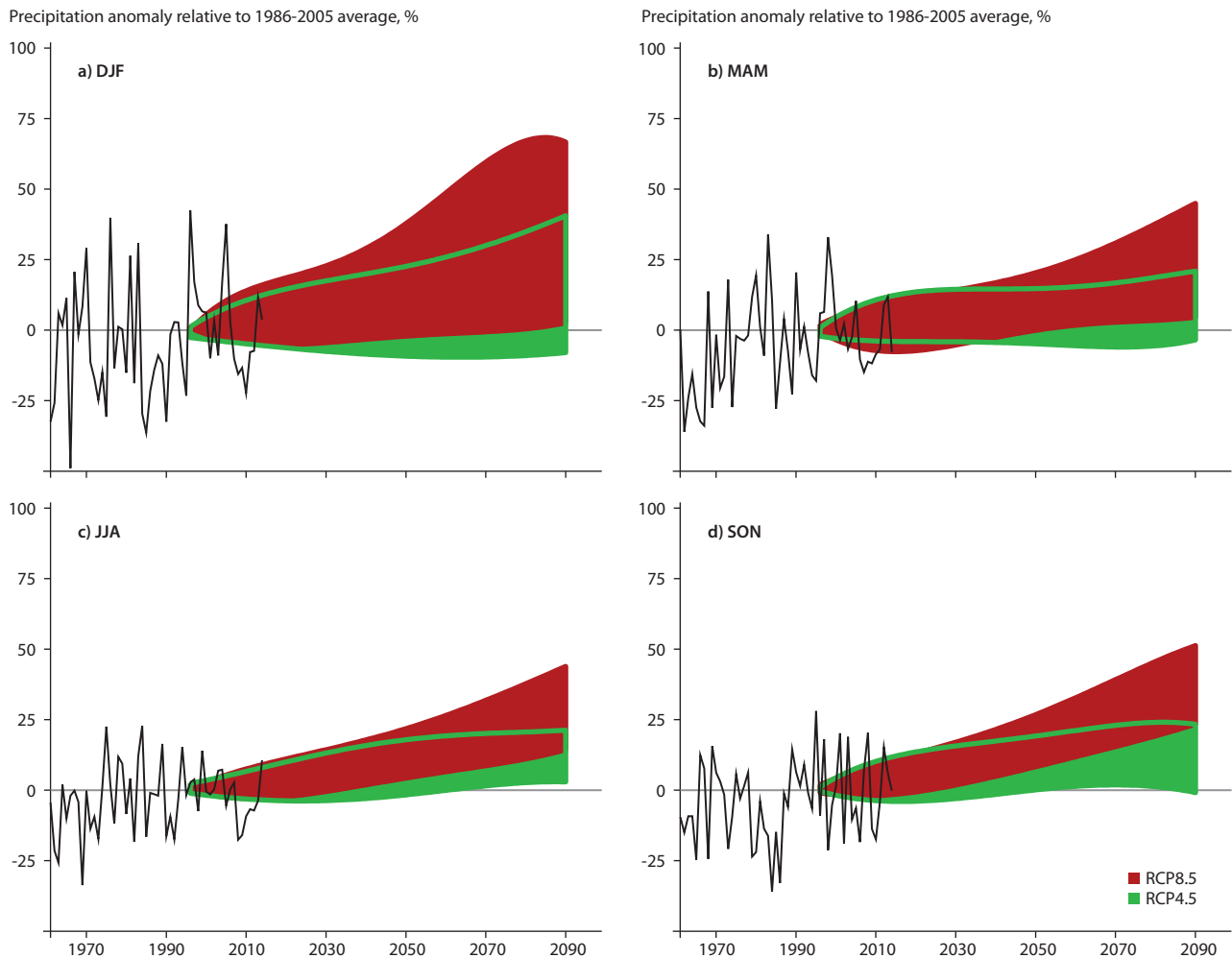


Figure 3.5 Same as Figure 3.1, but for anomalies in total (liquid and solid) precipitation. Changes are expressed as percentage differences with respect to the 1986–2005 average. The observational product is CRU TS 3.23 (pre), and the simulations are the same as those used for Figure 3.1.

1890–2012. While statistically significant trends were found, the results were spatially heterogeneous with both increasing and decreasing precipitation trends, even for sites a relatively short distance apart. None of the analyzed normal periods exhibited large-scale simultaneous agreement on positive or negative precipitation trends. Analysis of adjusted climate station precipitation data over the Canadian sector of the BBDS region from Mekis and Vincent (2011) shows evidence of statistically significant increases in precipitation over the 1950–2010 period: 5% per decade for rainfall and 3% per decade for snowfall (Brown et al., 2018). However, Rapačić et al. (2015) found that trends computed using the adjusted Mekis and Vincent (2011) station data were about two times larger than those obtained from a multi-data set estimate. They concluded that while there was strong evidence of long-term increases in precipitation over the Canadian Arctic, there were large uncertainties in the magnitude of the change. Hamilton and Wu (2013) reported a statistically significant trend of about +10 mm per decade from the 60-year precipitation record at Alert. The observed long-term increases in precipitation over the region are a response to both warming (warmer air can hold more water vapor) and loss of sea ice (Kopec et al., 2016; Thomas et al., 2016).

Projected changes

Precipitation is expected to increase over the BBDS region in response to warming and reductions in sea ice cover (Kattsov et al., 2007; Zhang et al., 2012; Bintanja and Selten, 2014; Kopec et al., 2016; Thomas et al., 2016). However, the climate change signal for precipitation is less marked than for air temperature.

Figure 3.5 shows the projected range in precipitation changes for the BBDS region (land only). The range of the RCP4.5 scenarios (green) is consistent with no change for some seasons. As with temperature, recent past interannual variability, as well as the range of future changes, is much larger in winter than in summer. RCP-related uncertainty becomes considerable around 2050, and both envelopes show ranges that widen with time due to model-related uncertainty and natural variability. It must be stressed that large relative changes can occur with small absolute changes for areas of the High Arctic where total precipitation amounts are low – e.g., the mean annual precipitation is only about 200 mm at Resolute in the Northwest Territories (Mekis and Vincent, 2011). Projections for changes in other variables of the atmospheric branch of the water cycle are discussed in the supplementary materials provided for this subchapter (Langen et al., 2016).

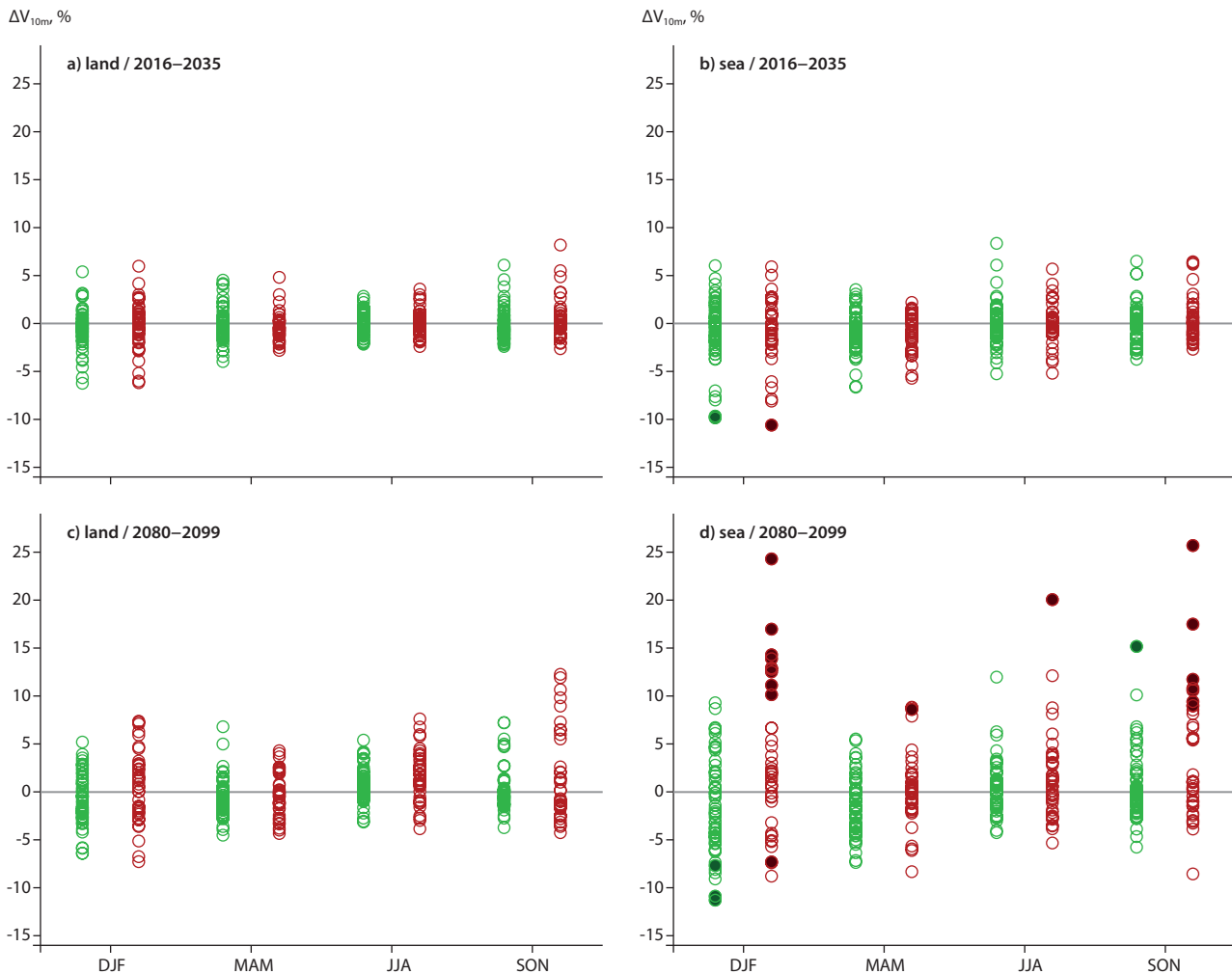


Figure 3.6 Same as Figure 3.2, but for anomalies in mean wind speed (ΔV_{10m}), expressed as percentage differences with respect to the 1986–2005 average.

3.1.2.3 Wind

Mean BBDS near-surface wind speeds are projected to change within $\pm 5\%$ by 2030 and $\pm 10\%$ by 2080 for all seasons. There is little information on projected changes in prevailing wind direction.

Observed trends

It is difficult to reach clear conclusions about wind-speed trends in the BBDS region. Trend analysis of surface wind speed observations is complicated by strong interannual variability and by the sensitivity of these observations to instrumentation (anemometer type and height) as well as the location and exposure of the observing site. There are relatively few studies of trends in wind speeds in the BBDS region. Wan et al. (2010) presented wind speed trend analysis results for homogenized wind speed records at a number of Canadian stations in the BBDS region over the period 1953–2006. The results show increasing wind speeds at Alert and Resolute but decreases at stations on Baffin Island. The observed increase in annual mean wind speed at Alert over the 1954–2011 period was $+0.33$ m/s per decade (Hamilton and Wu, 2013). Trends in geostrophic winds (the wind speed derived from surface pressure observations) indicate decreasing wind speeds over most of the BBDS region

(Wan et al., 2010). Stopa et al. (2016) report increasing over-water wind speeds in Baffin Bay for the recent 1992–2014 period (from the Climate Forecast System reanalysis).

Projected changes

During the current century, average near-surface wind speeds in the BBDS region are likely to remain close to the reference value. There are relatively few studies of projected changes in wind direction (e.g., McInnes et al., 2011; Gorter et al., 2014), and this aspect is not further discussed here.

Dynamical phenomena involved in future wind regime and storm activity changes are complex, not fully understood, and some of their effects work in opposite directions (Bengtsson et al., 2006; Harvey et al., 2013; Gorter et al., 2014). Hence, the sign of the sum (net) impact on surface winds at the scale of relatively small regions, such as the BBDS, is not consistent from one model to another. This inconsistency means that weak, positive, and negative 21st century changes all represent plausible outcomes. Figure 3.6 shows near-surface (10-meter) 20-year average wind speed anomalies relative to the period 1986–2005 for a large ensemble of CMIP5 simulations. This figure suggests that adaptation plans should consider $\pm 5\%$ changes in mean wind speed for the period 2016–2035 and $\pm 10\%$ changes for 2080–2099.

Examples of CMIP5 global models that project positive trends in surface wind speeds include EC-Earth; indeed, Dobrynin et al. (2012) find increases on the order of 0–10% over the maritime portion of the BBDS region from the mid-19th century to the end of the 21st century (with RCP4.5 and RCP8.5 emissions scenarios). Using an ensemble of CMIP3 models, McInnes et al. (2011) also obtained no consensus among models regarding the sign of the signal in mean wind speed over the BBDS region from 1981–2000 to 2081–2100. However, for some maritime parts of the BBDS region, at least two-thirds of the CMIP3 simulations do agree on a 0–10% reduction in winter wind speed.

3.1.2.4 Extreme events

Projections of weather extremes for the BBDS region show an increase in annual minimum and maximum temperatures and an increase in heavy precipitation. Annual minimum temperatures are projected to increase by 2–6°C in the medium-emissions scenarios and more than 6°C in the high-emissions scenarios by 2081–2100, relative to 1981–2000. Annual maximum temperatures increase somewhat less. Both quantities increase more on the Nunavut side of the region than on the Greenland side. Projections show large (40–150%) increases in the amount of precipitation during very wet days, as well as increases in the number of wet days and decreases in the length of dry spells. Projected changes in extreme winds have different signs across the region.

In climatology, an *extreme event* is the occurrence of a value near the lower or upper range of the distribution of all observed values (IPCC, 2012). Because extreme events occur only rarely, their frequency in observational records may not be representative of their true probability of occurrence, and theoretical assumptions must compensate for the small sample size (Coles, 2001; Katz, 2013). This consideration poses an additional difficulty for obtaining reliable scenarios for the distribution extremes (Wehner, 2013), whose climatic change is not necessarily the same as that of the distribution mean (Kunkel, 2003; Katz, 2010). Extreme atmospheric events manifest in different forms, and each application requires specific indicators. Several global studies have focused on indices for extreme temperature and precipitation, discussing observed recent trends (e.g., Alexander et al., 2006), the performance of global models during the recent past (e.g., Sillmann et al., 2013a), and model projections for the 21st century (e.g., Tebaldi et al., 2006; Orłowsky and Seneviratne, 2012). Extreme winds have been investigated somewhat less.

Observed trends

Analysis of surface stations (Peterson et al., 2008; Donat et al., 2013; Wang et al., 2014) shows the BBDS region following trends similar to those of the rest of the Arctic – toward significant warming of temperature-extreme indices, particularly for indices based on daily minimum temperatures. Matthes et al. (2015) find most of the BBDS experiencing significant increases (decreases) in the duration of winter warm (cold) spells over the 1979–2013 period (in the ERA-Interim reanalysis). Trends in precipitation extremes vary greatly among stations; hence there

is no clear regional pattern of change in extreme-precipitation indices over the region.

Projected changes

An analysis of CMIP5 simulations by Sillmann et al. (2013b) indicates that over the BBDS region (land only), between 1981–2000 and 2081–2100, the multi-model median of the average annual minimum temperature (index “TNn”) changes by about +2 to +6°C under RCP4.5 and by more than +6°C under RCP8.5. For the multi-model median of the average annual maximum temperature (“TXx”), the projected changes are about +0 to +4°C under RCP4.5 and +1 to +7°C under RCP8.5 (the ranges represent differences across the region). For both TNn and TXx, increases are larger on the Canadian side than on the Greenland side of the region. On a seasonal basis, increases in TNn are more pronounced for winter than summer. Sillmann et al. (2013b) also report decreases in cold spell duration indices and increases in warm spell duration indices. Regarding precipitation extremes over the BBDS region (land only), their study indicates that the multi-model median of the annual amount of precipitation falling during very wet days (index “R95p”) changes between about +40% and +100% under RCP4.5 and between +70% and +150% under RCP8.5. Also, the multi-model median of the annual number of days with precipitation above 10 mm (“R10mm”) increases by 0.5 to 4 days (RCP4.5) and by 0.5 to 10 days (RCP8.5), whereas the multi-model median of the length of the longest dry-day sequence (“CCD”) decreases by about 1 to 10 days (under both RCP4.5 and RCP8.5). For the CCD index, these results are not statistically significant over southern Greenland.

Only a few studies examine future wind extremes for the BBDS region. Using an ensemble of scenarios based on eight CMIP3 global climate models, Cheng et al. (2014) found that the annual number of hours with wind-gust speeds exceeding specific thresholds (28, 40, 70, and 90 km/h) is likely to increase at Resolute, Nunavut. The percentage increases are approximately 5–85% for 2046–2065 and approximately 15–170% for 2081–2100 (reference period 1994–2009; higher percentage increases associated with higher gust thresholds). Seasonal results for the 70 km/h threshold in 2081–2100 indicate a larger percentage increase in summer than in other seasons, partly due to lower summer values during the reference period. Wind-gust scenarios from Cheng et al. (2014) also indicate increases at Eureka, Pond Inlet, Clyde River, Hall Beach, and Iqaluit, though not in all seasons (a decrease is projected for Hall Beach in winter). Assuming that 850 hPa winds co-vary with near-surface winds, the results from Gastineau and Soden (2009) indicate geographical differences in 21st century changes in the annual frequency of extreme daily winds: a decrease over Davis Strait, an increase over the Canadian archipelago, and a relatively weak change over Baffin Bay. No equivalent multi-model results have been found for the Greenland side.

It is important to note that the reliability of scenarios for precipitation and wind extremes is tightly connected with the ability to model cyclones (McCabe et al., 2001; Pfahl and Wernli, 2012). In the BBDS region, these storms often enter from the south (Maxwell, 1981). Evaluating the cyclone climatologies of

climate models in this region is a challenge because estimates of the relative frequency of cyclones vary widely depending on which study periods, reanalysis data sets, and storm tracking algorithms are used (e.g., Zhang et al., 2004; Serreze and Barry, 2005; Vavrus, 2013; Tilinina et al., 2014). Models are found to perform well at capturing the spatial pattern and seasonal variations in cyclone frequency but with large between-model differences in the numbers of cyclones (Vavrus, 2013; Zappa et al., 2013). Topographically driven wind extremes, such as the katabatic piteraq events of southern Greenland, require high-resolution models (Moore et al., 2015) and cannot be represented in global climate models.

3.1.3 Terrestrial cryosphere

3.1.3.1 Snow

Projections of snow-cover duration for the end of the 21st century show a decrease of approximately 40–60 days. This change is mainly due to later snow onset, with reductions being most pronounced in coastal regions. The results are quite sensitive to the imposed emissions scenario – e.g., with stabilization by 2100 under the medium-emissions scenario and with accelerating decreases under the high-emissions scenario. Annual maximum snow depth shows little response to warming, but for the May–October period, large relative reductions in snowpack are projected.

Seasonal snow is present over most of the BBDS region from early October to mid-June, with permanent or semipermanent snow cover over higher elevations. Changes in snow cover timing and amount have important implications for living and non-living resources (see Chapters 6 and 7; Bokhorst et al., 2016; Brown et al., 2017). Such changes also influence the Arctic climate system and cryosphere due to the reflective and insulating properties of snow. For example, the timing and amount of snow accumulation on sea ice is an important

control on ice cover formation and growth (Barber et al., 2017). Snow accumulation varies considerably in space and time, with several variables exerting strong influences on maximum snow accumulation at regional to local scales: proximity to moisture sources, elevation, surface topography (exposure to wind), and prevailing vegetation. The regional patterns of snow cover duration (SCD) and of mean annual maximum snow accumulation (Figure 3.7) highlight the strong coastal gradients in snow cover around Baffin Bay.

Observed trends

The longest available satellite-based information for estimating trends in annual snow cover duration over the BBDS region is the U.S. National Oceanic and Atmospheric Administration (NOAA) climate data record (Estilow et al., 2015), with complete data since 1972. The utility of this data set is limited by its coarse resolution (190.5 km) and an absence of information over Greenland. However, the regionally averaged annual SCD series from NOAA agrees well with estimates obtained from in situ observations over the Canadian side of the BBDS (see Langen et al., 2016). The two series combined provide evidence of a decrease of approximately 3 weeks in the duration of snow on the ground since 1950. Station data show that most of the decrease is related to a later start to the snow cover season, which reflects the enhanced warming observed in autumn over the region (Rapačić et al., 2015).

There are large uncertainties in documenting trends in annual snow accumulation because of the sparse network of in situ measurements and the fact that snow-depth observations made at climate stations in open terrain may not be representative of snow conditions in the prevailing land cover. According to the available Canadian in situ snow-depth data, maximum snow depths have decreased over the Canadian side of the BBDS by an average of about 20% since 1950 (Brown et al., 2018).

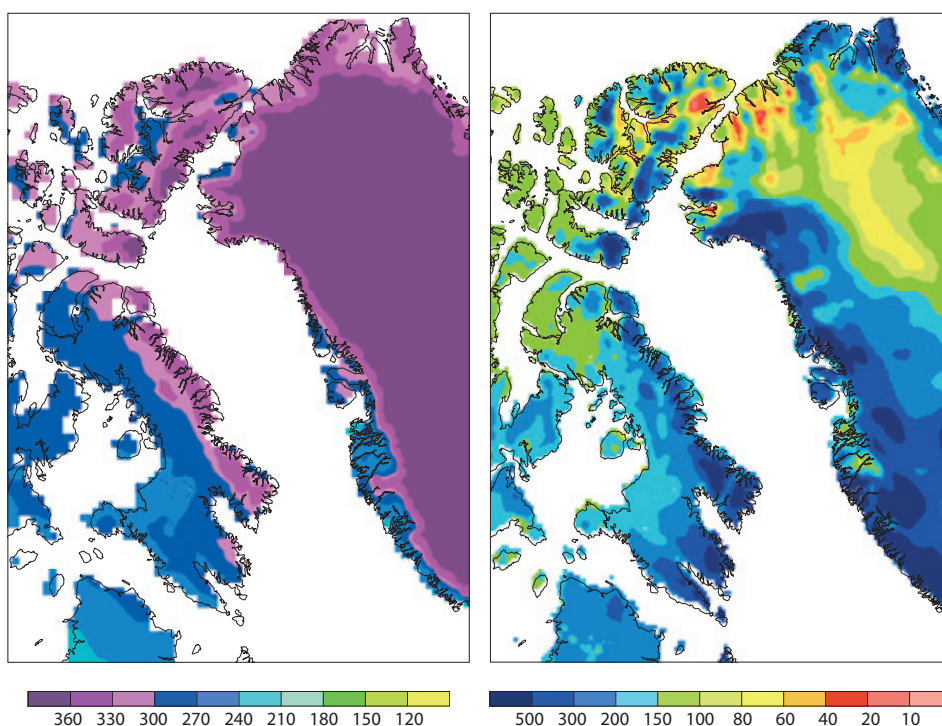


Figure 3.7 Left: Mean annual number of days with snow on the ground (snow cover duration, SCD) from the NOAA IMS 24 km daily snow cover analysis (Helfrich et al., 2007) over snow seasons 1998/99 to 2013/14. Right: Mean annual maximum snow water equivalent (SWE) (mm) over the 1979/80 to 2008/09 snow seasons, from the snow cover reconstruction of Liston and Hiemstra (2011).

Estimates of trends in maximum annual snow water equivalent (SWE_{max}) from other sources, such as passive microwave satellite data (GlobSnow; Takala et al., 2011) and the reanalysis-driven reconstruction of Liston and Hiemstra (2011), do not agree on the sign of change over the BBDS region in spite of evidence that precipitation is increasing over the region (AMAP, 2011; Lindsay et al., 2014; Vincent et al., 2015).

Projected changes

Projections of snow cover change for the BBDS region were obtained from the SWIPA 2017 report (Brown et al., 2017), which examines monthly snow cover and snow water equivalent (SWE) output from 16 independent CMIP5 models for 3 sets of experiments: historical (1986–2005), RCP4.5 (2006–2099), and RCP8.5 (2006–2099). Maps of relative change in annual snow cover duration and annual maximum SWE over Arctic land areas were generated for three 20-year scenario windows: near-term (2016–2035), mid-term (2046–2065), and long-term (2081–2100), all expressed with respect to the 1986–2005 reference period (shown in Langen et al., 2016). SCD was also computed for the first half of the snow season (August–January) and the second half (February–July), to capture changes in snow cover onset and snow-off (end of spring melt) dates. Regionally averaged results were computed over non-glacier gridpoints in the BBDS domain (approximated by the latitude/longitude

box of 60–85°N, 45–95°W). The following general points can be made from the CMIP5 model results:

- Annual maximum SWE shows little response to warming in the BBDS region (-10 to +15% range by 2100 for RCP8.5) and is relatively insensitive to emissions scenario (Figure 3.8, left panels). However, large relative reductions in SWE are projected to take place in the May–October period (Figure 3.8, right panels).
- Annual snow cover duration shows strong sensitivity to warming (Figure 3.9, top panels), with decreases of 15–25% projected by 2100 for RCP8.5. These percentage changes correspond to decreases of approximately 40–60 days, based on the mean annual SCD (255 days) observed at Canadian communities in the BBDS region (see Langen et al., 2016). SCD is also sensitive to emissions scenario: the RCP4.5 results indicate a stabilization of snow cover duration toward the end of this century, at levels about 5% lower than today, while the RCP8.5 results indicate accelerating reductions in snow cover throughout the century.
- Snow cover duration is projected to decrease more rapidly in the start of the snow season than at the end of the snow season (Figure 3.9, bottom panels). This feature is also found in snow cover trends from in situ observations and in high-resolution regional RCP4.5 and RCP8.5 model projections for Greenland (Christensen et al., 2015).

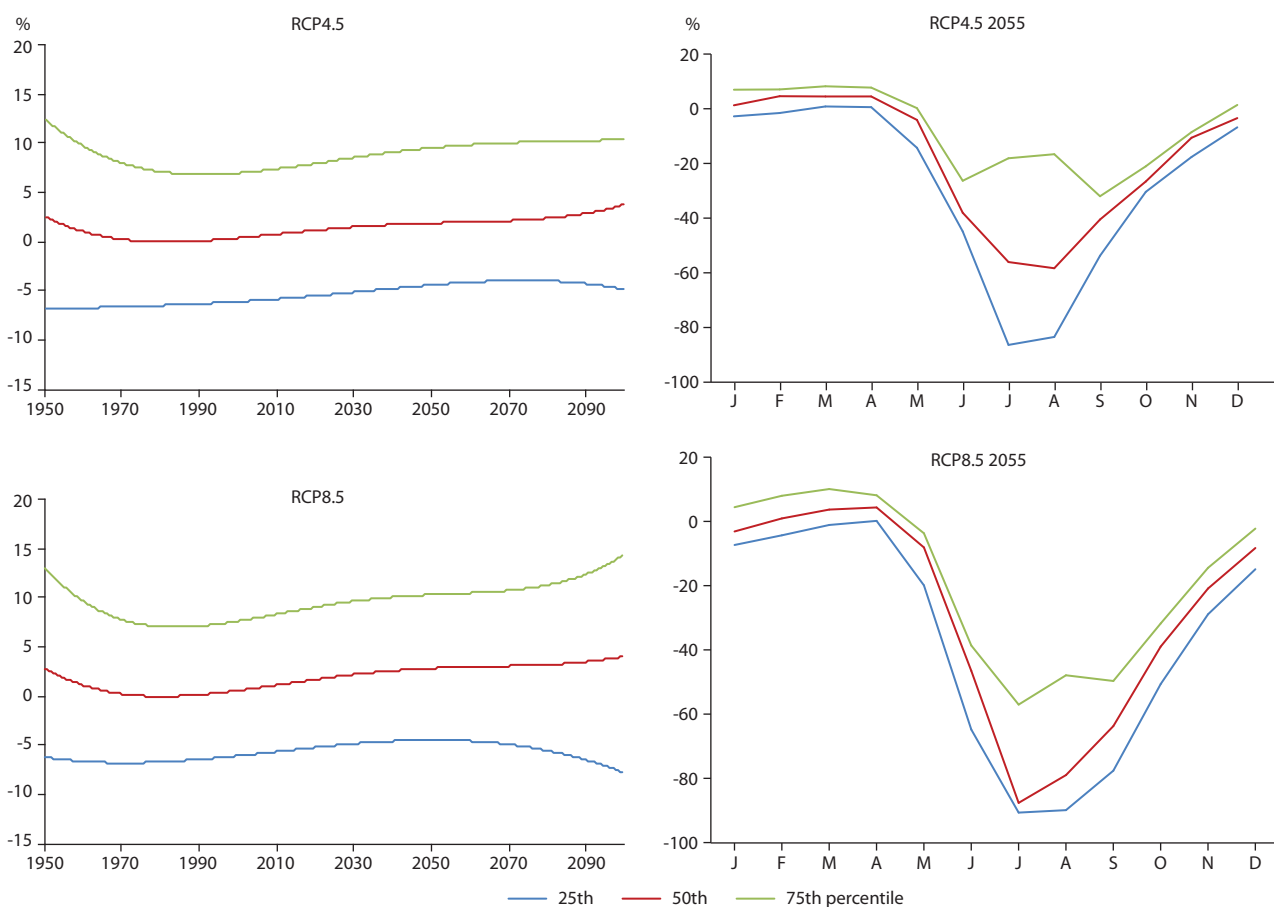


Figure 3.8 Left panels: Projected change (%) in BBDS-averaged maximum snow water equivalent (SWE_{max}) relative to 1986–2005, from 16 CMIP5 models: 25th, 50th and 75th percentiles (fourth-order polynomial smoothing). Right panels: Projected change (%) in monthly snow water equivalent (SWE) over BBDS non-glacier land areas for the year 2055 under the RCP4.5 and RCP8.5 scenarios: 25th, 50th, and 75th percentiles of 16 CMIP5 models. Results for the 2025 and 2090 periods are provided in the supplementary material for this subchapter (Langen et al., 2016).

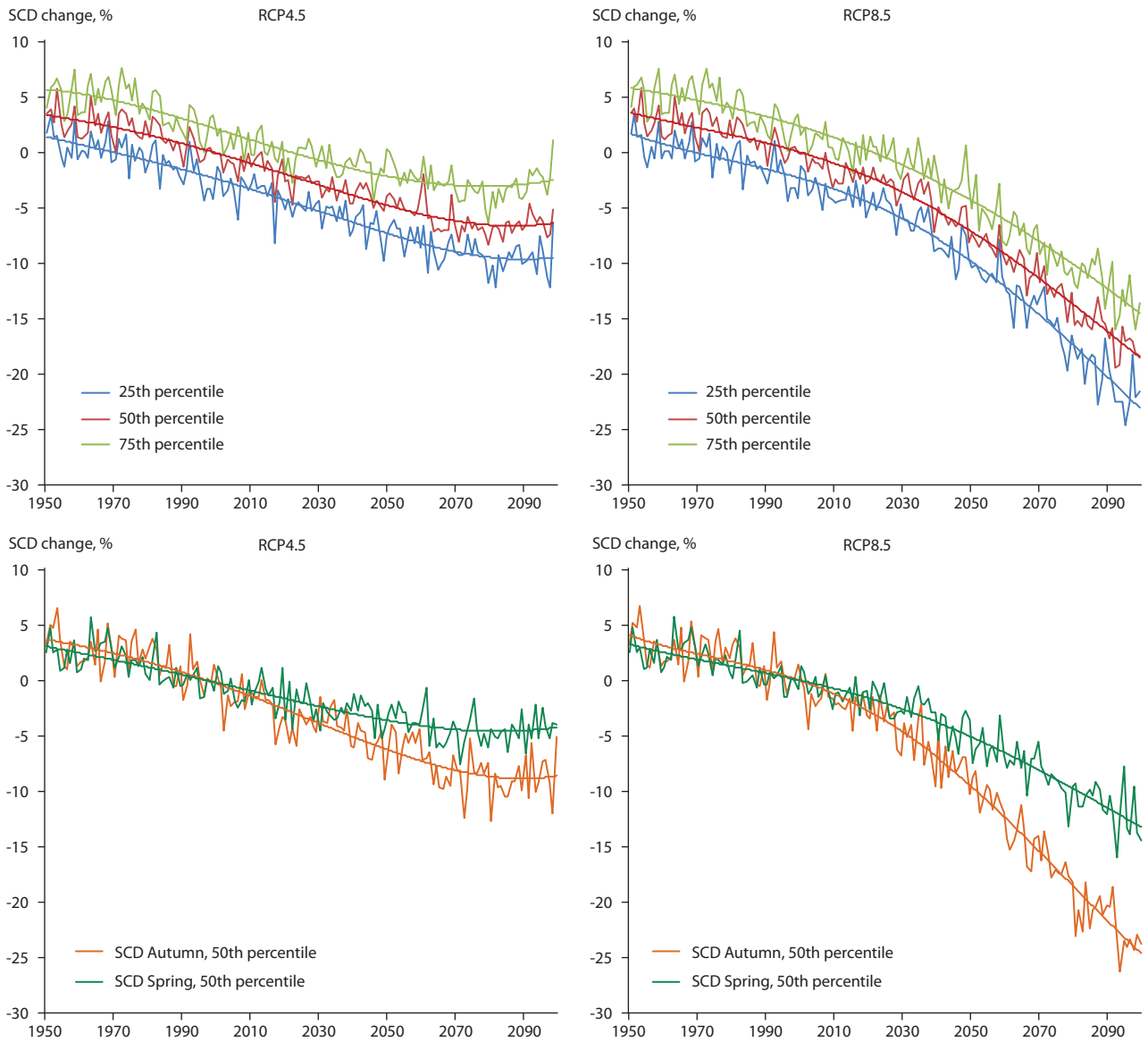


Figure 3.9 Top panels: Projected change (%) in annual snow cover duration relative to 1986–2005, averaged over non-glacier land points in the BBDS region, from 16 CMIP5 models: 25th, 50th, and 75th percentiles. Bottom panels: Projected change (%) in snow cover duration over the first half (SCD Autumn) and second half (SCD Spring) of the snow season, relative to 1986–2005, from 16 models: 50th percentiles.

More detailed information on the spatial pattern of projected snow cover changes from the CanRCM4 regional climate model (0.22° Arctic CORDEX experiment, run 1) (Scinocca et al., 2016; see Langen et al., 2016) shows evidence of strong coastal gradients in SWEmax change in several areas (e.g., southern Baffin Island, southwestern Greenland, Ellesmere Island), with decreases along the coastal margins and increases over higher elevations farther inland. The stronger climate response of snow cover in coastal regions is consistent with the conclusions of Brown and Mote (2009) regarding the higher climate sensitivity of snow cover in marine areas. This greater sensitivity is related to the warmer cold season temperatures and higher precipitation in these areas.

3.1.3.2 Permafrost

BBDS permafrost is projected to warm the most in the region’s coldest areas and to thaw considerably in the warmest areas. Ellesmere Island is an example of a cold

area that is projected to experience pronounced permafrost warming. Southwestern Greenland is an example of a relatively warm area that is projected to experience pronounced permafrost thawing.

The thermal state of the ground is closely linked to climate – particularly air temperature and precipitation, which are the main drivers influencing thermal-state variability and temporal and spatial changes. Other local environmental drivers – such as wind, snow drift dynamics (Stieglitz et al., 2003; Zhang, 2005), vegetation cover growth (Lantz et al., 2012), drainage, and subsurface material properties (including ice/moisture content) – greatly influence ground temperature and its spatial and temporal variability. In such contexts, trends in shallow ground temperature can be sensitive to short-duration variations and regional comparisons can be challenging. Deeper ground temperatures reflect longer-term trends in climate. A recent review of changing Arctic permafrost and the impacts of these changes is provided in Chapter 3 of the SWIPA update (Romanovsky et al., 2017).

Observed trends

Figure 3.10 shows permafrost temperatures for several sites in the BBDS region. On the Canadian side, the mean annual ground temperatures generally decrease with increasing latitude, ranging from about -5°C in the southern portion of Baffin Island to about -15°C at the northernmost sites of Ellesmere Island (e.g., Smith et al., 2010; Smith et al., 2013). On Baffin Island, the thickness of the active layer (the seasonally thawed surface layer above permafrost) ranges from less than 1 m to about 2 m (Ednie and Smith, 2010; Ednie and Smith, 2011); limited observations indicate thicknesses generally less than 1 m for the northernmost sites. Since the 1980s, permafrost temperatures at Alert have increased at rates of about 0.5 and 0.3°C per decade at depths of 15 and 24 m, respectively (Figure 3.11 and Table 3.1), which is consistent with air temperature trends (Smith et al., 2012; Romanovsky et al., 2015). Higher rates of permafrost warming were observed in the period 2000–2014, with a warming of 0.7 to 1°C per decade at 24 m depth and 1.3°C per decade at 15 m depth. Record-high permafrost temperatures were observed at Alert in 2012, with mean annual ground temperatures in the upper 25 m reaching more than -11°C at one site (Romanovsky et al., 2015). Shallow (<5 m) permafrost temperatures recorded in Iqaluit show warming rates of about 0.2°C per year between 1993 and 2004 (Throop et al., 2010). The shorter time series records (4–5 years) at 10 to 15 m depth at other sites on Baffin Island and the surrounding islands show warming patterns similar to those recently observed at Alert. These patterns are

Table 3.1 Change in permafrost temperature over time for selected sites in the BBDS region (Smith et al., 2012; Romanovsky et al., 2015; Throop et al., 2010; Ednie and Smith, 2015; plus updates).

Site (and measurement depth)	Time period	Rate of temperature change ($^{\circ}\text{C}$ per year)
Alert BH1 (24 m)	1978–2014	0.03
	2000–2014	0.07
Alert BH2 (24 m)	1978–2014	0.03
	2000–2014	0.10
Alert BH5 (15 m)	1978–2014	0.05
	2000–2014	0.13
Resolute (15 m)	2008–2012	0.33
Eureka (10 m)	2009–2012	0.29
Arctic Bay (15 m)	2008–2013	0.18
Pond Inlet (15 m)	2008–2013	0.15
Iqaluit (5 m)	1993–2004	0.20

part of a consistent pan-cryospheric response to warming (Derksen et al., 2012).

On the Greenland side of the BBDS region, permafrost temperatures are relatively warm (close to 0°C) in coastal zones and south of the Arctic Circle; inland and farther north, temperatures are colder. Data from four shallow boreholes covering the period 2007–2009 (Figure 3.10) indicate that mean

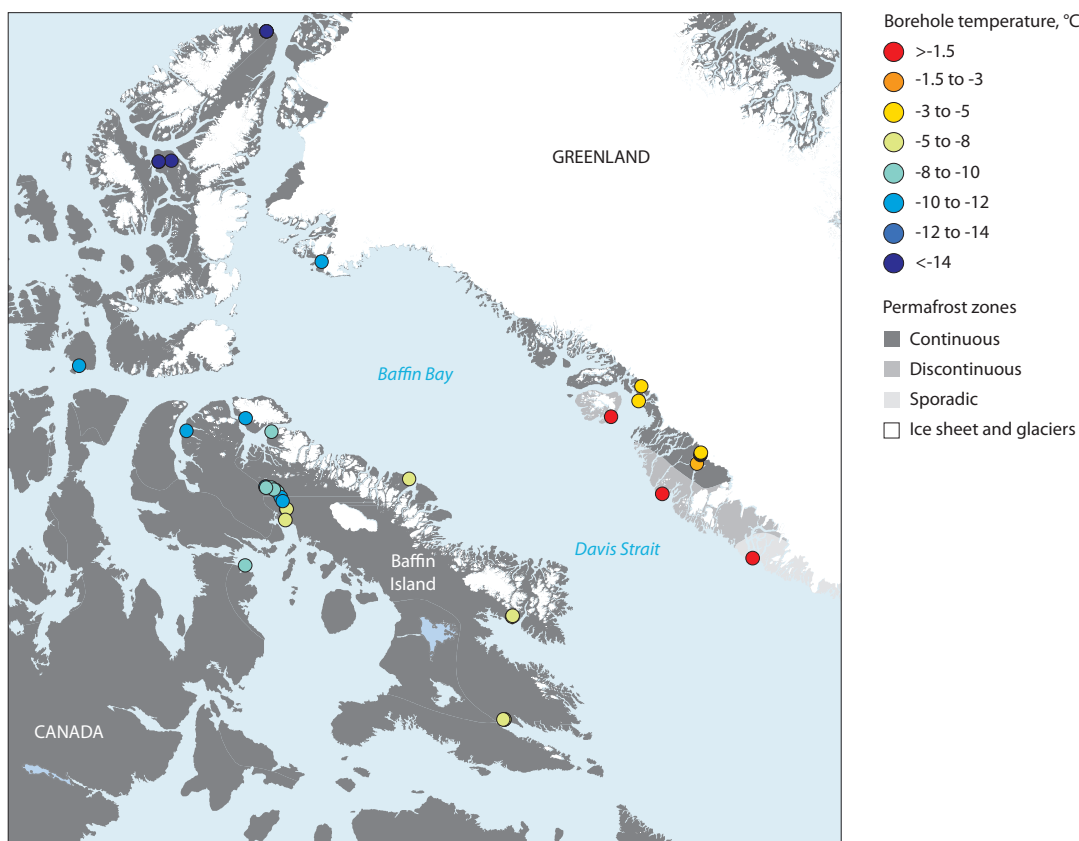


Figure 3.10 Permafrost temperatures (derived from Christiansen et al., 2010; Smith et al., 2013) and permafrost zones (from the map of Brown et al., 2014). The temperatures represent mean annual ground temperature at the depth of zero annual amplitude (the depth below which there is no significant seasonal variation in ground temperature) or at the depth of the closest measurement. The data were generally collected since 2008. The permafrost zone categories, indicated by the dark-to-light gray shading, are continuous (90–100% cover), discontinuous (50–90% cover), and sporadic (10–50% cover).

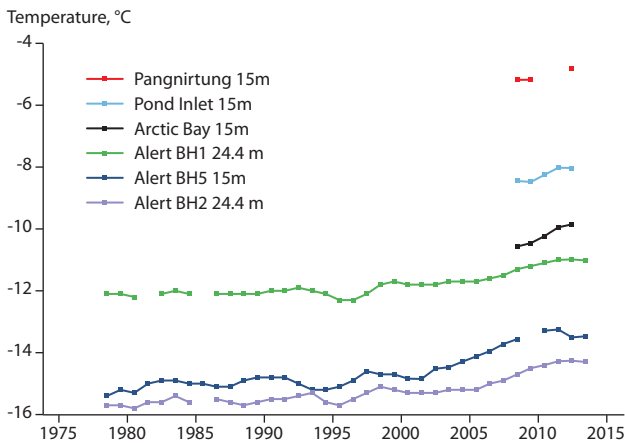


Figure 3.11 Permafrost temperature (annual mean) time-series records (reproduced from Smith et al., 2015) for Canadian Forces Station (CFS) Alert, at depths of 15 and 24 m (updated from Smith et al., 2012, and Romanovsky et al., 2015) and three communities on Baffin Island (data from Ednie and Smith, 2015, and Romanovsky et al., 2015). Alert BH1 is located near the coast and has greater snow cover than the other two Alert sites. (This figure is a copy of an official work published by the Government of Canada. This reproduction has not been produced in affiliation with or with the endorsement of the Government of Canada.)

annual ground temperatures at depths near 4 m range from 0.2°C at Nuuk (sporadic permafrost) to -3.4°C at Ilulissat (continuous permafrost) (Christiansen et al., 2010). The Ilulissat borehole is located in a fine-grained marine deposit with a residual salinity that increases with depth. The resulting depression of the freezing point (relative to zero-salinity conditions) means that permafrost at this site is relatively close to thawing (Ingeman-Nielsen et al., 2010). In the northernmost part of West Greenland, a borehole at Thule has a mean annual ground temperature of -10°C (Bjella, 2012). These observed values are in agreement with simulation results obtained from the Geophysical Institute Permafrost Lab (GIPL; University of Alaska, Fairbanks) model forced using year 2005 data from the Climate Research Unit 3.1 database (CRU-3.1).

Projected changes

The recent CMIP5 generation of climate and earth system models shows a wide range of abilities in the simulation of current permafrost distribution and active-layer characteristics. Most models are not designed to simulate deep ground temperatures. Computed temperatures are sensitive to soil layer and lithologic discretization, realistic representation of surface snowpack and organic soils, realistic treatment of heat and water flow in soils, and the numerical precision of the computer running the climate model (Paquin and Sushama, 2015). In addition, Slater and Lawrence (2013) found that some models had significant air temperature and snow depth biases that adversely affected their ability to simulate realistic permafrost conditions.

It is therefore practical to employ a dedicated permafrost model driven by climate model output. Figure 3.12 shows the result of one such experiment (using the model GIPL2; Marchenko et al., 2008). Under RCP4.5 (Figure 3.12, upper panels), the simulated permafrost temperatures at 5 m depth show warming of about 2–4°C over large areas of the cold permafrost regions on the Canadian side of the region by

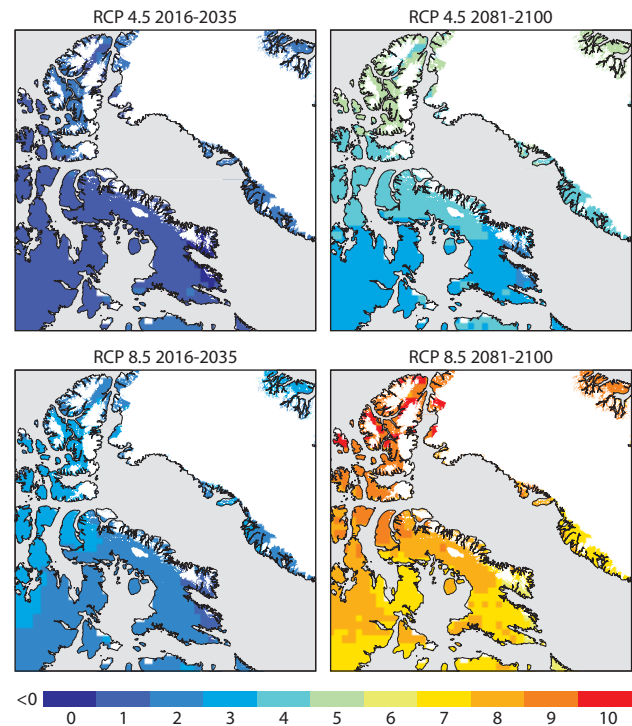


Figure 3.12 Projected change for BBDS permafrost, expressed as the change in average temperature (°C) at 5 m depth for the periods 2016–2035 (left panels) and 2081–2100 (right panels). The results are based on the GIPL2 transient permafrost model forced with the CCSM4 GCM and emission scenarios RCP4.5 (upper panels) and RCP8.5 (lower panels). Changes are computed relative to the reference period 1986–2005.

the years 2081–2100. The Greenland side also shows ground temperatures increasing by up to 2–4°C. This warming results in degradation of the permafrost, especially in the southern part of the region (Gent et al., 2011). Under RCP8.5 (Figure 3.12, lower panels), the largest increase in the 5 m temperature could reach 8–10°C by the 2081–2100 period; most of the permafrost on the Canadian side could warm by about 6–8°C. On the Greenland side, where the permafrost is already fairly warm (between 0 and -5°C), large areas are projected to have temperatures cross the 0°C threshold by 2081–2100. These results, which reflect only one model (GIPL2) and do not account for local variability, may not accurately correspond to site-specific observations.

3.1.3.3 Land ice

The Greenland Ice Sheet is projected to lose mass during the 21st century, with the primary mechanisms being increased freshwater runoff (up to a doubling or tripling) and glacier calving. Year-to-year variability in freshwater runoff is projected to increase. The Canadian Arctic glaciers and ice caps are similarly projected to lose mass due to increased runoff.

The BBDS region encompasses ice sheets and glaciers in both Greenland and the Canadian Arctic Archipelago. Ice sheets and glaciers gain mass through precipitation, and they lose mass primarily through meltwater runoff, iceberg calving, and melting in direct contact with ocean water. The difference between the mass gain and loss is called the total mass balance. The surface mass balance is the difference between accumulation from

precipitation and mass loss from surface ablation (sublimation, drifting snow erosion, and runoff of meltwater). The loss of mass through iceberg calving and melting in direct contact with the ocean is termed the dynamical mass loss. An Arctic-wide perspective on observed and projected changes in land ice is provided in Chapter 4 of the SWIPA update (Box et al., 2017).

Observed trends

According to a reconstruction by Box (2013), meltwater runoff from the Greenland Ice Sheet as a whole increased 63% over the 1840–2010 period. This reconstruction suggests that the ice sheet surface mass balance had an insignificant decreasing trend due to nearly equal increases in accumulation and runoff rates. In the early 1990s, the surface mass balance started to decrease, due almost entirely to increased melting and runoff, with changes in accumulation being small (Sasgen et al., 2012; Vernon et al., 2013). The increase in melting is driven by regional warming that is associated with both anthropogenic changes (e.g., Fyke et al., 2014b) and prevailing atmospheric circulation patterns that are favorable for melting (e.g., Fettweis et al., 2013).

The ice sheet changes led to 20–50% increases in freshwater input to the seas adjacent to Greenland between 1992 and 2010 (Bamber et al., 2012). Mernild and Liston (2012) modeled regional changes in the magnitude and timing of runoff since 1960. Runoff increase is attributed mainly to an increase in areal melt extent, with smaller contributions from an increase in melt duration and a countering decrease in melt rates. The length of the simulated discharge season was longest in the south (about 4–6 months) and shortest in the north (about 2–3 months). The length of the discharge season increased between 1960–1969 and 2000–2010, with changes ranging from 11 days in the north to 27 days in the south and southwest. The mass loss and ocean freshwater input from increased runoff has been augmented by an increased iceberg calving flux since the early 1990s from southern and western Greenland (Bigg et al., 2014).

Reconciliation of results from various methods estimating the total mass balance of the Greenland Ice Sheet (e.g., Shepherd et al., 2012) has documented a sharp increase in the total mass loss over recent decades. The IPCC's AR5 (IPCC, 2013a) reports an acceleration from 0.1 mm sea-level equivalent per year (1992–2001) to 0.6 mm per year (2002–2011). According to Enderlin et al. (2014), the relative contribution of dynamical mass loss to the total loss decreased from 58% before 2005 to 32% between 2009 and 2012. In the southwest, recent mass loss has been mainly through surface mass balance, while in the west and northwest, surface mass balance and dynamical mass loss contribute approximately equally. The majority of the current Greenland total mass loss (about 60%) is attributed to West Greenland (Andersen et al., 2015).

Outside the ice sheets of Greenland and Antarctica, the Canadian Arctic Archipelago (CAA) contains the largest area of land ice (~150,000 km²) on Earth. Recent estimates of mass loss identify the CAA as the single largest land ice contributor to sea level rise outside the two ice sheets (Gardner et al., 2011; Sharp et al., 2011; Gardner et al., 2013; Sharp et al., 2014). Observations show that most of the land ice in the CAA has

lost mass, thickness, and area over the past half century as a result of climate warming. Since 2007, more intense and sustained melt has occurred in response to a trend toward more frequent summer anticyclonic circulation over the region (Overland et al., 2012; Gascon et al., 2013; Sharp et al., 2014; Bezeau et al., 2015). The CAA mass losses are dominated by melt and runoff, with iceberg calving playing a varying but apparently minor role (Williamson et al., 2008; Van Wychen et al., 2014). Floating ice shelves at northern Ellesmere Island have also been strongly affected by the recent warming, with some fjords in the region now ice free for the first time in over 3,000 years (Sharp et al., 2014; White et al., 2014).

Projected changes

Although snowfall accumulation is projected to increase in the future (Krasting et al., 2013), all studies indicate that the Greenland surface mass balance will continue to decrease because projected increases in runoff are greater than projected increases in accumulation (Church et al., 2013a). Rae et al. (2012) compared regional climate models over Greenland, driven by different global models. Depending on the model combinations employed, projected runoff rates increase by about a factor of 2–3 over the 21st century in the A1B scenario (which lies between the RCP4.5 and RCP8.5 scenarios). In a single-model experiment using the RCP8.5 scenario, Fyke et al. (2014a) found an approximately 50% increase in year-to-year variability in surface mass balance; this increase was dominated by increased variability in runoff.

Increasing dynamical ice loss has been linked to the arrival of warm ocean water (Holland et al., 2008; Straneo et al., 2010, 2012) and a reduction of ice in the fjord ahead of a glacier terminus, thus increasing the calving rate (Amundson et al., 2010). As noted by Church et al. (2013a), 19 coupled global atmosphere–ocean climate models show a warming of about 2°C in scenario A1B around Greenland over the 21st century (Yin et al., 2011), indicating that the increased outflow may be expected to continue into the future. We do not currently have three-dimensional models of iceberg calving and energy exchange at the ice–ocean interface, but flowline modeling by Nick et al. (2013) suggests speed-ups of up to 70% for a suite of four major outlet glaciers. These speed-ups tend to occur mainly in the early part of the 21st century; after that, the speeds level out.

Model projections of future mass loss components were synthesized by Church et al. (2013a), and the projected Greenland Ice Sheet contribution to sea level rise is given in Table 3.2. The median total contribution is found to be about 10 cm of sea level, with an upper range of about 20 cm.

Table 3.2 Projected Greenland Ice Sheet contribution to sea level rise (in meters) by 2081–2100, relative to 1986–2005: median values [and likely ranges] (Church et al., 2013a).

	Surface mass balance (m)	Dynamical mass loss (m)	Total (m)
RCP4.5	0.04 [0.01 to 0.09]	0.04 [0.01 to 0.06]	0.08 [0.04 to 0.13]
RCP 8.5	0.07 [0.03 to 0.16]	0.05 [0.02 to 0.07]	0.12 [0.07 to 0.21]

As with the Greenland Ice Sheet, the indications are that the currently observed trend of CAA glacier mass loss will continue into the future, as enhanced meltwater runoff is not sufficiently compensated by increased snowfall (Lenaerts et al., 2013). However, it should be stressed that there is considerable model variability in the sign, magnitude, and timing of projected changes in snowfall and accumulated snow mass over the region; in addition, most climate models do not represent local moisture sources such as the North Water Polynya, which is an important contributor to the mass balance of the Manson and Prince of Wales ice fields (Boon et al., 2010). Radic et al. (2013) used downscaled output from 14 different global climate models forced by emissions scenarios RCP4.5 and RCP8.5 to drive a glacier mass balance model. For the period 2006–2100, they found glacier volume reductions of 10–60% in the Queen Elizabeth Islands and 20–100% in the Baffin/Bylot region. The glaciers of the Queen Elizabeth Islands have a relatively low sensitivity to the first 2°C of warming, but their sensitivity increases as warming increases beyond that point. Relative to other regions, the CAA has a relatively low sensitivity of mass balance to climate warming, but this still results in large projected mass losses due to the relatively large warming projected over this region.

3.1.3.4 Freshwater ice

Projections for lake ice in 2050 indicate a 10–15 day earlier break-up and a 5–10 day later freeze-up, with a 10–30 cm decrease in maximum ice thickness. Lake-ice response to warming is influenced by lake morphology (size and depth) and local changes in snow accumulation.

The following material is taken largely from the ArcticNet Eastern and Central Canadian Arctic Integrated Regional Impact Study (IRIS) report (Stern and Gaden, 2015) and the Eastern Canadian Arctic IRIS report (Brown et al., 2018).

Lake and river ice are integral components of the northern environment, and they influence a wide range of related climate-sensitive ecosystem services and numerous ecological and water quality characteristics (Beltaos and Prowse, 2009; Prowse et al., 2011a). Ice is also a critical component of cold-region hydrologic systems, affecting extreme floods and low winter flows (Beltaos and Prowse, 2009). Ice cover formation, melt, and dynamics are sensitive to a variety of meteorological variables, and changes in any of these variables can influence ice composition, thickness, and stability, as well as the complex interactions among hydrodynamic, mechanical, and thermal processes (Beltaos and Prowse, 2009). Lake and river ice regimes also respond to non-climatic controls such as lake morphology and depth (Brown and Duguay, 2010) and changes in the terrestrial hydrologic regime (Prowse et al., 2011a, 2011b).

Compiling information on trends in lake and river ice cover is a challenge. Few in situ records exist, and satellite observations have a variety of limitations related to resolution, frequency, consistency, and duration of coverage. Latifovic and Pouliot (2007) used Advanced Very High Resolution Radiometer (AVHRR) satellite imagery to analyze lake freeze-up/break-

up trends over the period 1985–2004, including four lakes distributed across the Canadian side of the BBDS region. Their analysis showed evidence that these lakes were part of a consistent Canadian Arctic-wide trend toward later freeze-up and earlier break-up. The average change observed over the four lakes for the 20-year period was a 15-day later freeze-up and a 24-day earlier break-up. Lake Hazen, near Alert, exhibited the largest trends and also the only statistically significant trends. Paquette et al. (2015) provided evidence of recent significant changes at Ward Hunt Lake on northern Ellesmere Island, from analysis of field records, aerial photographs, and satellite imagery. These records show that the summer perennial ice regime was relatively stable from 1953 to 2007 but then experienced rapid thinning in 2008 and became ice free in 2011. Further evidence of rapid lake ice changes over the region was provided by Surdu (2015), who observed widespread decreases in lake ice cover over the Canadian Arctic Archipelago from analysis of RADARSAT data for the 1997–2011 period. There is also evidence that some lakes may be transitioning from perennial to seasonal ice regimes (Mueller et al., 2009), which has major consequences for freshwater ecosystems and related ecosystem services (Vincent et al., 2012).

A variety of methods are used to generate scenarios of projected change in river and lake ice because these quantities are typically not resolved in global climate models. Recent studies have applied lake ice models to estimate the responses of lake ice characteristics to changes in temperature and precipitation: lake ice freeze-up/break-up, ice thickness, and the potential for white ice formation (Brown and Duguay, 2011; Dibike et al., 2011, 2012). White ice results from the incorporation of melted surface snow into the ice. Over the BBDS region, these studies project a 10–15 day earlier break-up and a 5–10 day later freeze-up for 2050. These numbers are comparable to an estimated decrease in river ice duration over most of Canada of approximately 20 days by 2050, provided by Prowse et al. (2007), based on the observed temperature sensitivity of river ice. Ice thickness is projected to decrease by 10–30 cm, with only small increases in the amount of white ice formation. These model simulations are based on an “idealized lake” of fixed depth. In reality, lake response will vary with lake morphology (size and depth) and local changes in snow accumulation, as shown by Brown and Duguay (2011).

3.1.4 Ocean

A freshening and warming of the Baffin Bay surface layer (about 0.2°C per decade over the next 50 years) is projected under the high-emissions scenario. This change is expected to reduce convection depth during winter and increase water column stability during the ice-free months. Models project an increased inflow of warm Atlantic-origin water into the bay, a decrease of cold Arctic water flow through the Canadian Arctic Archipelago, and an intensification of the counterclockwise circulation in Baffin Bay. Under these projected changes, the duration of ice bridges in Nares Strait, and thus the duration of the North Water Polynya, will likely decrease.

3.1.4.1 Physical oceanography of the region

Baffin Bay connects the Arctic Ocean with the western North Atlantic through three narrow CAA passages (Nares Strait, Jones Sound, and Lancaster Sound). Depth-averaged summer temperature and salinity over the upper 100 m (Figure 3.13) displays an east–west difference that reflects the relatively warm and salty West Greenland Current flowing northward along the west Greenland slope and the cold and fresh Arctic water flowing southward through the CAA and along the western side of Baffin Bay and Davis Strait. The relatively fresh water nearshore on the west Greenland shelf is a continuation of the East Greenland Coastal Current, which rounds the southern tip of Greenland to then flow northward, hugging the western Greenland coast; ice sheet runoff further freshens this water as it travels northward.

Vertically, Baffin Bay has a three-layer structure consisting of cold and fresh Arctic water in the top 300 m, a warm and salty middle layer from about 300 to 800 m, and a cold and slightly fresher deep layer (Tang et al., 2004). A similar three-layer structure is observed in Davis Strait (Figure 3.14) to the south, although the deep layer in the strait, in contrast to the bay, is not fresher than the middle layer. The winter mixed layer depth, resulting from wind mixing and sea ice formation, reaches about 100 m (Tang et al., 2004). In the summer, a strong, shallow pycnocline develops, reducing the mixed layer depth to about 10–30 m (e.g., Harrison et al., 1982; Jensen et al., 1999).

A summary of observation-based mean freshwater inputs and outputs for Baffin Bay is shown in Figure 3.15. The data upon which many of the numbers are based are extremely limited, and they do not reflect the strong interannual variability observed at locations where measurements have been taken long enough to identify lower-frequency variability as an important feature of these Arctic Ocean exports.

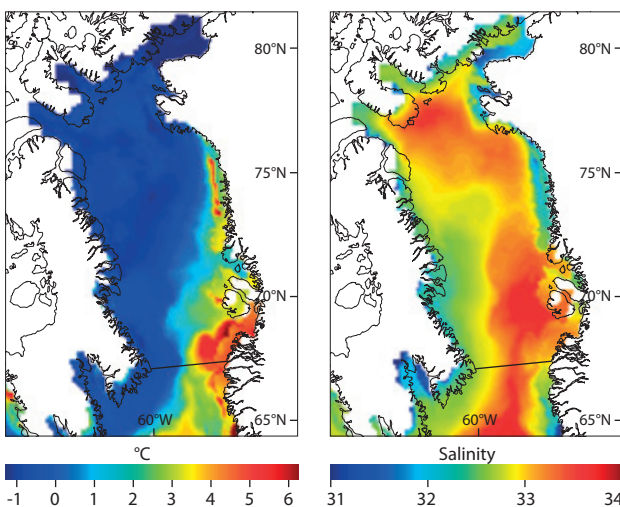


Figure 3.13 Summer (August to October) temperature (left panel) and salinity (right panel) in the upper 100 m of the Baffin Bay/Davis Strait water column. Derived from available archived data between 1910 and 2009. The transect line indicates the location of the cross-sections shown in Figure 3.14. (Modified from Hamilton and Wu, 2013; see their report for data-set details. © Her Majesty in Right of Canada, as presented by the Minister of Fisheries and Oceans.)

There are three principal inputs of fresh water to Baffin Bay: the CAA passages, the East Greenland Coastal Current extension, and the Greenland Ice Sheet. Combining estimates from the CAA passages (Melling et al., 2008; Munchow and Melling, 2008; Rabe et al., 2012; Peterson et al., 2012; Hamilton and Wu, 2013; see Langen et al., 2016, for Barrow Strait/Lancaster Sound time series) gives a mean volume transport through the entire CAA of about 1.5 Sv (1 Sv = 1 million m³ per second) and a freshwater transport of 81 mSv. These inputs show strong seasonal variability (with summer transport being 2–3 times larger than winter transport) and strong interannual variability (up to a factor of 4). Along West Greenland, Curry et al. (2014) derived northward mean volume transports of 0.4 Sv on the shelf and 0.7 Sv on the slope (Irminger Sea water) and a freshwater transport of 24 mSv. For the western half of Davis Strait, they reported a southward mean volume transport and freshwater transport in the Baffin Island Current of 2.9 Sv and 117 mSv, respectively. Glacial freshwater (solid and liquid) also enters Baffin Bay, principally off the Greenland Ice Sheet but also from glaciers on Baffin and Ellesmere islands. According to Bamber et al. (2012), 80% of the total Greenland discharge enters the ocean on the western and southeastern coasts. The rate of freshwater discharge from these glacial sources is increasing (Rignot et al., 2011; Bamber et al., 2012).

3.1.4.2 Observed trends

Hamilton and Wu (2013) used archived summer temperature and salinity data from 1950 to 2005 to derive trends in Baffin Bay and Davis Strait. Although interannual variability was high, particularly in the upper ocean, some significant trends were observed:

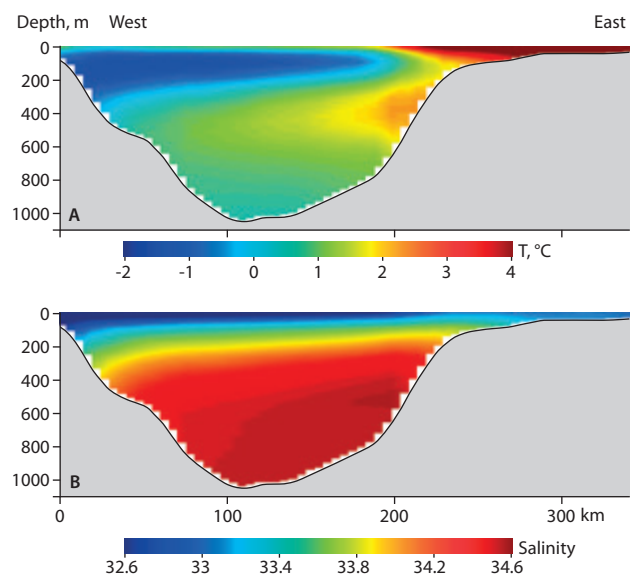


Figure 3.14 Davis Strait cross-sections of mean summer temperature (T, top) and salinity (S, bottom). Derived from available archived data between 1910 and 2009. The three-layer structure of Baffin Bay is also reflected in these Davis Strait data. The location of the cross-sections is indicated by the black transect line in Figure 3.13. (Reproduced from Hamilton and Wu, 2013; see their report for data-set details. © Her Majesty in Right of Canada, as presented by the Minister of Fisheries and Oceans.)

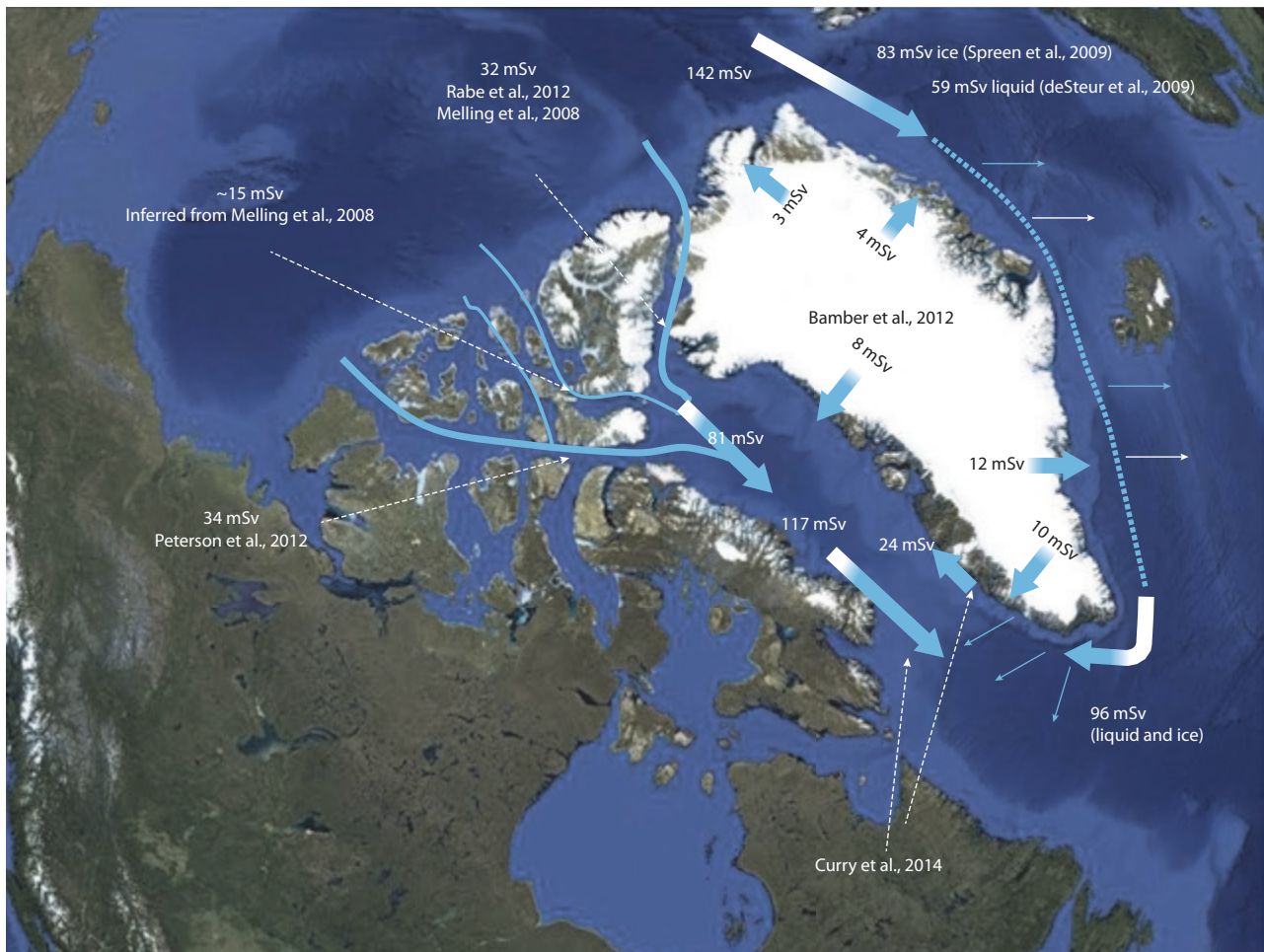


Figure 3.15 Mean freshwater fluxes (mSv) into Baffin Bay, based on observations reported by the referenced investigators. The coloring of the block arrows denotes the portion of the flux that is liquid (blue) versus ice (white).

- Freshening on the Baffin Island shelf (-0.06 psu per decade [psu is practical salinity unit]). This rate is similar to the findings of Zweng and Munchow (2006), who computed a freshening trend of -0.086 ± 0.039 psu per decade using data from 1916 to 2003. Most of the change occurred in the 1980–2005 period. Hamilton and Wu (2013) excluded data from the top 50 m, using data only within the 50–200 m interval because inclusion of the highly variable surface data masked the trend.
- Highly significant warming over the 600–800 m depth interval: 0.13°C per decade over the last 50 years (Hamilton and Wu, 2013). This observed warming trend is consistent with the finding of Zweng and Munchow (2006), who give $0.11 \pm 0.06^\circ\text{C}$ per decade for warming of the intermediate layer of Baffin Bay.

According to Vaughan et al. (2013), the rate of Greenland Ice Sheet mass loss during the decade 2002–2011 was 215 Gt/yr (7 mSv). Rignot et al. (2011) found this loss rate to be increasing at 0.76 mSv/yr (based on an 18-year record). This increase in rate is corroborated by Bamber et al. (2012), whose results further indicate that between 1992 and 2010, direct discharge along the shores of Baffin Bay, the Labrador Sea, and the Irminger Sea increased by 22%, 48%, and 49%, respectively.

3.1.4.3 Projected changes

Circulation

As noted in Section 3.1.1, projections of regional-scale changes are typically associated with large uncertainties, and ocean circulation changes are no exception, especially in the Northwest Atlantic/Baffin Bay region (e.g., Loder et al., 2015). Due to their coarse resolution, global models generally lack an adequate representation of the CAA channels, which, as mentioned above, are one of the main Arctic freshwater flux pathways (see the discussion above, regarding the region's general physical oceanography). Moreover, in these models, runoff from the Greenland Ice Sheet is often distributed uniformly over a large region of the northern North Atlantic, rather than close to the Greenland coast. Jahn et al. (2012) showed that a realistic representation of the CAA channel configuration, sea ice thickness, and local ice sheet runoff appears necessary to obtain consistent projections of circulation and freshwater flux changes in Baffin Bay.

High-resolution regional models, on the other hand, have a better representation of the CAA but do not necessarily include all forcings, such as changes in wind stress, large-scale sea surface height, and Greenland Ice Sheet melt. Nevertheless,

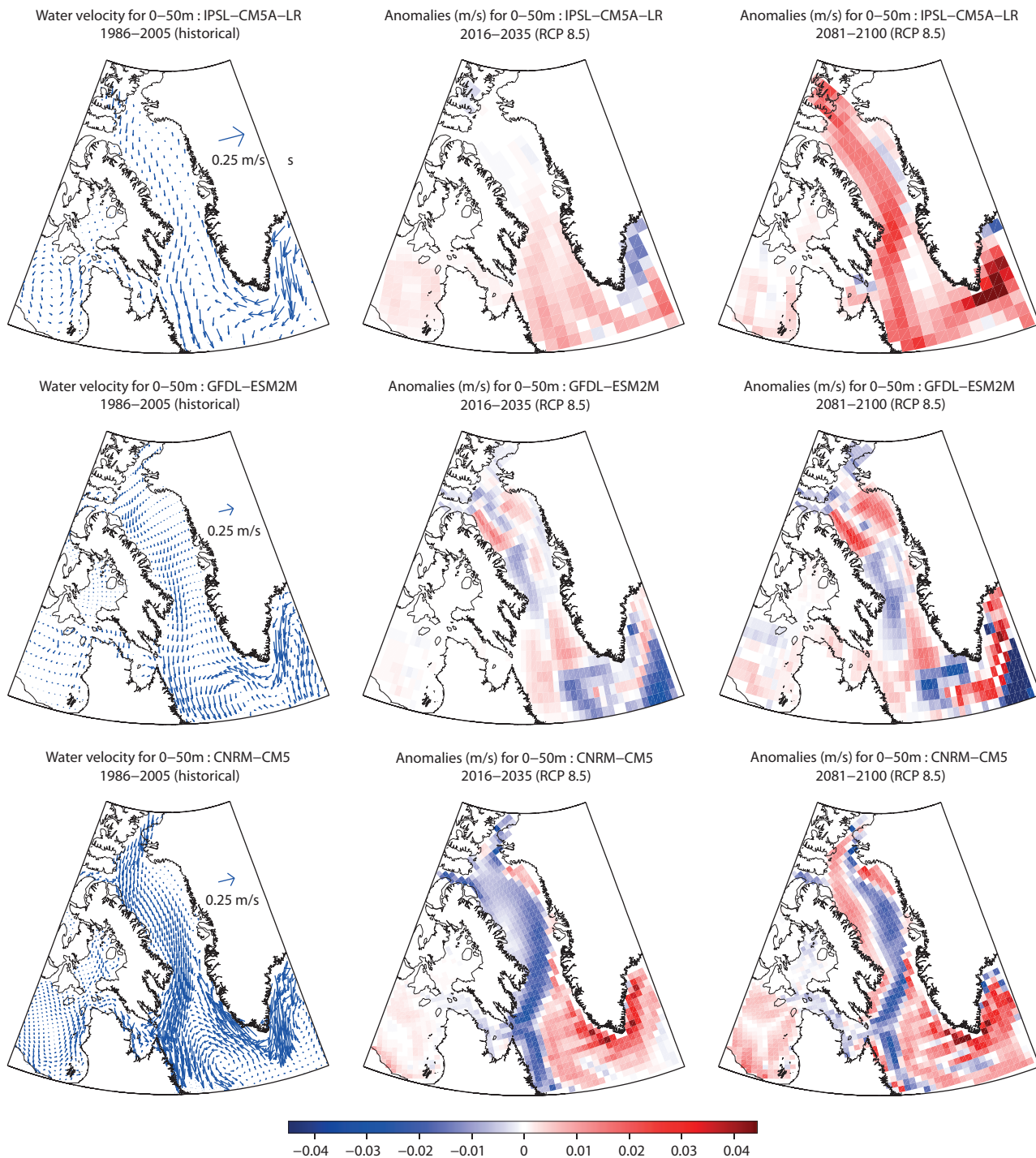


Figure 3.16 Labrador Sea/Baffin Bay mean near-surface current velocities (0–50 m) over the reference period (1986–2005), plus projected changes for the periods 2016–2035 and 2081–2100 under the RCP8.5 scenario. The projected changes are expressed as differences between the future period and the historical period. Each row shows the output of a different model.

some common trends do emerge when considering results from a few global and regional models.

Figure 3.16 shows projected changes in the strength of near-surface currents for the two periods 2016–2035 and 2081–2100 (relative to 1986–2005) for the RCP8.5 scenario for three global models (see Langen et al., 2016, for the RCP4.5 case). Of the seven available models that incorporated biogeochemistry at the time the Lavoie et al. (2013) study was initiated, these three provided a reasonable representation of the counterclockwise circulation in Baffin Bay (Figure 3.16, left column). In the projections of future conditions, this basic circulation pattern

generally persists across the different models. The strength of the circulation is the characteristic that changes.

As illustrated in Figure 3.16, the disagreement among the three global models in projected changes in current strengths is comparable in magnitude to the changes themselves. The models all include a representation of ice calving (Swingedouw et al., 2009; Dunne et al., 2012; Voldoire et al., 2013) but only in the GFDL-ESM2M model (Figure 3.16, middle row) is the meltwater distributed close to the ice sheet. This characteristic may explain the GFDL model's better agreement with the following regional model results.

Several regional model studies project a decrease in the flow of cold Arctic water through the CAA due to an increase in sea surface height in Baffin Bay, an intensification of the counterclockwise circulation, and an increased transport of freshwater along the west Greenland coast (Hu and Myers, 2014; Castro de la Guardia et al., 2015; Lique et al., 2015).

Mixed layer depth

Considering the different water masses flowing into Baffin Bay, the uncertainty in future circulation changes, and the low horizontal and vertical resolution of the global models, confidence in the details of projected mixed layer depth changes are low. However, based on recent and projected near-surface air temperature trends (Loder and van der Baaren, 2013; Steiner et al., 2015) and surface layer freshening (see below), some conclusions can be drawn.

The global models analyzed by Lavoie et al. (2013), as well as the regional North American Arctic–Nucleus for European Modelling of the Ocean (NAA-NEMO) model of Hu and Myers (2014), project a mean warming of the surface layer of about 0.2°C per decade over the next 50 years under the RCP8.5 scenario (see Steiner et al., 2015). A freshening trend of the sea surface layer is also projected by these models, although with a greater uncertainty. The multi-model ensemble mean trends calculated by Lavoie et al. (2013) are $-0.12 (\pm 0.12)$ and $-0.19 (\pm 0.12)$ psu per decade for RCPs 4.5 and 8.5 (with \pm indicating model spread). The regional NAA-NEMO model projects a freshening of about half that rate (i.e., -0.09 psu per decade; Steiner et al., 2015).

Warming and freshening of the surface layer is expected to stabilize the surface layer, reduce convection depth in winter, and increase water column stability during the ice-free months. The subset of models used by Lavoie et al. (2013) does project a modest decrease of the monthly maximum mixed layer depth. The multi-model ensemble mean trends are $-0.7 (\pm 0.6)$ m per decade for RCP4.5 and $-1.0 (\pm 0.6)$ m per decade for RCP8.5. The mean mixed layer depth trend is associated with an even higher uncertainty than the monthly maximum mixed layer depth. The projected shallowing is of only 2–3 m over the next 50 years. Warming and freshening of the surface layer thus appears to have a greater impact on stratification below the mixed layer, with strengthening stratification potentially resulting in reduced vertical mixing and a reduction of heat loss from the warm subsurface layer. A warming of the intermediate layer has indeed been simulated in different studies (e.g., Castro de la Guardia et al., 2015; Lique et al., 2015; and references therein).

Projections examined by Holland et al. (2007) consistently showed increased freshwater storage in the Arctic Ocean and increased freshwater export into the North Atlantic in response to increased precipitation, river runoff, and melting. However, the magnitude of these projected changes is highly uncertain. Possible changes in the relative importance of the pathways for freshwater export, i.e., Fram Strait versus CAA, are also unclear. The future impact of increased freshwater input on mixing and circulation in the North Atlantic will

depend on whether future conditions favor one pathway over the other.

3.1.4.4 The North Water Polynya

The North Water Polynya is one of the Arctic's largest and most productive polynyas (Deming et al., 2002; see also Chapters 2 and 6). The polynya forms seasonally under the action of strong northerly winds that push sea ice southward, away from an ice bridge that forms in Nares Strait/Smith Sound (at the constriction point between Greenland and Ellesmere Island), thus leaving behind an area of open water (Melling et al., 2001; Dumont et al., 2010). Once the polynya is open, upwelling of warm water along the Greenland coast contributes to its maintenance (Melling et al., 2001; Dumont et al., 2010).

Arctic waters, advected through Nares Strait, and Atlantic waters, advected with the West Greenland Current, are both present in the North Water Polynya (Melling et al., 2001; Lobb et al., 2003). Arctic waters cross the polynya as a southward flow, while the West Greenland Current, entering through Melville Bay, splits and then recirculates into the southward flow at different locations (Melling et al., 2001; Dumont et al., 2010). During northerly wind events, upwelling can occur both along the Greenland coast and along the landfast ice edge (ice bridge), depending on the ice configuration (Dumont et al., 2010). The warm upwelled waters, rich in nutrients, contribute to the high primary production reported for this area (Tremblay et al., 2002).

The presence of an ice bridge is necessary for the formation of the polynya (Melling et al., 2001). With the observed and projected changes (e.g., warming, freshening, thinning of sea ice; more mobile sea ice), the duration of ice bridges in Nares Strait/Smith Sound – and thus the duration of the North Water Polynya – will likely decrease. The existence of the North Water Polynya could be at risk in the future, with significant consequences for primary production (Michel et al., 2015). An important reduction in primary production in the polynya was indeed observed in the last decade and was attributed to freshening and increased stratification resulting from fresher Arctic water flowing through Nares Strait and from increased Greenland glacier melt (Bergeron and Tremblay, 2014). The changes in the ice bridge (i.e., its shorter duration) have also led to an increased advection of multi-year ice through Nares Strait and along the western side of Baffin Bay in recent years (Barber and Massom, 2007; Michel et al., 2015).

3.1.5 Sea ice

Climate models project the largest decreases in sea ice cover to occur in the autumn (15–20% reduction by 2080) due to later freeze-up, with smaller decreases in the spring (10–15% reduction) due to earlier ice break-up. Winter ice thickness is projected to decrease by about 20–30 cm, with the largest decreases in more northerly regions. The timing of the changes varies considerably across models. For the foreseeable future, multi-year ice is likely to remain a hazard for shipping in the Canadian Arctic Archipelago.

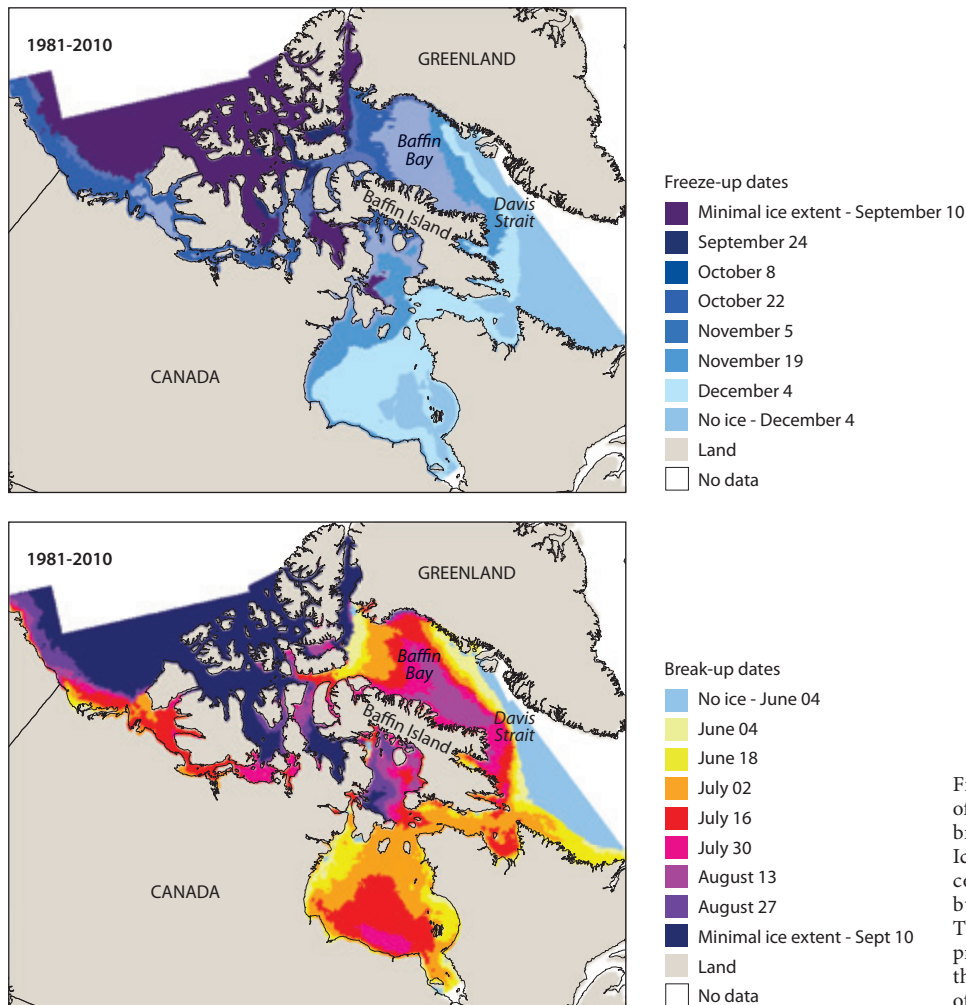


Figure 3.17 Mean dates (1981–2010) of sea ice freeze-up (upper panel) and break-up (lower panel) (Canadian Ice Service, 2011b.) (These maps are copies of official works published by the Government of Canada. These reproductions have not been produced in affiliation with or with the endorsement of the Government of Canada.)

The sea ice season in the BBDS region extends from approximately October to July (Figure 3.17), with seasonal concentration and thickness responding to the combined influences of air temperature, atmosphere and ocean circulation (winds, currents, sea surface temperatures), leads and polynyas, and, when ice is compressed against the west side of Baffin Bay, ridging and rafting. The influence of the North Water Polynya is clearly visible in the Figure 3.17 break-up plot (lower panel), with northern Baffin Bay being the first area to be ice-free. Break-up dates range from June to mid-August, with some northern areas of the region remaining ice covered for most of the year (e.g., Nares Strait, Kane Basin, and the northern coast of Ellesmere Island) (Tivy et al., 2011). On the Greenland side of the region, ice conditions are much lighter due to the influence of the relatively warm, north-flowing West Greenland Current. The ice cover in West Greenland is seasonal even in regions that receive imports of advected multi-year ice.

Only a small amount of multi-year ice enters Baffin Bay from Nares Strait and Lancaster Sound, and it is mainly restricted to the western side of the bay (Tang et al., 2004; Kwok et al., 2010). Sea ice is transported down the western side in the southward-flowing portion of the Baffin Bay gyre at speeds of up to 20–30 km/day (Canadian Ice Service, 2011a). The average ice drift velocity from northern Baffin Bay to the southern Labrador Sea is typically about 10–15 km/day but can exceed 20 km/day with variations in wind speed serving to speed up or slow down this motion (Kwok, 2007; Canadian Ice Service, 2011a).

Ice thickness can vary considerably over the region. For example, ice formed in newly opened leads is typically <0.5 m thick, whereas ice formed at the start of the winter season can eventually reach thicknesses of approximately 1.5 m (Tang et al. 2004). When the pack is compressed against the coastline, ridging and rafting can generate ice thicknesses of over 3 m. Weekly landfast ice thickness measurements made at Canadian coastal communities around Baffin Bay during the 1961–1990 period (Canadian Ice Centre, 1992) show average maximum ice thicknesses ranging from approximately 1.5 m around southern Baffin Island to over 2 m for Alert and Eureka on Ellesmere Island.

3.1.5.1 Observed trends

The BBDS region experienced a 20% loss in July–November sea ice extent over the period 1981–2014 (see Langen et al., 2016), with most of the change occurring in the time after 1998. The year 2006 had the lowest ice cover seen in the period of regular satellite observations. Analysis of trends in ice extent from passive microwave satellite data (Figure 3.18) shows decreases in nearly all months in the BBDS region, with Baffin Bay, Hudson Strait, and Davis Strait experiencing some of the largest Canadian Arctic decreases in summer total sea ice area and multi-year sea ice area (Howell et al., 2009; Tivy et al., 2011). Stroeve et al. (2014), using passive microwave satellite data, examined trends in the dates of first melt and first freeze-up of sea ice over the Baffin Bay region. For the 1979–2013

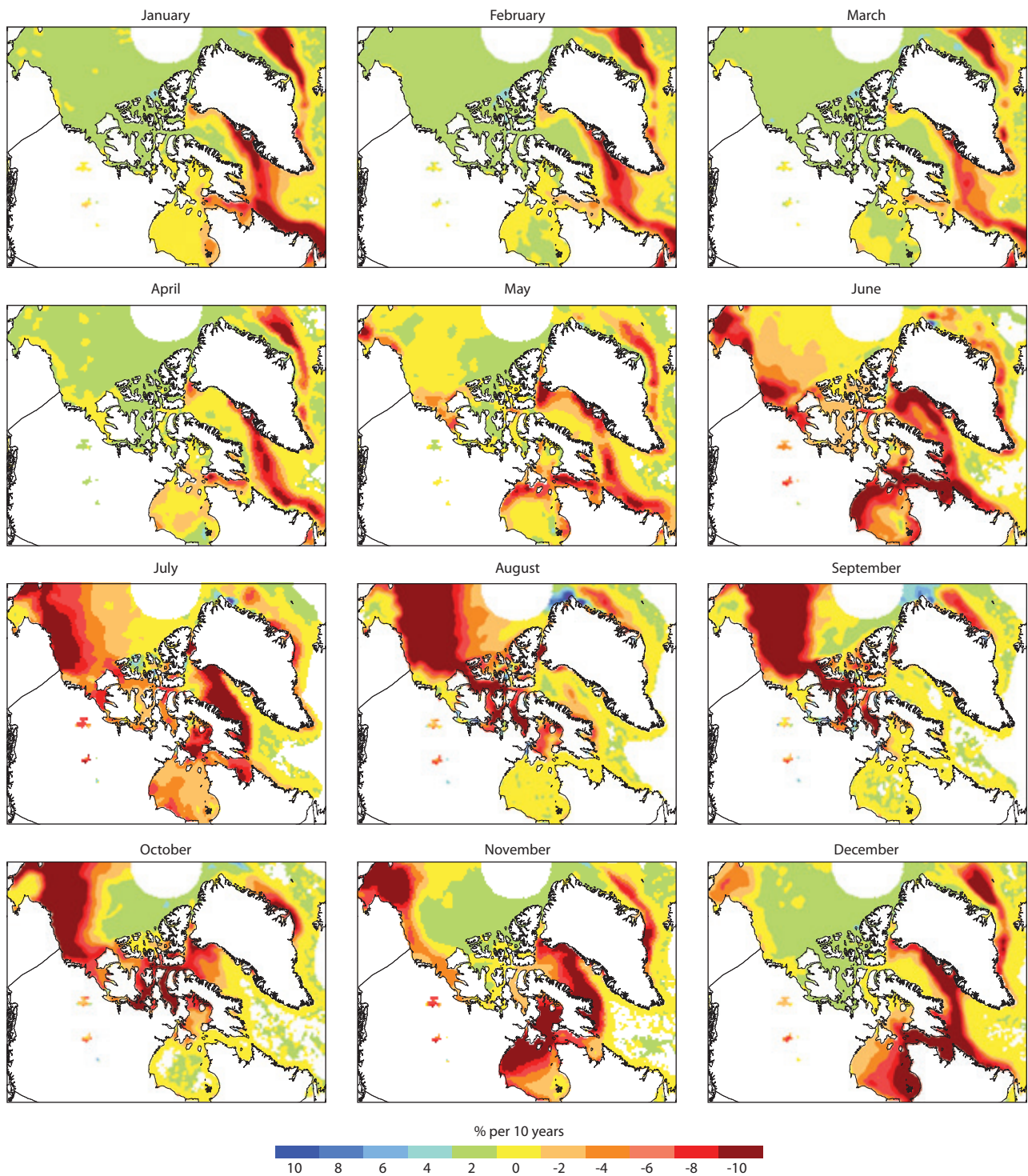


Figure 3.18 Trends in monthly average ice concentration (%) over the Canadian Arctic and adjacent waters, 1979–2012, expressed as percent change per decade (based on the passive microwave satellite data set of Cavalieri et al., 1996, updated to 2012).

period, they found a statistically significant trend to earlier melt onset, of 4.6 days per decade. There was also evidence of a trend to a later freeze-onset date of 0.8 days per decade, but this trend was not statistically significant. This Baffin Bay finding contrasts with the case of the CAA, which was dominated by significant trends to later freeze-up, of 2.2 days per decade. The larger changes in the freeze-up period over the CAA are consistent with recent temperature trends over the region, which show the strongest warming in the October–December season (Rapačić et al., 2015). These ice changes are a reaction

to (and in turn provide positive feedbacks to) the increasing air and sea surface temperatures and changes in atmospheric circulation (Overland et al., 2012; Sharp et al., 2014) that are driving the rapid rates of climate change observed over the region in the past decade.

Analyses of U.S. National Ice Center weekly sea ice charts from 1976 to 2007 by Yu et al. (2014) show that landfast ice extent around the Arctic Basin was relatively extensive from the early to mid-1980s but then declined in many coastal

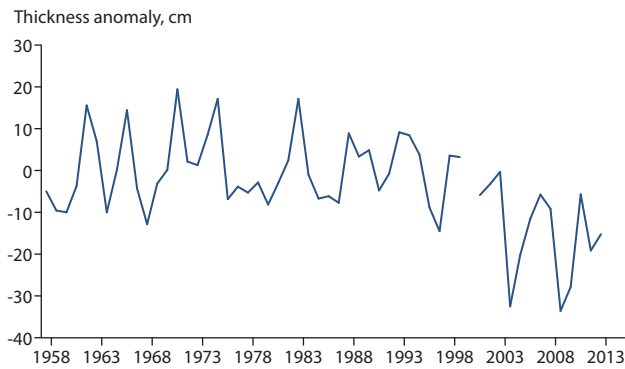


Figure 3.19 Regionally averaged annual anomalies in maximum ice thickness, 1958–2013 (with respect to a 1959–1987 average) from six Canadian BBDS stations with long-term weekly ice thickness measurements. (Ice thickness data were obtained from the Canadian Ice Service, www.ec.gc.ca/glaces-ice/.)

regions of the Arctic, particularly after the early 1990s. Yu et al. (2014) documented a 4.5% per decade decrease in winter landfast ice area over Baffin Bay over the 1976–2007 period, but this trend was not statistically significant. However, their Baffin Bay regional time series of winter landfast ice area (see Langen et al., 2016) shows a reduction of ~50% in landfast ice extent over the period 1994–2005. Analysis of Canadian landfast ice conditions with Canadian Ice Service digital charts from 1983 to 2009 by Galley et al. (2012) showed significant decreases in landfast ice cover duration over the CAA from later ice onset and/or earlier breakup. The study highlighted major reductions in landfast ice cover duration for most of Baffin Bay's coastal regions. Three BBDS communities (Arctic Bay, Pond Inlet, and Clyde River) were identified as being located in areas that were most affected by decreasing landfast ice duration. In the interior of the Northwest Passage, landfast sea ice duration was not observed to have undergone any statistically significant change over the period analyzed. These observed decreases in landfast ice duration are consistent with Inuit community observations of thinner ice and a shorter ice season (observations summarized by Gaden and Stern, 2015). The impacts of the changing ice regime on Inuit hunting are discussed in Section 6.5.2.

Analyses of weekly ice thickness data from six Canadian coastal BBDS communities with long-term weekly ice thickness measurements (since the late 1950s; Brown et al., 2018) show that maximum ice thicknesses experienced an abrupt decrease of approximately 20 cm after 2000. This decline represents about a 10% reduction in maximum thickness (Figure 3.19). The regionally averaged date of annual maximum ice thickness advanced by approximately 3 weeks over the same period in response to earlier melt.

3.1.5.2 Projected changes

CMIP5 models project a continuation of observed trends to a shorter ice season and thinner ice but with a large spread in the rate and timing of sea ice changes (Stroeve et al., 2012). Projected changes in autumn and winter ice concentration and ice thickness for RCP4.5 are shown in Figures 3.20 and 3.21, respectively. (Results for all seasons and for the RCP2.6

and RCP8.5 scenarios are shown in Langen et al., 2016.) The largest decreases in sea ice concentration (15–20% by 2080) are projected for the autumn (SON) season, related to a later freeze-up. Decreases of 10–15% are projected over most of the region in the summer (JJA), in response to earlier break-up. Winter ice thickness is projected to decrease by approximately 20–30 cm, with the largest decreases occurring in more northerly regions. A large spread in model-projected changes is evident over Baffin Bay and Foxe Basin.

It should be noted that the temporal evolution of simulated Arctic sea ice cover is strongly influenced by internal variability (Jahn et al., 2012; Stroeve et al., 2012) and that averaging over a model ensemble will smooth out the influence of those models that show early rapid ice loss events (Döscher and Koenigk, 2013). Wang and Overland (2012) determined a model consensus for nearly ice-free Arctic summers by the 2030s, using a subset of models that best represented the observed sea ice regime and historical trends. However, most of these models do not resolve the CAA and the regional ice dynamics that involve the import of multi-year ice from the Arctic Ocean (Howell et al., 2008, 2013). Sea ice change scenarios from a high-resolution coupled ice–ocean model for the Canadian Arctic (Hu and Myers, 2014) do not show completely ice-free summers in the CAA before 2100, in agreement with Sou and Flato (2009). The future response of multi-year ice in the CAA depends on other factors in addition to air temperature (Derksen et al., 2012). For the foreseeable future, ice is likely to remain a hazard for shipping (Haas and Howell, 2015). Additional simulations from high-resolution coupled ice–ocean models driven with a range of climate model outputs are needed to reach robust conclusions about the projected magnitude and timing of changes in BBDS sea ice cover in coastal waters.

3.1.6 Sea level

Relative sea level in the BBDS region is projected to fall at nearly all locations, despite projected global sea level rise. The BBDS pattern is mainly due to crustal uplift in response to past and projected ice mass decreases. For the high-emissions scenario, the projected median relative sea-level change (at 2100, relative to 1986–2005) ranges over the region from a fall of nearly 90 cm to a rise of nearly 10 cm.

3.1.6.1 Observed trends

Global sea level rose at a mean rate of 1.7 (± 0.2) mm/yr between 1901 and 2010 (Church et al. 2013a; IPCC, 2013a), with considerable decadal-scale variability of the average rate of rise during the 20th century (Church and White, 2006). Between 1993 and 2010, sea level rose at a faster rate of 3.2 (± 0.4) mm/yr (Church et al., 2013a).

Relative sea level, in contrast to global mean sea level, is the sea level experienced at a single fixed location on the earth's solid surface. Changes to relative sea level are the net effect of a combination of changes in global sea level, local vertical crustal motion, and other factors described below. If the land is rising, then (all else being equal) relative sea level is lowered; if the land is sinking, then relative sea level is increased. Vertical land

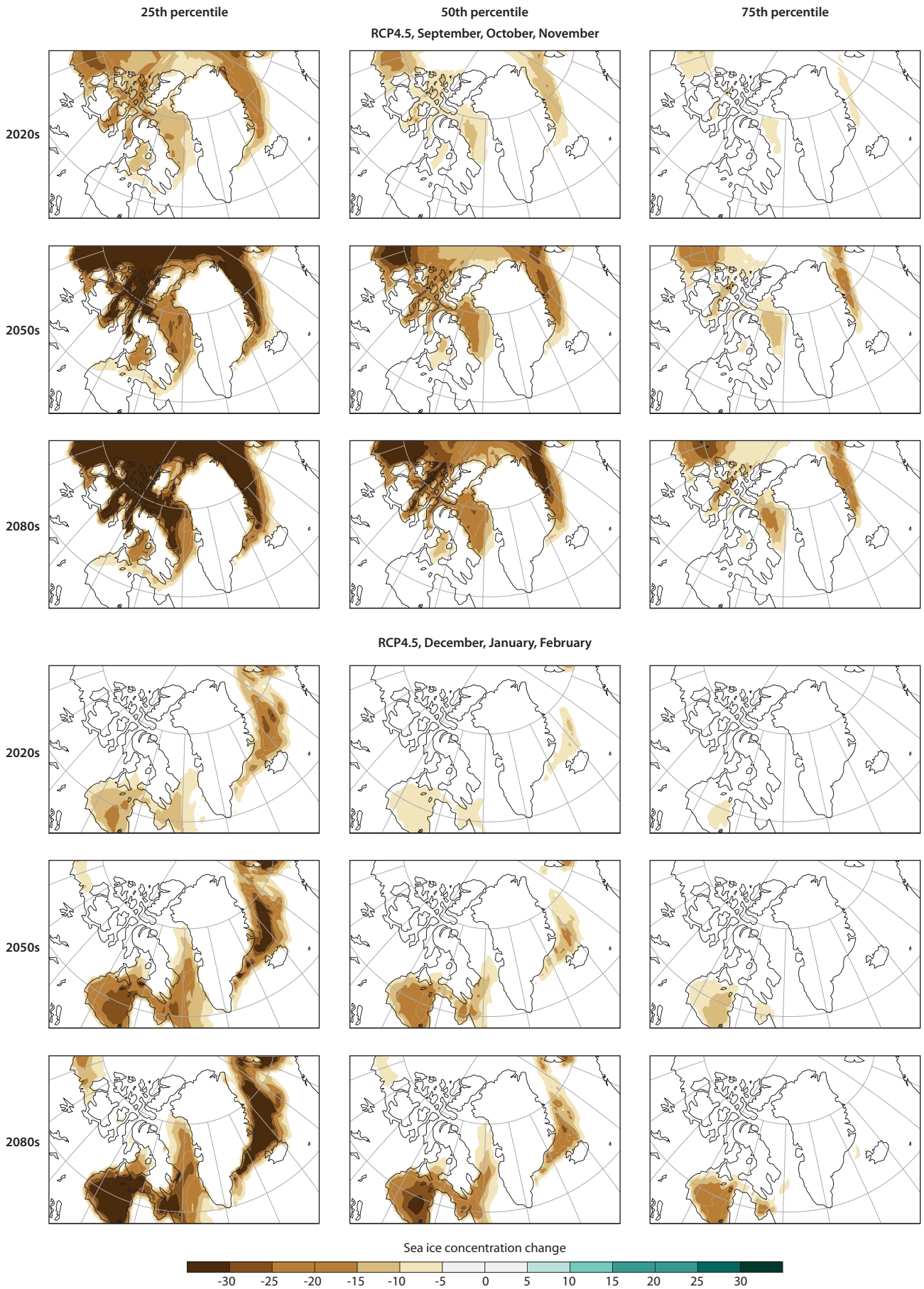


Figure 3.20 Projected change in autumn (SON) and winter (DJF) sea ice concentration (change in percent concentration relative to the 1986–2005 average) for the RCP4.5 scenario, according to a 29-member CMIP5 multi-model simulation. Results are shown for three periods in the future: 2016–2035 (labeled 2020s), 2046–2065 (labeled 2050s), and 2081–2100 (labeled 2080s). The figures illustrate the 25th, 50th, and 75th percentile changes projected by the CMIP5 models. For a list of the 29 models, see Table 4.1 of AMAP (2017a).

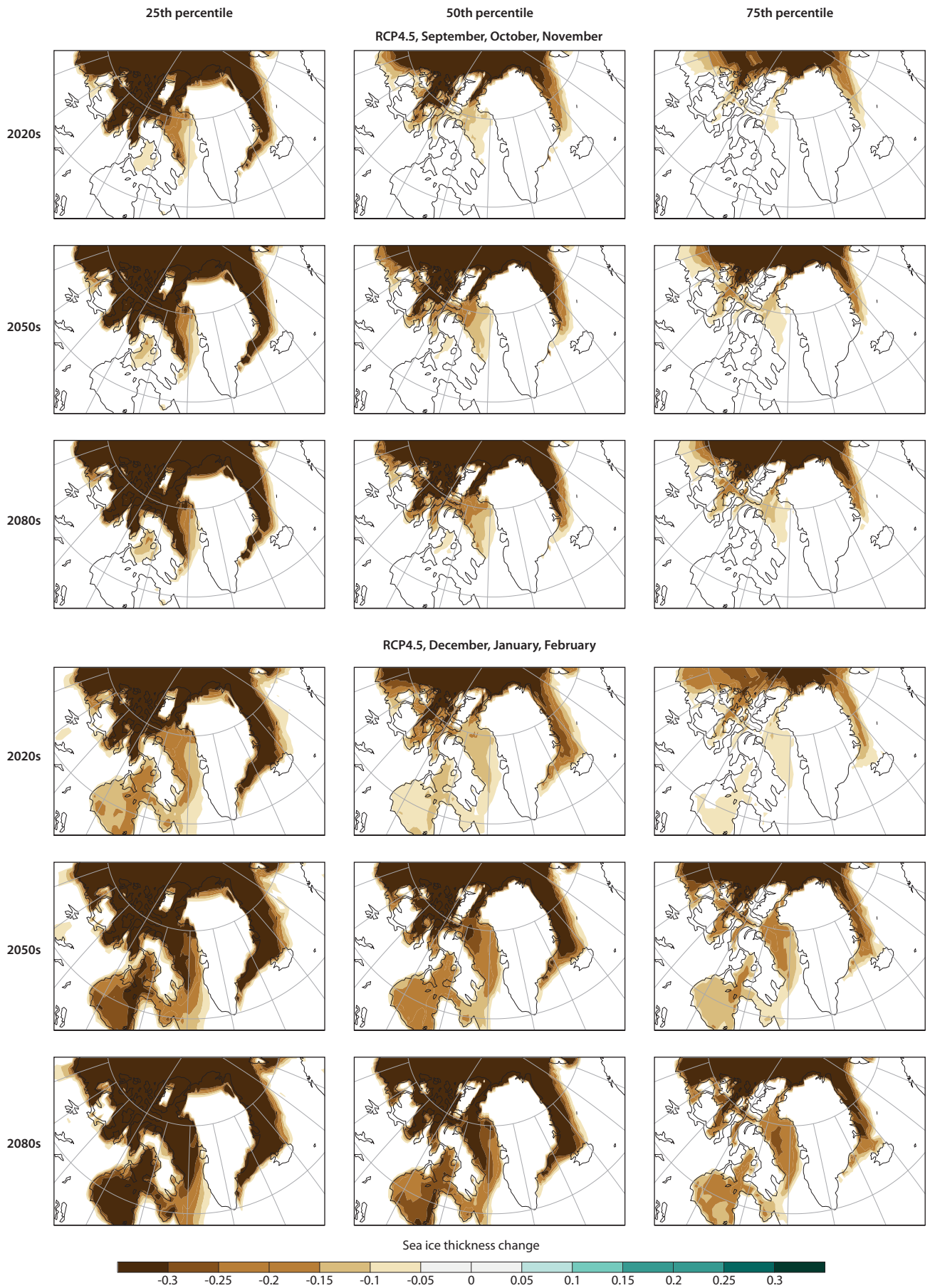


Figure 3.21 Projected change in autumn (SON) and winter (DJF) sea ice thickness (change in meters relative to the 1986–2005 average) for the RCP4.5 scenario, according to a 29-member CMIP5 multi-model simulation. See Figure 3.20 for an explanation of the panels.

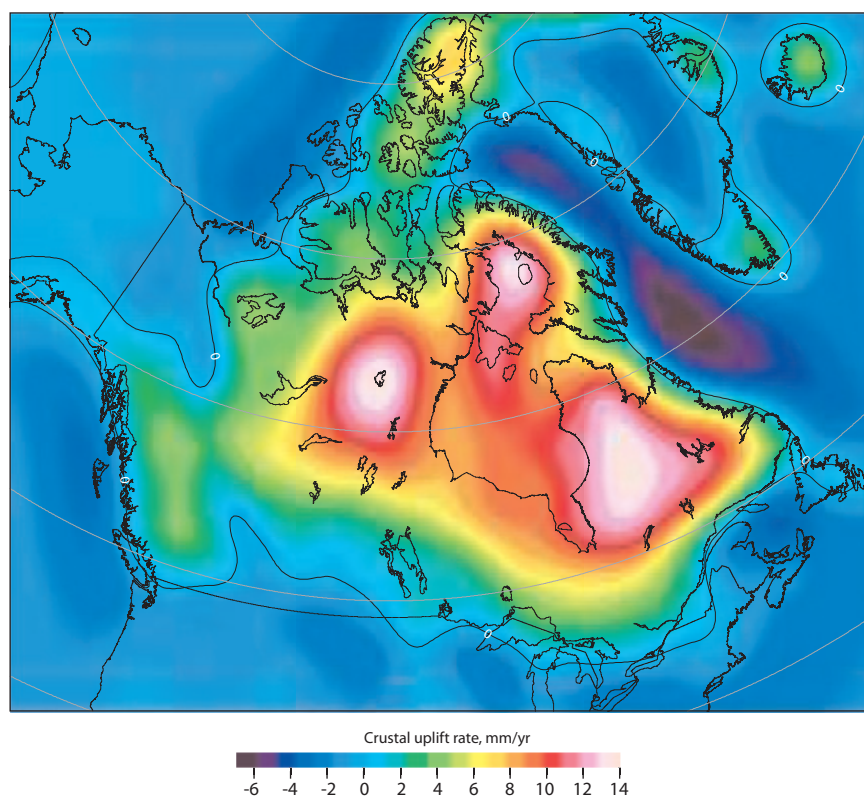


Figure 3.22 Present-day vertical crustal motion estimated by the ICE-6G glacial isostatic adjustment (GIA) model (described in Peltier et al., 2015). Regions of large uplift (warm colors) indicate former centers of the Laurentide Ice Sheet; subsiding regions (cool colors) were close to the ice-sheet margin or were peripheral to the ice sheets. In Greenland, the modest amounts of crustal uplift and subsidence are largely due to modeled changes in the Greenland Ice Sheet.

motion exerts a strong control on relative sea level changes in the Arctic region (Figure 3.22).

Glacial isostatic adjustment, also known as postglacial rebound, is the response of the solid earth to changes in glaciers and ice sheets. During ice ages, the glaciated surface of Earth is depressed beneath large ice sheets. At great depths within the planet, mantle material is displaced through slow, viscous flow. When glacial ice masses shrink and retreat, such as over much of Canada, the surface loading on the earth's surface is reduced. The earth responds, and areas that were depressed due to the weight of the ice begin to rise toward their previous elevations. This gradual process continues for thousands of years after ice loads have diminished. In regions that were once at the margins of the great ice sheets or were peripheral to the great ice sheets, the land rose during glaciation. Following deglaciation, these marginal and peripheral regions subside.

In areas such as Greenland and portions of the northern and eastern CAA, which are still glaciated, the solid earth also responds to past ice mass changes. Superposed on this viscous response to past ice mass changes is a faster elastic response of the solid earth to present-day ice mass changes. Close to ice masses that are presently undergoing large changes, this elastic crustal response can be large – up to a few millimeters per year. This response can provide a dominant contribution to observed or projected relative sea-level change.

Other factors that contribute to relative sea-level change, introducing additional spatial variability, include dynamic oceanographic effects, which add 15–20 cm to projected BBDS sea level rise by 2100 in the RCP8.5 scenario (e.g., Yin et al., 2010; Yin, 2012). The gravitational response of the ocean to ice mass changes (Mitrovica et al., 2001) is very important close

to large masses of ice that are undergoing large changes or are projected to undergo large changes. The reduced Greenland Ice Sheet, for example, now causes less gravitational upward “pull” of the surface of the ocean. Tide gauge records are sparse for the Arctic, but an intermittent record at Alert, at the northern tip of Ellesmere Island, indicates that sea level there has been falling at an average 1.5 mm/yr since the mid-1960s (Atkinson et al., 2016). In contrast, a tide gauge on the southwestern coast of Greenland at Nuuk indicates that relative sea level at that location has been rising at about 2 mm/yr for the time range 1958–2002 (Spada et al., 2014) – more slowly than the 1993–2010 global average of 3.2 mm/year (IPCC, 2013a).

3.1.6.2 Projected changes

Climate projections using the RCP scenarios (see Section 3.1.1) in the IPCC's AR5 (IPCC, 2013a) include global mean sea level change. Global sea level at 2100 is projected to be higher by 36–71 cm (RCP4.5) to 52–98 cm (RCP8.5), relative to 1986–2005 (Table 13.5 in Church et al., 2013a). In the BBDS region, relative sea-level projections depart strongly from global values and site-specific projections are required.

Relative sea-level projections have been generated for the Canadian side of the BBDS region (James et al., 2014, 2015). These projections utilized regional sea-level projections provided by the AR5 (Church et al., 2013b), incorporated vertical crustal motion from global positioning system (GPS) observations (James et al., 2014), and included regional dynamic oceanographic effects and the elastic crustal and gravitational effects of changing ice masses.

Under the high-emissions scenario (RCP8.5), relative sea level by 2100 is projected to fall at nearly all locations in the region

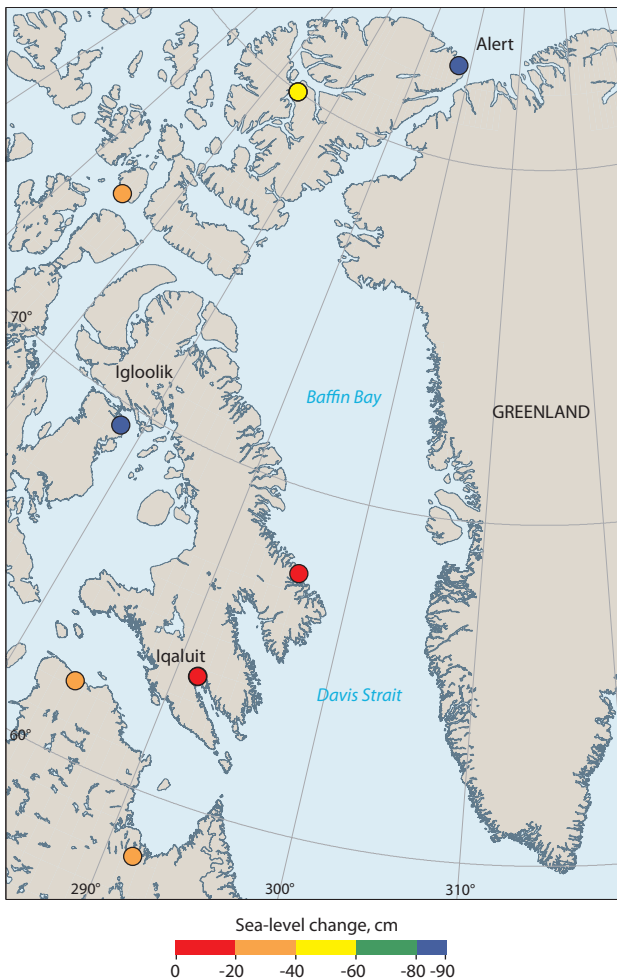


Figure 3.23 Projected relative sea-level change at the year 2100 (in cm) for the median RCP8.5 value at coastal locations in the Canadian sector of the Baffin Bay/Davis Strait region (after James et al., 2014). Values range from -84 cm to -1 cm and are relative to 1986–2005. Locations mentioned in the text are labeled.

(Figure 3.23), even though mean global sea level will have risen significantly by then. The projected sea level fall results from the combination of large amounts of crustal uplift at some sites, due to glacial isostatic adjustment (for example, Igloolik is measured to be rising at about 11.5 mm/yr, generating large projected sea level fall) and proximity to the Greenland Ice Sheet, which is projected to lose mass through the 21st century (Section 3.1.3). This latter effect is particularly strong at Alert, which is close to the Greenland Ice Sheet and has large values of projected sea level fall. Although proximity to the changing ice sheet makes detailed relative sea-level projections for sites on the Greenland coast less accurate under the present analysis, sea-level projections for western Greenland are also strongly negative (Church et al., 2013a).

Projections through the 21st century for Iqaluit (Figure 3.24, upper panel) show that the RCP8.5 projected relative sea level is higher (more positive) than the RCP4.5 case, similar to global projections in which larger emissions scenarios give larger projected global sea level rise. This correspondence is generally expected and projected at most locations. An exception is seen at Alert (Figure 3.24, lower panel), where the largest emissions scenario (RCP8.5) has the largest amount of projected relative sea-level fall. Here, the elastic crustal

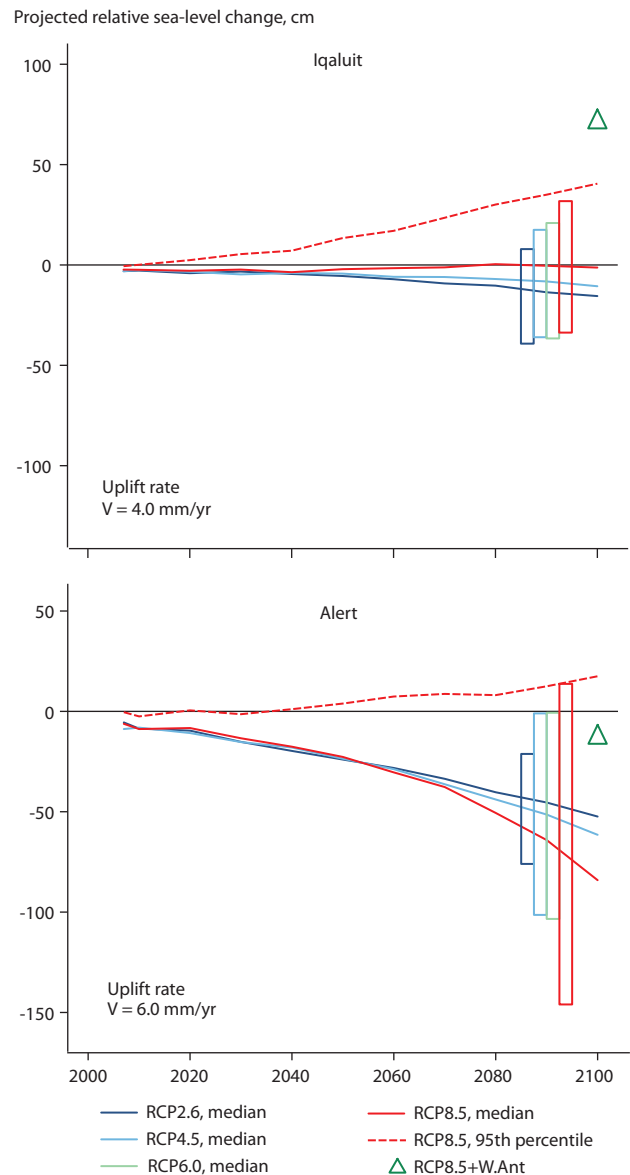


Figure 3.24 Projected relative sea-level change for Iqaluit and Alert (after James et al., 2014), based on the IPCC AR5 (Church et al., 2013a, 2013b) and also vertical crustal motion (uplift rate, given to nearest 0.5 mm/yr) derived from GPS observations. Projections are given through the century for the RCP2.6, RCP4.5, and RCP8.5 scenarios. The rectangles show the 90% confidence interval (5% to 95%) of the average projection for the period 2081–2100 for each of those three scenarios and also RCP6.0. The dashed red line gives the 95th percentile value for RCP8.5. The projected value at 2100 is also given for a scenario in which West Antarctica contributes an additional 65 cm of global sea level rise, added to the median projection of RCP8.5 (RCP8.5+W.Ant; green triangle).

response to projected shrinking of the ice sheet gives larger amounts of crustal uplift for larger scenarios, thus leading to larger amounts of projected sea level fall. This phenomenon is also expected for western Greenland.

For Iqaluit, uncertainties are such that sea level rise or fall on the order of 40 cm is possible for all RCP scenarios; at Alert, sea level fall is favored. A scenario that considers the effect of an additional 65 cm contribution to global sea level rise from partial collapse of the West Antarctic ice sheet, added to the median projection of RCP8.5, provides larger amounts of projected sea level rise or reduced amounts of sea level fall (green triangles in Figure 3.24).

Acknowledgments

We thank Robin Rong (Canadian Centre for Climate Modelling and Analysis) for generating the sea ice plots, Nicolas Lambert (Maurice-Lamontagne Institute, Fisheries and Oceans Canada) for preparing ocean model projection plots, and Rasmus A. Pedersen (Danish Meteorological Institute) for providing the near-surface air temperature percentile change maps. We would further like to acknowledge the Geological Survey of Canada, Natural Resources Canada, for supplying the borehole data for Arctic stations. The authors are also grateful to the Permafrost Laboratory of the University of Alaska for supplying the GIPL2 projections and to the CCSM4 GCM team and sponsors for supplying the permafrost model forcing data. This subchapter is Earth Sciences Sector (ESS) contribution number 20150100 of the Geological Survey of Canada.

References

- Alexander, L.V., X. Zhang, T.C. Peterson, J. Caesar, B. Gleason, A.M.G. Klein Tank, M. Haylock, D. Collins, B. Trewin, F. Rahimzadeh, A. Tagipour, K. Rupa Kumar, J. Revadekar, G. Griffiths, L. Vincent, D.B. Stephenson, J. Burn, E. Aguilar, M. Brunet, M. Taylor, M. New, P. Zhai, M. Rusticucci and J.L. Vazquez-Aguirre, 2006. Global observed changes in daily climate extremes of temperature and precipitation. *Journal of Geophysical Research*, 111:D05109, doi:10.1029/2005JD006290.
- Allard, M. and M. Lemay, 2012. Nunavik and Nunatsiavut: From Science to Policy. An Integrated Regional Impact Study (IRIS) of Climate Change and Modernization. ArcticNet Inc., Quebec City, Canada. 303pp.
- AMAP, 2011. Snow, Water, Ice and Permafrost in the Arctic (SWIPA): Climate Change and the Cryosphere. Arctic Monitoring and Assessment Programme (AMAP), Oslo, Norway. xii + 538pp.
- AMAP, 2017a. Adaptation Actions for a Changing Arctic: Perspectives from the Bering-Chukchi-Beaufort Region. Arctic Monitoring and Assessment Programme (AMAP), Oslo, Norway. xiv + 255pp.
- AMAP, 2017b. Snow, Water, Ice and Permafrost in the Arctic (SWIPA) 2017. Arctic Monitoring and Assessment Programme (AMAP), Oslo, Norway. xiv + 269pp.
- Amundson J.M., M. Fahnestock, M. Truffer, J. Brown, M.P. Lüthi and R.J. Motyka, 2010. Ice mélange dynamics and implications for terminus stability, Jakobshavn Isbræ, Greenland. *Journal of Geophysical Research*, 115:F01005.
- Andersen, M.L., L. Stenseng, H. Skourup, W. Colgan, S.A. Khan, S.S. Kristensen, S.B. Andersen, J.E. Box, A.P. Ahlstrøm, X. Fettweis and R. Forsberg, 2015. Basin-scale partitioning of Greenland ice sheet mass balance components (2007–2011). *Earth and Planetary Science Letters*, 409:89–95.
- Arrhenius, S., 1896. On the influence of carbonic acid in the air upon the temperature of the ground. *Philosophical Magazine Series 5*, 41(251):237–276.
- Atkinson, D.E., D.L. Forbes and T.S. James, 2016. Dynamic coasts in a changing climate. In: Lemmen, D.S., F.J. Warren, T.S. James and C.S.L. Mercer Clarke (Eds.). *Canada's Marine Coasts in a Changing Climate*, pp. 27–68. Government of Canada, Ottawa.
- Bamber, J., M. van den Broeke, J. Ettema, J. Lenaerts and E. Rignot, 2012. Recent large increases in freshwater fluxes from Greenland into the North Atlantic. *Geophysical Research Letters*, 39:L19501, doi:10.1029/2012GL052552.
- Barber, D.G. and R.A. Massom, 2007. The role of sea ice in Arctic and Antarctic polynyas. In: Smith, W.O. and D.G. Barber (Eds.). *Polynyas: Windows to the World*, pp. 1–54. Volume 74, Elsevier Oceanography Series, doi:10.1016/S0422-9894(06)74001-6.
- Barber, D., W. Meier and T. Lavergne, 2017. Arctic sea ice. In: *Snow, Water, Ice, Permafrost in the Arctic (SWIPA) 2017*. Arctic Monitoring and Assessment Programme (AMAP), Oslo, Norway.
- Barnes, E.A. and L.M. Polvani, 2015. CMIP5 projections of Arctic amplification, of the North American/North Atlantic circulation, and of their relationship. *Journal of Climate*, 28:5254–5271.
- Barrette, C., 2013. Initial Climate Change Projections for the Eastern Arctic, IRIS 2 Region. ArcticNet internal report. 26pp.
- Beltaos, S. and T. Prowse, 2009. River-ice hydrology in a shrinking cryosphere. *Hydrological Processes*, 23:122–144.
- Bengtsson, L., K.I. Hodges and E. Roeckner, 2006. Storm tracks and climate change. *Journal of Climate*, 19:3518–3543, doi:10.1175/JCLI3815.1.
- Bergeron, M. and J.-É. Tremblay, 2014. Shifts in biological productivity inferred from nutrient drawdown in the southern Beaufort Sea (2003–2011) and northern Baffin Bay (1997–2011), Canadian Arctic. *Geophysical Research Letters*, 41:3979–3987.
- Bezeau, P., M.J. Sharp and G. Gascon, 2015. Variability in summer anticyclonic circulation over the Canadian Arctic Archipelago and west Greenland in the late 20th/early 21st centuries and its effect on glacier mass balance. *International Journal of Climatology*, 35(4):540–557.
- Bigg, G.R., H.L. Wei, D.J. Wilton, Y. Zhao, S.A. Billings, E. Hanna and V. Kadiramanathan, 2014. A century of variation in the dependence of Greenland iceberg calving on ice sheet surface mass balance and regional climate change. *Proceedings of the Royal Society A: Mathematical, Physical and Engineering Sciences*, 470:20130662, doi:10.1098/rspa.2013.0662.
- Bintanja, R. and F.M. Selten, 2014. Future increases in Arctic precipitation linked to local evaporation and sea-ice retreat. *Nature*, 509:479–482.

- Bjella, K., 2012. Thule Air Base Airfield White Painting and Permafrost Investigation. ERDC/CRELL Technical Report TR-12.
- Blanchet, J.-P. and R. List, 1983. Estimation of optical properties of Arctic haze using a numerical model. *Atmosphere-Ocean*, 21(4):444-465, doi:10.1080/07055900.1983.9649179.
- Bokhorst, S., S.H. Pedersen, L. Brucker, O. Anisimov, J.W. Bjerke, R.D. Brown, D. Ehrich, R. Essery, A. Heilig, S. Ingvander and C. Johansson, 2016. Changing Arctic snow cover: A review of recent developments and assessment of future needs for observations, modelling, and impacts. *Ambio*, 45(5):516-537.
- Boon, S., D.O. Burgess, R.M. Koerner and M.J. Sharp, 2010. Forty-seven years of research on the Devon Island ice cap, Arctic Canada. *Arctic*, 63:13-29, doi:10.2307/40513366.
- Box, J.E., 2013. Greenland ice sheet mass balance reconstruction. Part II: Surface mass balance (1840-2010). *Journal of Climate*, 26:6974-6989.
- Box, J., M. Sharp, G. Aðalgeirsdóttir, M. Ananicheva, M.L. Andersen, R. Carr, G. Moholdt, C. Clason, W.T. Colgan, L. Copland, A. Glazovsky, A. Hubbard, K.K. Kjeldsen, B. Wouters, T. Wagner, and W. Van Wychen, 2017. Changes to Arctic land ice. In: *Snow, Water, Ice, Permafrost in the Arctic (SWIPA) 2017. Arctic Monitoring and Assessment Programme (AMAP)*, Oslo, Norway.
- Brown, L. and C.R. Duguay, 2010. The response and role of ice cover in lake-climate interactions. *Progress in Physical Geography*, 34(5):671-704, doi:10.1177/0309133310375653.
- Brown, L.C. and C.R. Duguay, 2011. The fate of lake ice in the North American Arctic. *The Cryosphere*, 5:869-892, doi:10.5194/tc-5-869-2011.
- Brown, R.D. and P.W. Mote, 2009. The response of Northern Hemisphere snow cover to a changing climate. *Journal of Climate*, 22:2124-2145, doi:10.1175/2008JCLI2665.1.
- Brown, J., O. Ferrians, J.A. Heginbottom and E. Melnikov, 2014. Circum-Arctic Map of Permafrost and Ground-Ice Conditions, extent data subset. National Snow and Ice Data Center, Boulder, USA. nsidc.org/data/docs/fgdc/ggd318_map_circumarctic/
- Brown, R., D. Vikhamar-Schuler, O. Bulygina, C. Derksen, K. Luoju, L. Mudryk, L. Wang and D. Yang, 2017. Arctic terrestrial snow cover. In: *Snow, Water, Ice and Permafrost in the Arctic (SWIPA) 2017*, pp. 25-64. Arctic Monitoring and Assessment Programme (AMAP), Oslo, Norway.
- Brown, R., C. Barrette, L. Brown, D. Chaumont, P. Grenier, S. Howell and M. Sharp, 2018. Climate variability, trends and projected change for the eastern Canadian Arctic. In: Bell, T. and T.M. Brown (Eds.). *From Science to Policy in the Eastern Canadian Arctic: An Integrated Regional Impact Study (IRIS) of Climate Change and Modernization*. ArcticNet, Quebec City.
- Canadian Ice Centre, 1992. *Ice Thickness Climatology, 1961-1990 Normals*. Ice Climatology Services Report Ice 2-91. Supply and Services Canada, Catalogue No. En57-28/1961-1990. 277pp.
- Canadian Ice Service, 2011a. *Sea Ice Climatic Atlas for the Northern Canadian Waters 1981-2010*. Ottawa. 995pp. www.ec.gc.ca/glaces-ice/?lang=En&n=4B35305B-1
- Canadian Ice Service, 2011b. Ice charts. In: *Sea Ice Climatic Atlas for the Northern Canadian Waters 1981-2010*. Last modified 4 October 2013. www.ec.gc.ca/glaces-ice/default.asp?lang=En&n=4B35305B-1&offset=3&toc=show
- Castro de la Guardia, L., X. Hu and P.G. Myers, 2015. Potential positive feedback between Greenland Ice Sheet melt and Baffin Bay heat content on the west Greenland shelf. *Geophysical Research Letters*, 42(12):4922-4930, doi:10.1002/2015GL064626.
- Cavalieri, D., C. Parkinson, P. Gloersen and H.J. Zwally, 1996, updated yearly. Sea Ice Concentrations from Nimbus-7 SMMR and DMSP SSM/I-SSMIS Passive Microwave Data. NASA DAAC at the National Snow and Ice Data Center, Boulder, USA. Accessed 07 November 2013. doi:10.5067/8GQ8LZQVL0VL.nsidc.org/data/docs/daac/nsidc0051_gsfsc_seaice.gd.html
- Charron, I., 2014. *A Guidebook on Climate Scenarios: Using Climate Information to Guide Adaptation Research and Decisions*. Ouranos. 86pp. www.ouranos.ca/publication-scientifique/GuideCharron2014_EN.pdf
- Cheng, C.S., E. Lopes, C. Fu and Z. Huang, 2014. Possible impacts of climate change on wind gusts under downscaled future climate conditions: Updated for Canada. *Journal of Climate*, 27:1255-1270.
- Christensen, J.H., M. Olesen, F. Boberg, M. Stendel and I. Koldtoft, 2015. *Future Climate Change in Greenland*. DMI Scientific Report 15-04. (In Danish). www.dmi.dk/laer-om/generelt/dmi-publikationer/videnskabelige-rapporter
- Christiansen, H.H., B. Eitzelmüller, K. Isaksen, H. Juliussen, H. Farbrot, O. Humlum, M. Johansson, T. Ingeman-Nielsen, L. Kristensen, J. Hjort, P. Holmlund, A.B.K. Sannel, C. Sigsgaard, H.J. Åkerman, N. Foged, L.H. Blikra, M.A. Pernosky and R.S. Ødegård, 2010. The thermal state of permafrost in the Nordic area during the International Polar Year 2007-2009. *Permafrost and Periglacial Processes*, 21:156-181, doi:10.1002/ppp.687.
- Church, J.A. and N.J. White, 2006. A 20th century acceleration in global sea-level rise. *Geophysical Research Letters*, 33:L01602, doi:10.1029/2005GL024826.
- Church, J.A., P.U. Clark, A. Cazenave, J.M. Gregory, S. Jevrejeva, A. Levermann, M.A. Merrifield, G.A. Milne, R.S. Nerem, P.D. Nunn, A.J. Payne, W.T. Pfeffer, D. Stammer and A.S. Unnikrishnan, 2013a. Sea level change. In: *Climate Change 2013: The Physical Science Basis*, pp. 1137-1216. Contribution of Working Group I to the Fifth Assessment Report of the Intergovernmental Panel on Climate Change (IPCC). Stocker, T.F., D. Quin, G.K. Plattner, M. Tignor, S.K. Allen, J. Boschung, A. Nauels, Y. Xia, V. Bex and P.M. Migdale (Eds.). Cambridge

University Press. www.ipcc.ch/pdf/assessment-report/ar5/wg1/WG1AR5_Chapter13_FINAL.pdf

Church, J.A., P.U. Clark, A. Cazenave, J.M. Gregory, S. Jevrejeva, A. Levermann, M.A. Merrifield, G.A. Milne, R.S. Nerem, P.D. Nunn, A.J. Payne, W.T. Pfeffer, D. Stammer and A.S. Unnikrishnan, 2013b. Sea level change supplementary material. In: *Climate Change 2013: The Physical Science Basis*, pp. 13SM-1-13SM-8. Contribution of Working Group I to the Fifth Assessment Report of the Intergovernmental Panel on Climate Change (IPCC). Stocker, T.F., D. Qin, G.K. Plattner, M. Tignor, S.K. Allen, J. Boschung, A. Nauels, Y. Xia, V. Bex and P.M. Migdley (Eds.). Cambridge University Press. www.ipcc.ch/pdf/assessment-report/ar5/wg1/supplementary/WG1AR5_Ch13SM_FINAL.pdf

Coles, S., 2001. *An Introduction to Statistical Modeling of Extreme Values*. Springer Series in Statistics. 208pp.

Cook, J., D. Nuccitelli, S.A. Green, M. Richardson, B. Winkler, R. Painting, R. Way, P. Jacobs and A. Skuce, 2013. Quantifying the consensus on anthropogenic global warming in the scientific literature. *Environmental Research Letters*, 8(2):024024, doi:10.1088/1748-9326/8/2/024024.

Cuerrier, A., N.D. Brunet, J. Gérin-Lajoie, A. Downing and E. Lévesque, 2015. The study of Inuit knowledge of climate change in Nunavik, Quebec: A mixed methods approach. *Human Ecology*, 43(3):379-394.

Curry, B., C.M. Lee, B. Petrie, R.E. Moritz and R. Kwok, 2014. Multiyear volume, liquid freshwater, and sea ice transports through Davis Strait, 2004-10. *Journal of Physical Oceanography*, 44:1244-1266, doi:10.1175/JPO-D-13-0177.1.

Deming, J.W., L. Fortier, and M. Fukuchi, 2002. The International North Water Polynya Study (NOW): A brief overview. *Deep-Sea Research II*, 49(22-23):4887-4892, doi:10.1016/S0967-0645(02)00168-6.

Derksen, C., S.L. Smith, M. Sharp, L. Brown, S. Howell, L. Copland, D.R. Mueller, Y. Gauthier, C. Fletcher, A. Tivy, M. Bernier, J. Bourgeois, R. Brown, C.R. Burn, C. Duguay, P. Kushner, A. Langlois, A.G. Lewkowicz, A. Royer, and A. Walker, 2012. Variability and change in the Canadian cryosphere. *Climatic Change*, 115:59-88, doi:10.1007/s10584-012-0470-0.

Deser, C., A.S. Phillips, M.A. Alexander and B.V. Smoliak, 2014. Projecting North American climate over the next 50 years: Uncertainty due to internal variability. *Journal of Climate*, 27:2271-2296, doi:10.1175/JCLI-D-13-00451.1.

Dibike, Y., T. Prowse, T. Saloranta and R. Ahmed, 2011. Response of Northern Hemisphere lake-ice cover and lake-water thermal structure patterns to a changing climate. *Hydrological Processes*, 25(19):2942-2953.

Dibike, Y., T. Prowse, B. Bonsal, L.D. Rham and T. Saloranta, 2012. Simulation of North American lake-ice cover characteristics under contemporary and future climate conditions. *International Journal of Climatology*, 32(5):695-709.

Dobrynin, M., J. Murawsky and S. Yang, 2012. Evolution of the global wind wave climate in CMIP5 experiments. *Geophysical Research Letters*, 39:L18606, doi:10.1029/2012GL052843.

Donat, M.G., L.V. Alexander, H. Yang, I. Durre, R. Vose, R.J.H. Dunn, K.M. Willett, E. Aguilar, M. Brunet, J. Caesar, B. Hewitson, C. Jack, A.M.G. Klein Tank, A.C. Kruger, J. Marengo, T.C. Peterson, M. Renom, C. Oria Rojas, M. Rusticucci, J. Salinger, A.S. Elayah, S.S. Sekele, A.K. Srivastava, B. Trewin, C. Villarreal, L.A. Vincent, P. Zhai, X. Zhang and S. Kitching, 2013. Updated analyses of temperature and precipitation extreme indices since the beginning of the twentieth century: The HadEX2 dataset. *Journal of Geophysical Research: Atmospheres*, 118(5):2098-2118.

Döscher, R. and T. Koenigk, 2013. Arctic rapid sea ice loss events in regional coupled climate scenario experiments. *Ocean Science*, 9(2):217-248.

Dumont, D., Y. Gratton and T.E. Arbetter, 2010. Modeling wind-driven circulation and landfast ice-edge processes during polynya events in northern Baffin Bay. *Journal of Physical Oceanography*, 40:1356-1372.

Dunne, J. P., J.G. John, A.J. Adcroft, S.M. Griffies, R.W. Hallberg, E. Shevliakova, R.J. Stouffer, W. Cooke, K.A. Dunne, M.J. Harrison, J.P. Krasting, S.L. Malyshev, P.C.D. Milly, P.J. Phillips, L.T. Sentman, B.L. Samuels, M.J. Spelman, M. Winston, A.T. Wittenberg and N. Zadeh, 2012. GFDL's ESM2 global coupled climate-carbon earth system models. Part I: Physical formulation and baseline simulation characteristics. *Journal of Climate*, 25(19):6646-6665, doi:10.1175/Jcli-D-11-00560.1.

Ednie, M. and S.L. Smith, 2010. Establishment of community-based permafrost monitoring sites, Baffin Region, Nunavut. In: *Geo2010, 63rd Canadian Geotechnical Conference & 6th Canadian Permafrost Conference*, pp. 1205-1211. Calgary.

Ednie, M. and S.L. Smith, 2011. Establishment of Community-based Permafrost Monitoring Sites and Initial Ground Thermal Data, Baffin Region, Nunavut, Ottawa. Geological Survey of Canada, Open File 6727, doi:10.4095/287873. geoscan.nrcan.gc.ca/starweb/geoscan/servlet.starweb?path=geoscan/shorte.web&search1=R=287873

Ednie, M. and S.L. Smith, 2015. Permafrost Temperature Data 2008-2014 From Community-based Monitoring Sites in Nunavut. Geological Survey of Canada, Open File 7784, doi:10.4095/296705. geoscan.nrcan.gc.ca/starweb/geoscan/servlet.starweb?path=geoscan/fulle.web&search1=R=296705

Enderlin, E.M., I.M. Howat, S. Jeong, M.-J. Noh, J.H. van Angelen and M.R. van den Broeke, 2014. An improved mass budget for the Greenland ice sheet. *Geophysical Research Letters*, 41:866-872.

Estilow, T.W., A.H. Young and D.A. Robinson, 2015. A long-term Northern Hemisphere snow cover extent data record for climate studies and monitoring. *Earth System Science Data*, 7:137-142.

- Fettweis, X., E. Hanna, C. Lang, A. Belleflamme, M. Erpicum and H. Gallée, 2013. Brief communication: Important role of the mid-tropospheric atmospheric circulation in the recent surface melt increase over the Greenland Ice Sheet. *The Cryosphere*, 7(1):241-248, doi:10.5194/tc-7-241-2013.
- Fyke, J.G., M. Vizcaíno, W. Lipscomb and S. Price, 2014a. Future climate warming increases Greenland ice sheet surface mass balance variability. *Geophysical Research Letters*, 41:470-475, doi:10.1002/2013GL058172.
- Fyke, J.G., M. Vizcaíno and W.H. Lipscomb, 2014b. The pattern of anthropogenic signal emergence in Greenland Ice Sheet surface mass balance. *Geophysical Research Letters*, 41:6002-6008, doi:10.1002/2014GL060735.
- Gaden, A. and G.A. Stern, 2015. Navigating the North: A snapshot of the western and central Canadian Arctic. In: Stern, G.A. and A. Gaden (Eds.). *From Science to Policy in the Western and Central Canadian Arctic: An Integrated Regional Impact Study (IRIS) of Climate Change and Modernization*, chapter 1. ArcticNet, Quebec City.
- Galley, R.J., B.G.T. Else, S.E.L. Howell, J.V. Lukovich and D.G. Barber, 2012. Landfast sea ice conditions in the Canadian Arctic: 1983-2009. *Arctic*, 65:133-144.
- Gardner, A.S., G. Moholdt, B. Wouters, G.J. Wolken, D.O. Burgess, M.J. Sharp, J.G. Cogley, C. Braun and C. Labine, 2011. Sharply increased mass loss from glaciers and ice caps in the Canadian Arctic Archipelago. *Nature*, 473:357-360, doi:10.1038/nature10089.
- Gardner, A.S., G. Moholdt, J.G. Cogley, B. Wouters, A.A. Arendt, J. Wahr, E. Berthier, R. Hock, W.T. Pfeffer, G. Kaser, S.R. Ligtenberg, T. Bolch, M.J. Sharp, J.-O. Hagen, M. van den Broeke and F. Paul, 2013. A reconciled estimate of glacier contributions to sea level rise: 2003-2009. *Science*, 340:852-857.
- Gascon, G., M. Sharp, D. Burgess, P. Bezeau and A.B.G. Bush, 2013. Changes in accumulation-area firn stratigraphy and meltwater flow during a period of climate warming: Devon Ice Cap, Nunavut, Canada. *Journal of Geophysical Research: Earth Surface*, 118:2380-2391, doi:10.1002/2013JF002838.
- Gastineau, G. and B.J. Soden, 2009. Model projected changes of extreme wind events in response to global warming. *Geophysical Research Letters*, 36:L10810, doi:10.1029/2009GL037500.
- Gent, P.R., G. Danabasoglu, L.J. Donner, M.M. Holland, E.C. Hunke, S.R. Jayne, D.M. Lawrence, R.B. Neale, P.J. Rasch, M. Vertenstein, P.H. Worley, Z.L. Yang and M. Zhang, 2011. The Community Climate System Model version 4. *Journal of Climate*, 24:4973-4991, doi:10.1175/2011JCLI4083.1.
- Gorter, W., J.H. van Angelen, J.T.M. Lenaerts and M.R. van den Broeke, 2014. Present and future near-surface wind climate of Greenland from high resolution regional climate modelling. *Climate Dynamics*, 42:1595, doi:10.1007/s00382-013-1861-2.
- Grenier, P., R. de Elía and D. Chaumont, 2015. Chances of short-term cooling estimated from a selection of CMIP5-based climate scenarios during 2006-35 over Canada. *Journal of Climate*, 28:3232-3249, doi:10.1175/JCLI-D-14-00224.1.
- Haas, C. and S.E.L. Howell, 2015. Ice thickness in the Northwest Passage. *Geophysical Research Letters*, 42:7673-7680, doi:10.1002/2015GL065704.
- Hamilton, J.M. and Y. Wu, 2013. Synopsis and Trends in the Physical Environment of Baffin Bay and Davis Strait. *Canadian Technical Report of Hydrography and Ocean Sciences* 282. vi + 39pp.
- Harris, I., P.D. Jones, T.J. Osborn and D.H. Lister, 2014. Updated high-resolution grids of monthly climatic observations - the CRU TS3.10 dataset. *International Journal of Climatology*, 34:623-642, doi:10.1002/joc.3711.
- Harrison, W.G., T. Platt and B. Irwin, 1982. Primary production and nutrient assimilation by natural phytoplankton populations of the eastern Canadian Arctic. *Canadian Journal of Fisheries and Aquatic Sciences*, 39(2):335-345.
- Harvey, B.J., L.C. Shaffrey and T.J. Woollings, 2013. Equator-to-pole temperature differences and the extra-tropical storm track responses of the CMIP5 climate models. *Climate Dynamics*, 43:1171-1182, doi:10.1007/s00382-013-1883-9.
- Hawkins, E. and R. Sutton, 2009. The potential to narrow uncertainty in regional climate predictions. *Bulletin of the American Meteorological Society*, 90:1095-1107, doi:10.1175/2009BAMS2607.1.
- Helfrich, S.R., D. McNamara, B.H. Ramsay, T. Baldwin and T. Kasheta, 2007. Enhancements to, and forthcoming developments in the Interactive Multisensor Snow and Ice Mapping System (IMS). *Hydrological Processes*, 21:1576-1586, doi:10.1002/hyp.6720.
- Hewitson, B.C., J. Daron, R.B. Crane, M.F. Zermoglio and C. Jack, 2014. Interrogating empirical-statistical downscaling. *Climatic Change*, 122(4):539-554.
- Hinzman, L.D., C.J. Deal, A.D. McGuire, S.H. Mernild, I.V. Polyakov and J.E. Walsh, 2013. Trajectory of the Arctic as an integrated system. *Ecological Applications*, 23(8):1837-1868.
- Holland, M.M., J. Finnis, A.P. Barrett and M.C. Serreze, 2007. Projected changes in Arctic Ocean freshwater budgets. *Journal of Geophysical Research*, 112:GO4S55, doi:10.1029/2006JG000354.
- Holland, D.M., R.H. Thomas, B. De Young, M.H. Ribergaard and B. Lyberth, 2008. Acceleration of Jakobshavn Isbræ triggered by warm subsurface ocean waters. *Nature Geoscience*, 1:659-664.
- Hopkinson, R.F., D.W. McKenney, E.J. Milewska, M.F. Hutchinson, P. Papadopol and L.A. Vincent, 2011. Impact of aligning climatological day on gridding daily maximum-minimum temperature and precipitation over Canada. *Journal*

of Applied Meteorology and Climatology, 50(8):1654-1665, doi:10.1175/2011JAMC2684.1.

Howell, S.E.L., A. Tivy, J.J. Yackel, B.G.T. Else and C.R. Duguay, 2008. Changing sea ice melt parameters in the Canadian Arctic Archipelago: Implications for the future presence of multiyear ice. *Journal of Geophysical Research*, 113:C09030, doi:10.1029/2008JC004730.

Howell, S.E.L., C.R. Duguay and T. Markus, 2009. Sea ice conditions and melt season duration variability within the Canadian Arctic Archipelago: 1979-2008. *Geophysical Research Letters*, 36:L10502, doi:10.1029/2009GL037681.

Howell, S.E.L., T. Wohlleben, M. Daboor, C. Derksen, A. Komarov and L. Pizzolato, 2013. Recent changes in the exchange of sea ice between the Arctic Ocean and the Canadian Arctic Archipelago. *Journal of Geophysical Research: Oceans*, 118: doi:10.1002/jgrc.20265.

Hu, X. and P.G. Myers, 2014. Changes to the Canadian Arctic Archipelago sea ice and freshwater fluxes in the twenty-first century under the Intergovernmental Panel on Climate Change A1B climate scenario. *Atmosphere-Ocean*, 52:331-350, doi:10.1080/07055900.2014.942592.

Huard, D., D. Chaumont, T. Logan, M.-F. Sottile, R.D. Brown, B. Gauvin St-Denis, P. Grenier and M. Braun, 2014. A decade of climate scenarios: The Ouranos Consortium modus operandi. *Bulletin of the American Meteorological Society*, 95:1213-1225, doi:10.1175/BAMS-D-12-00163.1.

Ingeman-Nielsen, T., N. Foged, V. Romanovsky, S. Marchenko, R. Daanen and K.H. Svendsen, 2010. Geotechnical implications of a warming climate in Greenland evaluated on the basis of permafrost temperature reanalysis and model projections. In: *Proceedings of the 3rd European Conference on Permafrost*, p. 612533.

IPCC, 2012. *Managing the Risks of Extreme Events and Disasters to Advance Climate Change Adaptation: A Special Report of Working Groups I and II of the Intergovernmental Panel on Climate Change*. Field, C.B., V. Barros, T.F. Stocker, D. Qin, D.J. Dokken, K.L. Ebi, M.D. Mastrandrea, K.J. Mach, G.-K. Plattner, S.K. Allen, M. Tignor and P.M. Midgley (Eds.). Cambridge University Press.

IPCC, 2013a. *Summary for Policymakers*. In: *Climate Change 2013: The Physical Science Basis. Contribution of Working Group I to the Fifth Assessment Report of the Intergovernmental Panel on Climate Change*, pp. 3-29. Stocker, T.F., D. Qin, G.-K. Plattner, M. Tignor, S.K. Allen, J. Boschung, A. Nauels, Y. Xia, V. Bex and P.M. Midgley (Eds.). Cambridge University Press. www.ipcc.ch/pdf/assessment-report/ar5/wg1/WG1AR5_SPM_FINAL.pdf

IPCC, 2013b. *Annex I: Atlas of Global and Regional Climate Projections*. van Oldenborgh, G.J., M. Collins, J. Arblaster, J.H. Christensen, J. Marotzke, S.B. Power, M. Rummukainen and T. Zhou (Eds.). In: *Climate Change 2013: The Physical Science Basis. Contribution of Working Group I to the Fifth Assessment*

Report of the Intergovernmental Panel on Climate Change. Stocker, T.F., D. Qin, G.-K. Plattner, M. Tignor, S.K. Allen, J. Boschung, A. Nauels, Y. Xia, V. Bex and P.M. Midgley (Eds.). Cambridge University Press.

Jahn, A., K. Sterling, M.M. Holland, J.E. Kay, J.A. Maslanik, C.M. Bitz, D.A. Bailey, J. Stroeve, E.C. Hunke, W.H. Lipscomb and D.A. Pollak, 2012. Late-twentieth-century simulation of Arctic sea ice and ocean properties in the CCSM4. *Journal of Climate*, 25(5):1431-1452.

James, T.S., J.A. Henton, L.J. Leonard, A. Darlington, D.L. Forbes and M. Craymer, 2014. *Relative Sea-level Projections in Canada and the Adjacent Mainland United States*. Geological Survey of Canada, Open File 7737. 72pp. doi:10.4095/295574.

James, T.S., J.A. Henton, L.J. Leonard, A. Darlington, D.L. Forbes and M. Craymer, 2015. *Tabulated Values of Relative Sea-Level Projections in Canada and the Adjacent Mainland United States*. Geological Survey of Canada, Open File 7942. 81 pp. doi:10.4095/297048.

Jensen, H.M., L. Pedersen, A. Burmeister and B.W. Hansen, 1999. Pelagic primary production during summer along 65 to 72 degrees N off West Greenland. *Polar Biology*, 21(5):269-278, doi:10.1007/s003000050362.

Kandlikar, M., J. Risbey and S. Dessai, 2005. Representing and communicating deep uncertainty in climate-change assessments. *External Geophysics, Climate and Environment*, 337:443-455, doi:10.1016/j.crte.2004.10.010.

Kattsov, V.M., J.E. Walsh, W.L. Chapman, V.A. Govorkova, T.V. Pavlova and X. Zhang, 2007. Simulation and projection of Arctic freshwater budget components by the IPCC AR4 global climate models. *Journal of Hydrometeorology*, 8(3):571-589.

Katz, R.W., 2010. Statistics of extremes in climate change. *Climatic Change*, 100:71-76, doi:10.1007/s10584-010-9834-5.

Katz, R., 2013. *Statistical methods for nonstationary extremes*. In: *Extremes in a Changing Climate: Detection, Analysis and Uncertainty*. Volume 65 in *Water Science and Technology Library*, Springer. 423pp.

Kopec, B.G., X. Feng, F.A. Michel and E.S. Posmentier, 2016. Influence of sea ice on Arctic precipitation. *Proceedings of the National Academy of Sciences of the United States of America*, 113(1):46-51.

Krasting, J.P., A.J. Broccoli, K.W. Dixon and J.R. Lanzante, 2013. Future changes in Northern Hemisphere snowfall. *Journal of Climate*, 26(20):7813-7828.

Kunkel, K.E., 2003. North American trends in extreme precipitation. *Natural Hazards*, 29:291-305.

Kwok, R., 2007. Baffin Bay ice drift and export: 2002-2007. *Geophysical Research Letters*, 34:L19501, doi:10.1029/2007GL031204.

- Kwok, R., L. Toudal Pedersen, P. Gudmandsen and S.S. Pang, 2010. Large sea ice outflow into the Nares Strait in 2007. *Geophysical Research Letters*, 37:L03502, doi:10.1029/2009GL041872.
- Langen, P.L., P. Grenier and R. Brown, 2016. Supplementary Material for Section 3.1 Climatic Drivers. <https://www.amap.no/> -> Documents -> Documents -> Assessment Reports -> Scientific -> Adaptation Actions for a Changing Arctic: Perspectives from the Baffin Bay-Davis Strait Region -> AACA-BBDS Supplementary information.zip -> Section 3.1 Climate drivers
- Lantz, T.C., P. Marsh and S.V. Kokelj, 2012. Recent shrub proliferation in the Mackenzie Delta uplands and microclimatic implications. *Ecosystems*, 16(1):47-59, doi:10.1007/s10021-012-9595-2.
- Latifovic, R. and D. Pouliot, 2007. Analysis of climate change impacts on lake ice phenology in Canada using historical satellite data record. *Remote Sensing of Environment*, 106:492-507.
- Lavoie, D., N. Lambert and A. van der Baaren, 2013. Projections of Future Physical and Biogeochemical Conditions in Hudson and Baffin Bays from CMIP5 Global Climate Models. Canadian Technical Report of Hydrography and Ocean Sciences 289. xiii + 129pp.
- Lenaerts, J.T.M., J.H. van Angelen, M.R. van den Broeke, S. Gardner, B. Wouters and E. van Meijgaard, 2013. Irreversible mass loss of Canadian Arctic Archipelago glaciers. *Geophysical Research Letters*, 40(5):870-874, doi:10.1002/grl.50214.
- Lindsay, R., M. Wensnahan, A. Schweiger and J. Zhang, 2014. Evaluation of seven different atmospheric reanalysis products in the Arctic. *Journal of Climate*, 27:2588-2606, doi:10.1175/JCLI-D-13-00014.
- Lique, C., H.L. Johnson, Y. Plancherel and R. Flanders, 2015. Ocean change around Greenland under a warming climate. *Climate Dynamics*, 45:1235.
- Liston, G.E. and C.A. Hiemstra, 2011. The changing cryosphere: Pan-Arctic snow trends (1979-2009). *Journal of Climate*, 24:5691-5712, doi:10.1175/JCLI-D-11-00081.1.
- Lobb, J., E.C. Carmack, R.G. Ingram and A.J. Weaver, 2003. Structure and mixing across an Arctic/Atlantic front in northern Baffin Bay. *Geophysical Research Letters*, 30:1833, doi:10.1029/2003GL017755.
- Loder, J.W. and A. van der Baaren, 2013. Climate Change Projections for the Northwest Atlantic from Six CMIP5 Earth System Models. Canadian Technical Report of Hydrography and Ocean Sciences 286. xiv + 112pp.
- Loder, J.W., A. van der Baaren and I. Yashayaev, 2015. Climate comparisons and change projections for the Northwest Atlantic from six CMIP5 models. *Atmosphere-Ocean*, doi:10.1080/07055900.2015.1087836.
- Maraun, D., F. Wetterhall, A.M. Ireson, R.E. Chandler, E.J. Kendon, M. Widmann, S. Brienen, H.W. Rust, T. Sauter, M. Themeßl, V.K.C. Venema, K.P. Chun, C.M. Goodess, R.G. Jones, C. Onof, M. Vrac and I. Thiele-Eich, 2010. Precipitation downscaling under climate change: Recent developments to bridge the gap between dynamical models and the end user. *Reviews of Geophysics*, 48:RG3003, doi:10.1029/2009RG000314.
- Marchenko, S., V. Romanovsky and B. Tipenko, 2008. Numerical modeling of spatial permafrost dynamics in Alaska. In: Kane, D. and K. Hinkel (Eds.). *Proceedings of the Ninth International Conference on Permafrost*, University of Alaska Fairbanks, June 29-July 3, 2008. Volume 2, pp. 1125-1130.
- Matthes, H., A. Rinke and K. Dethloff, 2015. Recent changes in Arctic temperature extremes: Warm and cold spells during winter and summer. *Environmental Research Letters*, 10(11):114020.
- Maxwell, J.B., 1981. Climatic regions of the Canadian Arctic Islands. *Arctic*, 34(3):225-240.
- McCabe, G.J., M.P. Clark and M.C. Serreze, 2001. Trends in Northern Hemisphere surface cyclone frequency and intensity. *Journal of Climate*, 14:2763-2768.
- McInnes, K.L., T.A. Erwin and J.M. Bathols, 2011. Global climate model projected changes in 10 m wind speed and direction due to anthropogenic climate change. *Atmospheric Science Letters*, 12:325-333, doi:10.1002/asl.341.
- Mearns, L.O., M. Hulme, T.R. Carter, R. Leemans, M. Lal, P. Whetton, L. Hay, R.N. Jones, R. Katz, T. Kittel, J. Smith and R. Wilby, 2001. Climate scenario development. In: *Climate Change 2001. Working Group I: The Scientific Basis. Third Assessment Report of the Intergovernmental Panel on Climate Change*, pp. 739-768. Mata, L.J. and J. Zillman (Eds.). Cambridge University Press.
- Mekis, É. and L.A. Vincent, 2011. An overview of the second generation adjusted daily precipitation dataset for trend analysis in Canada. *Atmosphere-Ocean*, 49(2):163-177.
- Melling, H., Y. Gratton and R.G. Ingram, 2001. Ocean circulation within the North Water polynya of Baffin Bay. *Atmosphere-Ocean*, 39:301-325.
- Melling, H., T.A. Agnew, K.K. Falkner, D.A. Greenberg, C.M. Lee, A. Münchow, B. Petrie, S.J. Prinsenberg, R.M. Samelson and R.A. Woodgate, 2008. Fresh-water fluxes via Pacific and Arctic outflows cross the Canadian polar shelf. In: Dickson, R.R., J. Meinke and P. Rhines (Eds.). *Arctic-Subarctic Ocean Fluxes: Defining the Role of the Northern Seas in Climate*, chapter 9. Springer-Verlag Publishers.
- Mernild, S.H. and G.E. Liston, 2012. Greenland freshwater runoff. Part II: Distribution and trends, 1960-2010. *Journal of Climate*, 25:6015.
- Mernild, S.H., E. Hanna, J.R. McConnell, M. Sigl, A.P. Beckerman, J.C. Yde, J. Cappelen, K.K. Malmros and K. Steffen, 2014.

- Greenland precipitation trends in a long-term instrumental climate context (1890–2012): Evaluation of coastal and ice core records. *International Journal of Climatology*, 35:303–320, doi:10.1002/joc.3986.
- Michel, C., J. Hamilton, E. Hansen, D. Barber, M. Reigstad, J. Iacozza, L. Seuthe and A. Niemi, 2015. Arctic Ocean outflow shelves in the changing Arctic: A review and perspectives. *Progress in Oceanography*, doi:10.1016/j.pocean.2015.08.007.
- Mitrovica, J.X., M.E. Tamisiea, J.L. Davis and G.A. Milne, 2001. Recent mass balance of polar ice sheets inferred from patterns of global sea-level change. *Nature*, 409(6823):1026–1029.
- Moore, G.W.K., I.A. Renfrew, B.E. Harden and S.H. Mernild, 2015. The impact of resolution on the representation of southeast Greenland barrier winds and katabatic flows. *Geophysical Research Letters*, 42(8):3011–3018.
- Mortin, J., R.G. Graversen and G. Svensson, 2014. Evaluation of pan-Arctic melt-freeze onset in CMIP5 climate models and reanalyses using surface observations. *Climate Dynamics*, 42:2239–2257, doi:10.1007/s00382-013-1811-z.
- Mote, P., L. Brekke, P.B. Duffy and E. Maurer, 2011. Guidelines for constructing climate scenarios. *Eos, Transactions, American Geophysical Union*, 92(31):257–258.
- Mueller, D.R., P. Van Hove, D. Antoniadis, M.O. Jeffries and W.F. Vincent, 2009. High Arctic lakes as sentinel ecosystems: Cascading regime shifts in climate, ice cover, and mixing. *Limnology and Oceanography*, 54:2371–2385.
- Munchow, A. and H. Melling, 2008. Ocean current observations from Nares Strait to the west of Greenland: Interannual to tidal variability and forcing. *Journal of Marine Research*, 66:801–833.
- Nick, F.M., A. Vieli, M. Langer Andersen, I. Joughin, A. Payne, T.L. Edwards, F. Pattyn and R.S.W. van de Wal, 2013. Future sea-level rise from Greenland's major outlet glaciers in a warming climate. *Nature*, 497:235–238.
- Oreskes, N., 2004. Beyond the ivory tower: The scientific consensus on climate change. *Science*, 306:1686, doi:10.1126/science.1103618.
- Orlowsky, B. and S.I. Seneviratne, 2012. Global changes in extreme events: Regional and seasonal dimension. *Climatic Change*, doi:10.1007/s10584-011-0122-9.
- Overland, J.E., J.A. Francis, E. Hanna and M. Wang, 2012. The recent shift in early summer Arctic atmospheric circulation. *Geophysical Research Letters*, 39:1–6, doi:10.1029/2012GL053268.
- Overland, J., J. Walsh and V. Kattsov, 2017. Arctic trends, feedbacks, and thresholds – Multiple causes for rapid change. In: *Snow, Water, Ice and Permafrost in the Arctic (SWIPA) 2017. Arctic Monitoring and Assessment Programme (AMAP)*, Oslo, Norway.
- Paquette, M., D. Fortier, D.R. Mueller, D. Sarrazin and W.F. Vincent, 2015. Rapid disappearance of perennial ice on Canada's most northern lake. *Geophysical Research Letters*, 42:1433–1440, doi:10.1002/2014GL062960.
- Paquin, J.-P. and L. Sushama, 2015. On the Arctic near-surface permafrost and climate sensitivities to soil and snow model formulations in climate models. *Climate Dynamics*, 44:203–228, doi:10.1007/s00382-014-2185-6.
- Peltier, W.R., D.F. Argus and R. Drummond, 2015. Space geodesy constrains ice-age terminal deglaciation: The global ICE-6G_C (VM5a) model. *Journal of Geophysical Research: Solid Earth*, 120:450–487, doi:10.1002/2014JB011176.
- Peterson, T.C., X. Zhang, M. Brunet-India and J. L. Vázquez-Aguirre, 2008. Changes in North American extremes derived from daily weather data. *Journal of Geophysical Research*, 113:D07113, doi:10.1029/2007JD009453.
- Peterson, I., J. Hamilton, S. Prinsenberg and R. Pettipas, 2012. Wind-forcing of volume transport through Lancaster Sound. *Journal of Geophysical Research*, 117:C11018, doi:10.1029/2012JC008140.
- Pfahl, S. and H. Wernli, 2012. Quantifying the relevance of cyclones for precipitation extremes. *Journal of Climate*, 25:6770–6780.
- Pithan, F. and T. Mauritsen, 2014. Arctic amplification dominated by temperature feedbacks in contemporary climate models. *Nature Geoscience*, 7:181–184, doi:10.1038/ngeo2071.
- Prowse, T.D., B.R. Bonsal, C.R. Duguay and M.P. Lacroix, 2007. River-ice break-up/freezing-up: A review of climatic drivers, historical trends and future predictions. *Annals of Glaciology*, 26:443–451.
- Prowse, T., K. Alfredsen, S. Beltaos, B. Bonsal, C. Duguay, A. Korhola, J. McNamara, R. Pienitz, W.F. Vincent, V. Vuglinsky and G.A. Weyhenmeyer, 2011a. Past and future changes in Arctic lake and river ice. *Ambio*, 40:53–62, doi:10.1007/s13280-011-0216-7.
- Prowse, T., K. Alfredsen, S. Beltaos, B. Bonsal, C. Duguay, A. Korhola, J. McNamara, W.F. Vincent, V. Vuglinsky and G.A. Weyhenmeyer, 2011b. Arctic freshwater ice and its climatic role. *Ambio*, 40:46–52, doi:10.1007/s13280-011-0214-9.
- Rabe, B., H.L. Johnson, A. Münchow and H. Melling, 2012. Geostrophic ocean currents and freshwater fluxes across the Canadian polar shelf via Nares Strait. *Journal of Marine Research*, 70:603–640.
- Radic, V., A. Bliss, A.C. Beedlow, R. Hock, E. Miles and J.G. Cogley, 2013. Regional and global projections of twenty-first century glacier mass changes in response to climate scenarios from global climate models. *Climate Dynamics*, doi:10.1007/s00382-013-1719-7.

- Rae, J., G. Aðalgeirsdóttir, T. Edwards, X. Fettweis, G. Gregory, H. Hewitt, J.A. Lowe, P. Lucas-Picher, R.H. Mottram, A.J. Payne, J.K. Ridley, S.R. Shannon, W.J. van de Berg and M. van den Broeke, 2012. Greenland ice sheet surface mass balance: Evaluating simulations and making projections with regional climate models. *The Cryosphere*, 6:1275-1294.
- Rapaić, M., R. Brown, M. Marković and D. Chaumont, 2015. An evaluation of temperature and precipitation surface-based and reanalysis datasets for the Canadian Arctic, 1950-2010. *Atmosphere-Ocean*, 53(3):283-303.
- Rignot, E., I. Velicogna, M. van der Broeke, A. Monaghan and J. Lenaerts, 2011. Acceleration of the contribution of the Greenland and Antarctic ice sheets to sea level rise. *Geophysical Research Letters*, 38:L05503, doi:10.1029/2011GL046583.
- Romanovsky, V.E., S.L. Smith, H.H. Christiansen, N.I. Shiklomanov, D.A. Streletskiy, D.S. Drozdov, G.V. Malkova, N.G. Oberman, A.L. Kholodov and S.S. Marchenko, 2015. Terrestrial permafrost. In: Blunden, J. and D. Arndt (Eds.). *State of the Climate in 2014. Special Supplement to the Bulletin of the American Meteorological Society*, 96(7):S139-S141.
- Romanovsky, V.E. K. Isaksen, D. Drozdov, O. Anisimov, A. Instanes, M. Leibman, A.D. McGuire, N. Shiklomanov, S. Smith, D. Walker, G. Grosse, B.M. Jones, M.T. Jorgensen, M. Kanevskiy, A. Kizyakov, A. Lewkowicz, G. Malkova, S. Marchenko, D.J. Nicolsky, D. Sterletskiy and S. Westermann, 2017. Changing permafrost and its impacts. In: *Snow, Water, Ice and Permafrost in the Arctic (SWIPA) 2017. Arctic Monitoring and Assessment Programme (AMAP)*, Oslo, Norway.
- Rowell, D.P., 2006. A demonstration of the uncertainty in projections of UK climate change resulting from regional model formulation. *Climatic Change*, 79(3-4):243-257.
- Sasgen, I., M. van den Broeke, J.L. Bamber, E. Rignot, L.S. Sørensen, B. Wouters, Z. Martinec, I. Velicogna and S.B. Simonsen, 2012. Timing and origin of recent regional ice-mass loss in Greenland. *Earth and Planetary Science Letters*, 333-334:293-303.
- Scinocca, J.F., V.V. Kharin, Y. Jiao, M.W. Qian, M. Lazare, L. Solheim, G.M. Flato, S. Biner, M. Desgagne and B. Dugas, 2016. Coordinated global and regional climate modelling. *Journal of Climate*, 29:17-35.
- Seidel, K.H., 1987. *The Climate of Auyuittuq National Park Reserve: A Review. Report prepared for Environment Canada - Parks. Government of the Northwest Territories, Department of Renewable Resources*. 36pp.
- Serreze, M. and R. Barry, 2005. *The Arctic Climate System*. Cambridge University Press.
- Sharp, M., D.O. Burgess, J.G. Cogley, M. Ecclestone, C. Labine, and G.J. Wolken, 2011. Extreme melt on Canada's Arctic ice caps in the 21st century. *Geophysical Research Letters*, 38: doi:10.1029/2011GL047381.
- Sharp, M., D.O. Burgess, F. Cawkwell, L. Copland, J.A. Davis, E.K. Dowdeswell, J.A. Dowdeswell, A.S. Gardner, D. Mair, L. Wang, S.N. Williamson, G.J. Wolken and F. Wyatt, 2014. Recent glacier changes in the Canadian Arctic. In: Kargel, J.S., M.P. Bishop, A. Kaab, B.H. Raup and G. Leonard (Eds.). *Global Land Ice Measurements from Space: Satellite Multispectral Imaging of Glaciers*, pp. 205-228. Springer-Praxis.
- Shepherd, A., E.R. Ivins, G. A. V.R. Barletta, M.J. Bentley, S. Bettadpur, K.H. Briggs, D.H. Bromwich, R. Forsberg, N. Galin, M. Horwath, S. Jacobs, I. Joughin, M.A. King, J.T.M. Lenaerts, J. Li, S.R.M. Ligtenberg, A. Luckman, S.B. Luthcke, M. McMillan, R. Meister, G. Milne, J. Mouginot, A. Muir, J.P. Nicolas, J. Paden, A.J. Payne, H. Pritchard, E. Rignot, H. Rott, L.S. Sørensen, T.A. Scambos, B. Scheuchl, E.J.O. Schrama, B. Smith, A.V. Sundal, J.H. van Angelen, W.J. van de Berg, M.R. van den Broeke, D.G. Vaughan, I. Velicogna, J. Wahr, P.L. Whitehouse, D.J. Wingham, D. Yi, D. Young and H.J. Zwally, 2012. A reconciled estimate of ice-sheet mass balance. *Science*, 338:1183-1189.
- Sillmann, J., V.V. Kharin, X. Zhang, F.W. Zwiers and D. Bronaugh, 2013a. Climate extremes indices in the CMIP5 multimodel ensemble: Part 1. Model evaluation in the present climate. *Journal of Geophysical Research: Atmospheres*, 118: doi:10.1002/jgrd.50203.
- Sillmann, J., V.V. Kharin, F.W. Zwiers, X. Zhang and D. Bronaugh, 2013b. Climate extremes indices in the CMIP5 multimodel ensemble: Part 2. Future climate projections. *Journal of Geophysical Research: Atmospheres*, 118: doi:10.1002/jgrd.50188.
- Slater, A.G. and D.M. Lawrence, 2013. Diagnosing present and future permafrost from climate models. *Journal of Climate*, 26(15):5608-5623, doi:10.1175/JCLI-D-12-00341.1.
- Smith, S.L., V.E. Romanovsky, A.G. Lewkowicz, C.R. Burn, M. Allard, G.D. Clow, K. Yoshikawa and J. Throop, 2010. Thermal state of permafrost in North America: A contribution to the International Polar Year. *Permafrost and Periglacial Processes*, 21:117-135.
- Smith, S.L., J. Throop and A.G. Lewkowicz, 2012. Recent changes in climate and permafrost temperatures at forested and polar desert sites in northern Canada. *Canadian Journal of Earth Sciences*, 49: 914-924.
- Smith, S.L., D.W. Riseborough, M. Ednie and J. Chartrand, 2013. *A Map and Summary Database of Permafrost Temperatures in Nunavut, Canada. Geological Survey of Canada Open File 7393*, doi:10.4095/292615. geoscan.nrcan.gc.ca/starweb/geoscan/servlet.starweb?path=geoscan/shorte.web&search1=R=292615
- Smith, S.L., A.G. Lewkowicz, C. Duchesne and M. Ednie, 2015. Variability and change in permafrost thermal state in northern Canada. Paper 237. In: *GEOQuébec 2015. Proceedings of the 68th Canadian Geotechnical Conference and 7th Canadian Conference on Permafrost, Québec. GEOQuébec 2015 Organizing Committee*.

- Sou, T. and G. Flato, 2009. Sea ice in the Canadian Arctic Archipelago: Modeling the past (1950-2004) and the future (2041-60). *Journal of Climate*, 22:2181-2198, doi:10.1175/2008JCLI2335.1.
- Spada, G., G. Galassi and M. Olivieri, 2014. A study of the longest tide gauge sea-level record in Greenland (Nuuk/Godthab, 1958-2002). *Global and Planetary Change*, 118:42-51, doi:10.1016/j.gloplacha.2014.04.001.
- Steiner, N., K. Azetsu-Scott, J. Hamilton, K. Hedges, X. Hu, M.Y. Janjua, D. Lavoie, J. Loder, H. Melling, A. Merzouk, W. Perrie, I. Peterson, M. Scarratt, T. Sou and R. Tallmann, 2015. Observed trends and climate projections affecting marine ecosystems in the Canadian Arctic. *Environmental Reviews*, 23(2):191-239.
- Stern, G.A. and A. Gaden, 2015. From Science to Policy in the Western and Central Canadian Arctic: An Integrated Regional impact Study (IRIS) of Climate Change and Modernization. ArcticNet, Quebec City. 432pp.
- Stieglitz, M., S.J. Dery, V.E. Romanovsky and T.E. Osterkamp, 2003. The role of snow cover in the warming of arctic permafrost. *Geophysical Research Letters*, 30(13):4. doi:10.1029/2003gl017337.
- Stopa, J.E., F. Ardhuin and F. Girard-Ardhuin, 2016. Wave climate in the Arctic 1992-2014: Seasonality and trends. *The Cryosphere*, 10:1605-1629, doi:10.5194/tc-2016-37.
- Straneo, F., G.S. Hamilton, D.A. Sutherland, L.A. Stearns, F. Davidson, M.O. Hammill, G.B. Stenson and A. Rosing-Asvid, 2010. Rapid circulation of warm subtropical waters in a major glacial fjord in East Greenland. *Nature Geoscience*, 3:182-186.
- Straneo, F., D.A. Sutherland, D. Holland, C. Gladish, G.S. Hamilton, H.L. Johnson, E. Rignot, Y. Xu and M. Koppes, 2012. Characteristics of ocean waters reaching Greenland's glaciers. *Annals of Glaciology*, 53:202-210.
- Stroeve, J.C., V. Kattsov, A. Barrett, M. Serreze, T. Pavlova, M. Holland and W.N. Meier, 2012. Trends in Arctic sea ice extent from CMIP5, CMIP3 and observations. *Geophysical Research Letters*, 39: doi:10.1029/2012GL052676.
- Stroeve, J.C., T. Markus, L. Boisvert, J. Miller and A. Barrett, 2014. Changes in Arctic melt season and implications for sea ice loss. *Geophysical Research Letters*, 41:1216-1225, doi:10.1002/2013GL058951.
- Surdu, C.M., 2015. Spaceborne monitoring of Arctic lake ice in a changing climate. PhD Thesis. University of Waterloo. hdl.handle.net/10012/9184 2015-02-19
- Swingedouw, D., J. Mignot, P. Braconnot, E. Mosquet, M. Kageyama and R. Alkama, 2009. Impact of freshwater release in the North Atlantic under different climate conditions in an OAGCM. *Journal of Climate*, 22(23):6377-6403, doi:10.1175/2009jcli3028.1.
- Takala, M., K. Luojus, J. Pulliainen, C. Derksen, J. Lemmetyinen, J.-P. Kärnä, J. Koskinen and B. Bojkov, 2011. Estimating Northern Hemisphere snow water equivalent for climate research through assimilation of space-borne radiometer data and ground-based measurements. *Remote Sensing of Environment*, 115(12):3517-3529.
- Tang, C.C., C.K. Ross, T. Yao, B. Petrie, B.M. DeTracey and E. Dunlap, 2004. The circulation, water masses and sea-ice of Baffin Bay. *Progress in Oceanography*, 63(4):183-228.
- Taylor, K.E., R.J. Stouffer and G.A. Meehl, 2011. An overview of CMIP5 and the experiment design. *Bulletin of the American Meteorological Society*, 93:485-498, doi:10.1175/bams-d-11-00094.1.
- Tebaldi, C., K. Hayhoe, J.M. Arblaster and G.A. Meehl, 2006. Going to the extremes: An intercomparison of model-simulated historical and future changes in extreme events. *Climatic Change*, doi: 10.1007/s10584-006-9051-4.
- Thomas, E.K., J.P. Briner, J.J. Ryan-Henry and Y. Huang, 2016. A major increase in winter snowfall during the middle Holocene on western Greenland caused by reduced sea ice in Baffin Bay and the Labrador Sea. *Geophysical Research Letters*, 43:5302-5308, doi:10.1002/2016GL068513.
- Throop, J., S.L. Smith, and A.G. Lewkowicz, 2010. Observed recent changes in climate and permafrost temperatures at four sites in northern Canada. In: *Proceedings of the 63rd Canadian Geotechnical Conference & 6th Canadian Permafrost Conference*, Calgary, pp. 1265-1272.
- Tilinina, N., S.K. Gulev and D.H. Bromwich, 2014. New view of Arctic cyclone activity from the Arctic system reanalysis. *Geophysical Research Letters*, 41:1766-1772, doi:10.1002/2013GL058924.
- Tivy, A., S.E.L. Howell, B. Alt, S. McCourt, R. Chagnon, G. Crocker, T. Carrieres and J.J. Yackel, 2011. Trends and variability in summer sea ice cover in the Canadian Arctic based on the Canadian Ice Service Digital Archive, 1960-2008 and 1968-2008. *Journal of Geophysical Research*, 116:C03007, doi:10.1029/2009JC005855.
- Tremblay J.-É., Y. Gratton, E.C. Carmack, C.D. Payne and N.M. Price, 2002. Impact of the large-scale Arctic circulation and the North Water Polynya on nutrient inventories in Baffin Bay. *Journal of Geophysical Research*, 107(C8), doi:10.1029/2000JC000595.
- Twomey, S., 1977. The influence of pollution on the shortwave albedo of clouds. *Journal of Atmospheric Science*, 34:1149-1152.
- van Vuuren, D.P., J. Edmonds, M. Kainuma, K. Riahi, A. Thomson, K. Hibbard, G.C. Hurtt, T. Kram, V. Krey, J.-F. Lamarque, T. Masui, M. Meinshausen, J. Nakicenovic, S.J. Smith and S.K. Rose, 2011. The representative concentration pathways: An overview. *Climatic Change*, 109:5-31, doi:10.1007/s10584-011-0148-z.

- Van Wychen, W., D.O. Burgess, L. Gray, L. Copland, M. Sharp, J.A. Dowdeswell and T.J. Benham, 2014. Glacier velocities and dynamic ice discharge from the Queen Elizabeth Islands, Nunavut. *Geophysical Research Letters*, 41:484-490, doi:10.1002/2013GL058558.
- Vaughan, D.G., J.C. Comiso, I. Allison, J. Carrasco, G. Kaser, R. Kwok, P. Mote, T. Murray, F. Paul, J. Ren, E. Rignot, O. Solomina, K. Steffen and T. Zhang, 2013. Observations: Cryosphere. In: *Climate Change 2013: The Physical Science Basis; Contribution of Working Group I to the Fifth Assessment Report of the Intergovernmental Panel on Climate Change*. Stocker, T.F., D. Qin, G.-K. Plattner, M. Tignor, S.K. Allen, J. Boschung, A. Nauels, Y. Xia, V. Bex and P.M. Midgley (Eds.). Cambridge University Press.
- Vavrus, S.J., 2013. Extreme Arctic cyclones in CMIP5 historical simulations. *Geophysical Research Letters*, 40:6208-6212, doi:10.1002/2013GL058161.
- Vernon, C.L., J.L. Bamber, J.E. Box, M.R. van den Broeke, X. Fettweis, E. Hanna and P. Huybrechts, 2013. Surface mass balance model intercomparison for the Greenland ice sheet. *The Cryosphere*, 7:599-614.
- Vincent, W.F., I. Laurion, R. Pienitz, K.M.W. Anthony and M. Katey, 2012. Climate impacts on Arctic lake ecosystems. In: *Climatic Change and Global Warming of Inland Waters: Impacts and Mitigation for Ecosystems and Societies*, pp. 27-42. Wiley-Blackwell.
- Vincent, L.A., X. Zhang, R.D. Brown, Y. Feng, É. Mekis, E.J. Milewska, H. Wan and X.L. Wang, 2015. Observed trends in Canada's climate and influence of low frequency variability modes. *Journal of Climate*, doi:10.1175/JCLI-D-14-00697.1.
- Voltaire, A., E. Sanchez-Gomez, D. Salas y Méliá, B. Decharme, C. Cassou, S. Sénési, S. Valcke, I. Beau, A. Alias, M. Chevallier, M. Déqué, J. Deshayes, H. Douville, E. Fernandez and G. Madec, 2013. The CNRM-CM5.1 global climate model: Description and basic evaluation. *Climate Dynamics*, 40(9-10):2091-2121, doi:10.1007/s00382-011-1259-y.
- Wan H., X.L. Wang and V.R. Swail, 2010. Homogenization and trend analysis of Canadian near-surface wind speeds. *Journal of Climate*, 23:1209-1225, doi:10.1175/2009JCLI3200.1.
- Wang, M. and J.E. Overland, 2012. A sea ice free summer Arctic within 30 years: An update from CMIP5 models. *Geophysical Research Letters*, 39:L18501, doi:10.1029/2012GL052868.
- Wang, X.L., Y. Feng and L.A. Vincent, 2014. Observed changes in one-in-20 year extremes of Canadian surface air temperatures. *Atmosphere-Ocean*, 52(3):222-231, doi:10.1080/00559900.2013.818526.
- Way, R.G. and A.E. Viau, 2014. Natural and forced air temperature variability in the Labrador region of Canada during the past century. *Theoretical and Applied Climatology*, doi:10.1007/s00704-014-1248-2.
- Wehner, M., 2013. Methods of projecting future changes in extremes. In: *Extremes in a Changing Climate: Detection, Analysis and Uncertainty*. Volume 65 in *Water Science and Technology Library*, Springer. 423pp.
- White, A., L. Copland, D. Mueller and W. Van Wychen, 2014. Assessment of historical changes (1959-2012) and the causes of recent break-ups of the Petersen Ice Shelf, Nunavut, Canada. *Annals of Glaciology*, 56(69):65-76.
- Williamson, S., M. Sharp, J. Dowdeswell and T. Benham, 2008. Iceberg calving rates from northern Ellesmere Island ice caps, Canadian Arctic, 1999-2003. *Journal of Glaciology*, 54:391-400, doi:10.3189/002214308785837048.
- Yin, J., 2012. Century to multi-century sea level rise projections from CMIP5 models. *Geophysical Research Letters*, 39:L17709, doi:10.1029/2012GL052947.
- Yin, J., S.M. Griffies and R.J. Stouffer, 2010. Spatial variability of sea level rise in twenty-first century projections. *Journal of Climate*, 23(17):4585-4607.
- Yin, J., J.T. Overpeck, S.M. Griffies, A.X. Hu, J.L. Russell and R.J. Stouffer, 2011. Different magnitudes of projected subsurface ocean warming around Greenland and Antarctica. *Nature Geoscience*, 4:524-528.
- Yu, Y., H. Stern, C. Fowler, F. Fetterer and J. Maslanik, 2014. Interannual variability of Arctic landfast ice between 1976 and 2007. *Journal of Climate*, 27:227-243, doi:10.1175/JCLI-D-13-00178.1.
- Zappa, G., L.C. Shaffrey, K.I. Hodges, P.G. Sansom and D.B. Stephenson, 2013. A multimodel assessment of future projections of North Atlantic and European extratropical cyclones in the CMIP5 climate models. *Journal of Climate*, 26:5846-5862, doi:10.1175/JCLI-D-12-00573.1.
- Zhang, T., 2005. Influence of the seasonal snow cover on the ground thermal regime: An overview. *Review of Geophysics*, 43:RG4002, doi:10.1029/2004RG000157.
- Zhang, X., J.E. Walsh, J. Zhang, U.S. Bhatt and M. Ikeda, 2004. Climatology and interannual variability of Arctic cyclone activity: 1948-2002. *Journal of Climate*, 17:2300-2317.
- Zhang, X., J. He, J. Zhang, I. Polyakov, R. Gerdes, J. Inoue and P. Wu, 2012. Enhanced poleward moisture transport and amplified northern high-latitude wetting trend. *Nature Climate Change*, 3, doi:10.1038/nclimate1631.
- Zweng, M.M. and A. Muchow, 2006. Warming and freshening of Baffin Bay, 1916-2003. *Journal of Geophysical Research*, 111:C07016, doi: 10.1029/2005JC0030.